

Ngoc Tu Tran

Creating material properties for thermoset injection
molding simulation process

Ngoc Tu Tran

**Creating material properties for thermoset
injection molding simulation process**



TECHNISCHE UNIVERSITÄT
CHEMNITZ

**Universitätsverlag Chemnitz
2020**

Impressum

Bibliografische Information der Deutschen Nationalbibliothek

Die Deutsche Nationalbibliothek verzeichnet diese Publikation in der Deutschen Nationalbibliografie; detaillierte bibliografische Angaben sind im Internet über <http://www.dnb.de> abrufbar.

Titelgrafik: Ngoc Tu Tran
Satz/Layout: Ngoc Tu Tran

Technische Universität Chemnitz/Universitätsbibliothek
Universitätsverlag Chemnitz
09107 Chemnitz
<https://www.tu-chemnitz.de/ub/univerlag>

readbox unipress
in der readbox publishing GmbH
Rheinische Straße 171
44147 Dortmund
<https://www.readbox.net/unipress>

ISBN 978-3-96100-114-9

<http://nbn-resolving.de/urn:nbn:de:bsz:ch1-qucosa2-383802>

Creating material properties for thermoset injection molding simulation process

Von der Fakultät für Maschinenbau der
Technischen Universität Chemnitz

genehmigte

Dissertation

zur Erlangung des akademischen Grades

Doktoringenieur
(Dr.-Ing.)

Vorgelegt

von M. Sc. Ngoc Tu Tran

geboren am 20.02.1987 in Phu Tho, Vietnam

Tag der Einreichung: 03.04.2019

Tag der Verteidigung: 03.12.2019

1. Gutachter: Prof. Dr.-Ing. Michael Gehde

2. Gutachter: Prof. Dr.-Ing. Thomas Seul

Prüfungsvorsitzender: Prof. Dr.-Ing. Guntram Wagner

Bibliographic description

Tran, Ngoc Tu

Creating material properties for thermoset injection molding simulation process

Dissertation from Professorship of Plastic Materials, Department of Mechanical Engineering, Chemnitz University of Technology, Chemnitz, 2019

115 pages, 84 Figures, 11 Tables, 100 Literatures

Abstract

To simulate the injection molding process, it is necessary to set material data. With thermosets injection molding simulation, its material data sheet is found in limited sources and is seldom available from data bank of simulation tools. Therefore, before setting material data, it is necessary to create its own material data sheet that requires an extensive knowledge in measurement of rheological and thermal properties as well as optimization algorithm. In addition, to simulate exactly the thermosets injection molding compound process, it requires a profound knowledge in the mold filling characteristics of thermoset injection molding compounds. However, investigation of flow behavior of thermosets injection molding compounds inside the mold has not been adequately described. Up to now, there is still a big question related to whether there is slip or no slip phenomenon between thermosets melt and the wall surface during filling the cavity, for which has not yet been found an exact answer. Because of this the effect of wall slip on the cavity surface is still ignored during injection molding simulation process. This thesis focuses on developing method to study slip phenomenon of polymer melt during filling the cavity, firstly. Experimental injection studies under different processing conditions were performed. It was found that there was a strong slip on the interface between the phenolic polymer and the mold wall surface, which was not found for the thermoplastic injection molding. Secondly, the rheological and thermal properties of thermoset injection molding compounds was measured successfully. After that, the numerical method was developed and written to not only create its material data sheets, but also predict master curves of viscosity and cure kinetics at any heating rate. Finally, the generated data sheets that has not yet been found in data bank of any simulation tool were used to investigate the application of simulation tools in

simulation of the injection molding process with considering slip boundary condition. The results of this thesis are beneficial for understanding the slip phenomenon comprehensively, opening a new thinking about influence of slip on analysis, calculation and simulation of fiber orientation during the filling process of glass fiber reinforced thermoset injection molding compounds. Furthermore, with the developed numerical method, simulation guides become independent users of material data bank from simulation tools. Finally, it is impossible to neglect the influence of wall slip on the mold filling behavior of the thermoset injection molding compounds during simulation.

Keywords

Thermoset injection molding, Wall slip, Material properties, Reactive viscosity models, Cure kinetics models, Material data sheet, Computers simulation, Slip boundary condition.

Acknowledgement

I would like to deliver all my sincere thankfulness to all people who educated me, enlightened me and supported me.

Great thanks to Prof. Dr.-Ing. Michael Gehde, Institute of Conveying and Plastics in Chemnitz University of Technology, for providing me the important opportunity to study in this famous and outstanding institute. He was extraordinarily patient with me and squeezed time for the work of my doctoral thesis. He guided me to the right way step by step and gave me numerous critical suggestions.

I would like to show my gratitude to Prof. Dr.-Ing. Günter Mennig. I was convinced by his broad and profound knowledge in the field of mechanical engineering, especially, polymer science and engineering. He spent a lot of time in discussing with me about from general frame to every little detail of my doctoral thesis.

Many thanks to Prof. Dr.-Ing. Thomas Seul for reviewing my dissertation and constructive suggestions.

I appreciate Dr.-Ing. Tham Nguyen Chung. He introduced me to Prof. Dr.-Ing. Günter Mennig and Prof. Dr.-Ing. Michael Gehde to help me continue my academic pursuit at the Technische Universität Chemnitz. He guided me walking on the research road of plastic proceeding and injection molding simulation during the period of Ph.D. program.

I must also extend my thankfulness to other colleges in Institute of Conveyors and Plastics. Special thanks to Dr.-Ing. Brit Clauß, Dr.-Ing. Sascha Englich, Dr.-Ing. Thomas Scheffler and M.Sc. Nils Schmeißer for their kind help and encouragement. I would like also to appreciate Rocco Sickel, Frank Werner, Christian Uhlmann, Sven Mauersberger for their help in the experiments of my work.

Great thanks to my parents for raising and supporting me. I would like to appreciate sincere support from my family members during doing Ph.D. program. Special thanks to my sweet lover for her constant accompanying and understanding.

Chemnitz, December 2019

Tran, Ngoc Tu

Content

Bibliographic description	7
Acknowledgement.....	9
Content	11
1 Introduction and research objects	15
2 State of art	19
2.1 Thermoset injection molding process.....	19
2.1.1 Thermoset injection machine.....	19
2.1.2 Thermoset injection molding cycle	20
2.1.3 Mold filling behavior of thermoset injection molding compounds.....	22
2.2 Injection molding simulation process.....	25
2.2.1 Material properties.....	27
2.2.2 Influence of material properties on simulation process	36
2.2.3 Modelling material properties	38
2.2.4 Reactive injection molding simulation	41
3 Experiment	43
3.1 Selecting experimental material	43
3.2 Rheological measurement	43
3.2.1 Rheometer samples.....	43
3.2.2 Rotational rheometer tests	44
3.3 Thermal properties measurement	44
3.3.1 Cure kinetics measurement.....	44
3.3.2 Heat capacity measurement	44
3.3.3 Thermal conductivity measurement	44
3.4 Injection molding experiment	45
3.4.1 Developing technical method for investigating wall slip phenomenon	45
3.4.2 Study cavities	46

3.4.3	Experimental procedure	46
3.5	Summary of chapter.....	48
4	Experimental results.....	49
4.1	Material properties	49
4.1.1	Viscosity	49
4.1.2	Cure kinetics	50
4.1.3	Heat capacity.....	51
4.1.4	Thermal conductivity	51
4.2	Injection molding results	51
4.2.1	Slip phenomenon in the presence of a wall surface	51
4.2.2	Difference in the mold filling behavior between thermosetting and thermoplastic materials.....	54
4.2.3	Mechanism of slip phenomenon between thermoset polymer and cavity surface.....	55
4.2.4	Wall contact of thermoset melts.....	56
4.2.5	Weld line formation of thermoset polymer	57
4.2.6	Degree of cure	58
4.3	Summary of chapter.....	60
5	Creating thermoset material data for simulation process.....	61
5.1	Modelling cure kinetics	61
5.2	Modelling reactive viscosity	66
5.3	Prediction of viscosity	69
5.4	Summary of chapter.....	72
6	Simulation model	73
6.1	Characteristics of Moldex3D simulation tool	73
6.1.1	Meshing and numerical methods.....	73
6.1.2	Slip boundary condition	77
6.2	Filling and curing phase simulation	79
6.2.1	Importing generated material properties	79

6.2.2	Study cavities and sensor nodes	81
6.2.3	Simulation procedure.....	82
6.3	Simulation results	82
6.3.1	Predicted melt front and position of weld line.....	82
6.3.2	Predicted filling results	84
6.3.3	Predicted curing results	88
6.3.4	Influence of initial conversion on simulation results	91
6.4	Summary of chapter	92
7	Validation simulation results with experimental results	93
7.1	Filling results.....	93
7.2	Curing results	96
7.3	Results of different phenolic injection molding compounds	97
7.4	Summary of chapter	100
8	Summary.....	101
8.1	Conclusions	101
8.2	Future work	102
9	References.....	105
10	List of symbols and abbreviations	113

1 Introduction and research objects

Due to the outstanding process ability and high performance-price ratio, plastic component plays a significant role in daily life of everyone. With development of new additives and addition of reinforcing materials, properties of plastic have been remarkably improved, and its application field has been clearly expanded. It makes the plastic displacing dominant materials used in different fields possible. Based on their response to temperature, plastics materials could be classified into two main categories: thermoplastics and thermosets [1].

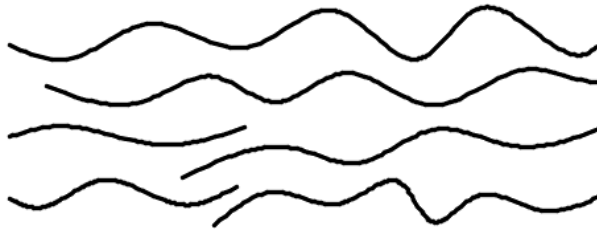


Figure 1.1 Thermoset before crosslinking or thermoplastic [2]

Before hardening, thermosets like thermoplastics are independent macromolecules. However, in their final state, after hardening, they have a three-dimensional structure obtained by chemical crosslinking produced after (spray-up molding or filament winding) or during the processing (compression or injection molding, for example) [2]. Figure 1.1 and Figure 1.2 illustrate the molecular arrangements of the polymers.

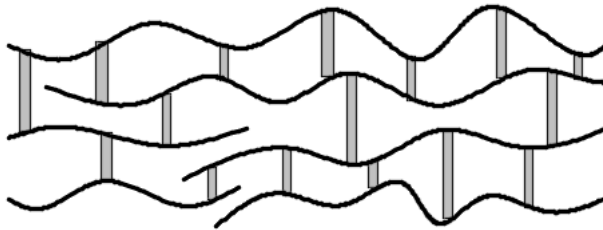


Figure 1.2 Thermoset after crosslinking [2]

As one of the most commonly applied processing methods for plastic compounds, injection molding has received a substantial amount of study and attention in recent years. In the field of injection molding process, computer simulation has been widely used to simulate the entire injection molding process. With computer simulation, potential defects, such as air trap, weld line positions and sink mark, emerging during injection molding process before doing in the

reality can be predicted, and therefore mistake of design can be modified without overfull expense of time and money. In addition, computer simulation is able to accomplish the experiments which can be difficultly operated in reality. Therefore, it can help to analyze and thus improve the whole process, raise success rate of first molding trial, reduce cost of manufacture and shorten the development cycle. With thermoplastics injection molding, there have been some significant achievements in application of simulation packages to simulate the entire phases of thermoplastics injection molding process. The computations are found in good agreement with experiments. Meanwhile, application of computer simulation in thermoset injection molding simulation and comparison between experimental and simulation results seem to be found in limited knowledge because of not only lacking material data sheet for simulation process that requires an extensive knowledge in measurement of rheological and thermal properties as well as optimization algorithm, but also complication in analysis of the mold filling characteristics of thermoset resin compounds. Up to now, investigation of flow behavior of thermoset resin compounds inside a mold has not been adequately described so that an existing question concerning whether there is slip or no slip on the interface between thermoset melt and cavity has not yet been found an exact answer. Therefore, the applicability of thermoplastics injection molding simulation concepts for thermosets is still available question that should be answered.

The aim of this work is firstly innovation of a method to study the mold filling behavior of thermosets injection molding compounds. Secondly, developing and writing a numerical method for creating thermoset material data sheet for investigation of the application of simulation tools in simulation the filling and curing phase of thermoset injection molding process. The developed numerical method helps simulation guides will become independent users of material data bank from simulation tools and evaluate the similarity and difference in the mold filling characteristics of thermoset injection molding compounds generated by both experiment and simulation. To complete these aims, following objectives and assignments were achieved and accomplished in this dissertation.

- a. A new method, namely, the spotwise painting of the mold wall surface was developed to investigate the slip phenomenon of polymer on the interface between polymer and cavity surface.
- b. The flow behavior of glass-fiber reinforced phenolic thermoset resin in the presence of the wall surface during injection molding under various processing parameters has been studied by applying the spotwise painting of the mold wall surface. The experimental results clearly show

a strong slip of the phenolic melt on the cavity surface. The complete difference in the flow behavior of thermosets and thermoplastics polymer on the cavity surface in the process of filling a mold was shown, which will lead to a new thinking of taking the influence of wall slips not only on measuring rheological properties of thermosets resins into account but also on calculation, analysis and simulation of the flow of the glass fiber reinforced thermosets resins during the injection molding filling process.

- c. Rheological and thermal properties of thermoset injection molding compounds were successfully measured. Furthermore, a new numerical methodology has been written to not only create material data bank of some thermoset injection molding compounds, but also predict the rheological and cure kinetics of thermosets resins at multiple heating rates different from the preset heating rates in a fast way. Finally, the generated material data sheets that has not yet been found in any simulation tool was directly imported into Moldex3D simulation tool for simulating the filling and curing process with and without considering slip boundary conditions.
- d. Comparison in the mold filling characterization of the thermoset injection molding compounds between experimental and simulation results was conducted to evaluate the application of simulation tools in simulation of thermoset injection molding process.

2 State of art

2.1 Thermoset injection molding process

Injection molding, defined by a cycle and automated process for manufacturing identical plastic articles from mold, is the most widely used polymer operation [3]. The process can manufacture either very small or very large parts using virtually any plastic material [4]. The injection molding is itself a very complex system composed of multiple components, which are subjected to many cycles of temperatures and stresses [5]. Injection molding has several features; including direct path from resin to finished part, i.e. no or only minimal finishing of the molded part necessary, and process can be fully automated and good reproducibility of production. So that the main advantage of this process is the capacity of repetitively and economically fabricating parts with complex geometries at a high production rate [6]. It presents the most important process for manufacturing plastics parts and is suitable for mass producing components. Typical injection molding could be found everywhere in daily life, e.g. automotive parts, consumer electronics wares and increasing number of construction part made from fiber reinforced plastic.

2.1.1 Thermoset injection machine

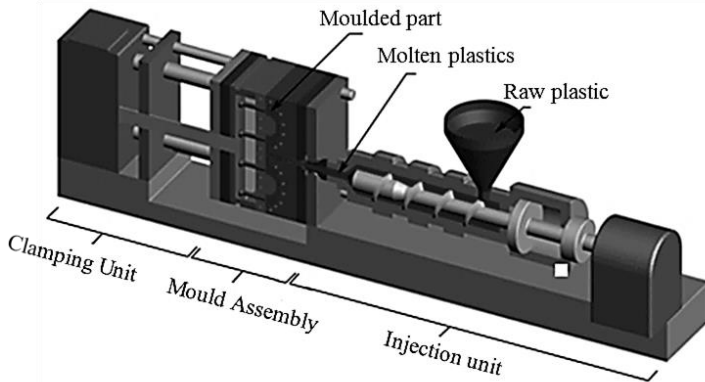


Figure 2.1 Plastic injection machine

The basic molding equipment consists of an injection molding machine, an injection mold, and a mold temperature control unit. These three components can influence the manufacture process directly and decide its success or failure. Figure 2.1 is an example of an injection molding machine. The injection molding

machine can be defined as a machine which produces formed component in a repeated manner from polymer materials [7, 8]. An injection molding machine can be broken down into the following components: Plasticizing/injection unit, clamping unit, control system and tempering devices for the mold. The main tasks of the plasticizing units are to heat and melt the polymer pellets entering from the hopper and inject the melt into the cavity of mold. Since injection molding is a discontinuous process, the machine must be able to open the mold for demolding and close it again for the next shot. The clamping unit accomplishes this. Because the polymer is pressed under high pressure into the mold, the clamping unit must also be able to keep the mold tightly sealed during the filling and holding pressure stages. At present, clamping units are available on the market in three different forms [9, 10]. These are known as mechanical, hydraulic, hydraulic mechanical and electro-mechanical systems. Driving unit provides necessary pressure of hydraulic oil or kinetic energy from electric motor. And the sequence of injection molding cycle is manipulated by a control unit, the function of which are to coordinate the machine sequence, to keep certain machine parameters constant, and to optimize individual steps in the process [11]. The control unit is integrated within the machine and operated through a touch screen nowadays.

2.1.2 Thermoset injection molding cycle

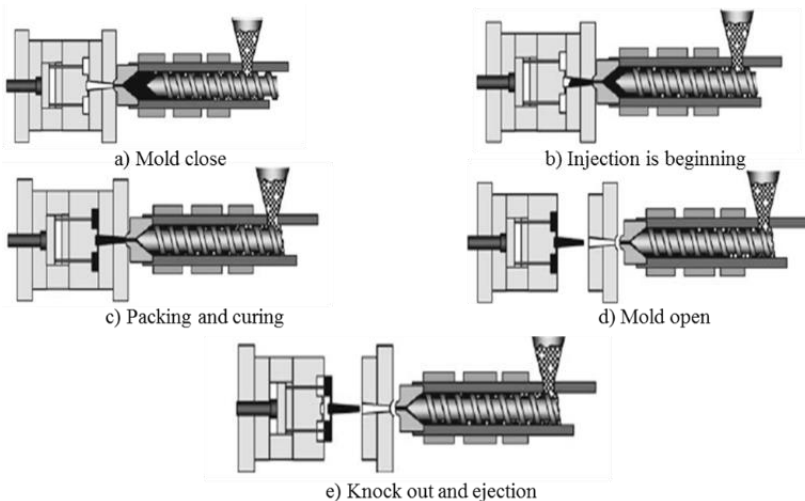


Figure 2.2 Schematic of injection molding system [12, 13, 14, 15]

The entire injection molding process for thermoset molding compounds is a consecutive process that includes a series of sequential steps, which partly overlap one another. To understand the entire thermoset injection molding process and the influence of each process phase on the quality of the moldings, we find it helpful to break the process into five sequences of phases as shown in Figure 2.2. At the beginning of thermoset injection molding process, the granular molding compound is poured or conveyed directly into the injection machine hopper. Then, the screw rotates and moves the granules forward the screw barrel. The polymer is plasticized from solid granules through the combined effect of heat conduction from the heated barrel and internal shear heating caused by rotation of the screw. Normally, the thermoset injection molding compounds are plasticized below cure temperature (circa from 80°C to 100°C). When the required volume of molding compound has been plasticized, the screw stops rotating. It moves forward axially without rotation, acting as a ram, forcing the plasticized compound through the sprue, runners, gates, and into the hot mold cavities (circa from 160°C to 190°C) thus forming the final shape of plastic component [16, 17]. As the cavity is filled, the screw moves with a small displacement to maintain a holding pressure and provides additional material into the cavity to ensure complete filling and detailed replication as far as possible. After the polymer melt ceases to flow, the cavity pressure gradually decreases to zero or a very low value. Simultaneously, the screw starts rotating and moving backward, and the plasticizing stage of next cycle starts. In the meantime, the injected polymer in the cavity goes through the curing process. In the filling and curing process, the temperature of injected polymer increases significantly due to conversion of mechanical energy (pressure) to heat, the shear heating or frictional heating, the heat transfers from the cavity wall to the polymer and the heat generated by chemical reaction between substances inside thermoset injection molding compounds. After the required cure time, the molded part has achieved final cure and become stiff enough, the mold opens, and the component can be ejected by ejector pin, sometimes with the help of robot. After this stage, an injection cycle has been completed, and the next cycle can start.

2.1.3 Mold filling behavior of thermoset injection molding compounds

The most important stage in injection molding is the mold filling process because several quality-related properties are strongly influenced by the flow and cooling processes that take place in the filling phase [18, 19, 20]. The injection molding of thermosets has received much less attention in comparison with thermoplastics injection molding. Except for a few reports, mainly mathematical in nature, very little has been published in relation to the molding injection molding of thermosets [21, 22]. This is not surprising, since the reactive nature of thermosets adds a new dimension to the process which serves only to increase the complexity of the modelling problem. Furthermore, the complexity of characterizing thermosets has contributed to the scarcity of useful data relating to the critical thermal, rheological, and thermodynamic properties of these materials which are essential for adequate modelling and analysis of the phenomena involved in thermoset processing [23].

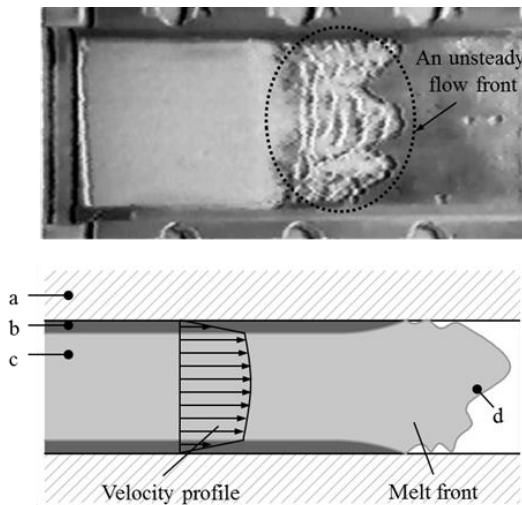


Figure 2.3 An unsteady flow front of thermosets polymer (above) and supposed flow characteristic of thermosets (below) (a) Mold; (b) Low viscosity skin layer; (c) High viscosity core region; (d) uncompacted zone [24]

Up to now, investigation of flow behavior of thermoset resin compounds inside a mold has not been adequately described. Only a few studies in this field have been reported. Thienel et al. [24] studied the mold filling behavior of thermoset resin compounds inside a rectangular cavity with a core using a mold with a glass window for observing the flow behavior directly. Castro et.al observed the flow

front of polyurethane by using a mold with a polycarbonate window [25]. They reported that there was an unsteady flow front of polymer during filling phase, as shown in Figure 2.3 (above). The mold filling seems to be plug-like flow and a supposed flow characteristic of thermoset is shown in Figure 2.3 (below). Nevertheless, to protect the glass window, experiments were conducted with low injection pressure so that the flow behavior under practical conditions of high pressure has not yet been observed.

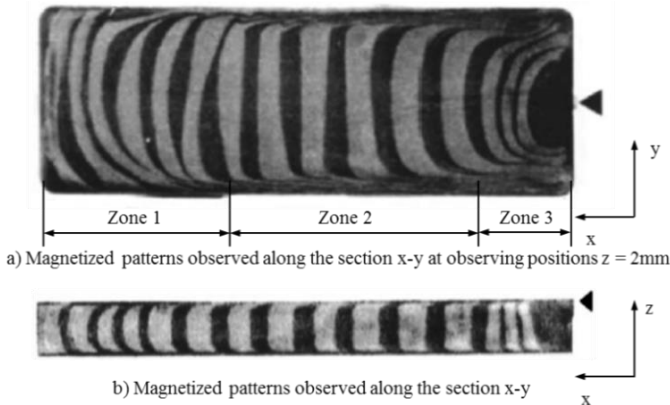


Figure 2.4 Flow behavior of thermoset phenolic resin by gate magnetization method [26]

Regarding to flow behavior of thermoset phenolic resin under high pressure with various processing conditions, Ohta [26] investigated the flow behavior of glass-fiber reinforced phenolic resin compound inside a rectangular mold under different injection molding conditions by using the gate-magnetization method developed by Yokoi and coworkers [27]. With the gate-magnetization method, magnetic particles, namely, anisotropic strontium ferrite particle, were premixed into the resin, which was magnetized at the gate by a pulsed magnetic field. The time for magnetization was controlled by a computer system. Three-dimensional flow patterns were analyzed by measuring the distribution of magnetized patterns at different sections of the molded part. The magnetized particles in the section were detected by using magneto detection liquid, which reacts to small amounts of magnetism. By observing the magnetized patterns, it was found that plug-like flow builds up in the cavity in both the horizontal and vertical sections as shown in Figure 2.4. A slip between the resin compound and the cavity wall occurred during the filling process. The flow behavior inside the cavity, as shown in Figure 2.4 (a), was observed in three characteristic zones by the forms of the magnetized patterns: asymmetric flow zone (zone 1), symmetric flow zone (zone 2) and arc-flow zone (zone 3) at the gate. However, the short-shot molded

part has not been done and this measuring method seems to be very complicated because of the complex design and operation of magnetization circuit. In addition, the magneto detection liquid can only react to small amounts of magnetism, which leads to difficulty in visual analysis of magnetized particles at different sections of a molded part. Furthermore, the slip on the interface between the polymer and the cavity surface is not clear.

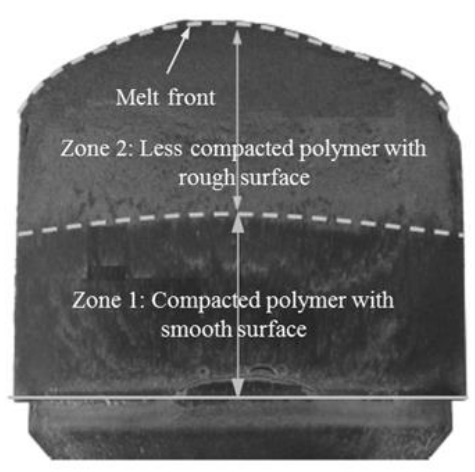


Figure 2.5 Mold filling study of thermoset phenolic injection molding compounds [28]

Recently, English [29] studied the influence of processing conditions such as injection speed, mold temperature on mold filling characteristics and fiber orientation of glass fiber reinforced phenol-formaldehyde resins in a rectangular mold. In his PhD thesis, a series of the short-molded parts were molded with different size of film gates and different processing conditions. Experimental results show that with each short-molded part, there were two characteristic zones, as shown in Figure 2.5. Zone 1 was located close to the gate. In this area, the polymer contacted the wall surface and the melt was compacted. Zone 2 was located next to zone 1, the melt was less compacted and next to the melt front there was no contact between the phenolic polymer and the wall surface. According to the variation of the surface roughness of the short-molded parts, he also supposed that the mold filling behavior seems to show a plug-like flow, which means there may be a wall slip between the phenolic polymer and the cavity surface.

In summary, the molding filling characteristics of glass fiber reinforced thermoset injection molding compounds has not yet physically explained.

Therefore, the existing question whether there is or no slip of thermoset injection molding compounds during the filling phase has not yet found an exact answer.

2.2 Injection molding simulation process

One of the most revolutionary technologies to affect injection molding in the past decades certainly is computer applications in the industrial production process. In the injection molding industry, computers permeate all aspects from the concept of a product design, mold manufacturing, raw material processing, marketing and sales, recycling, to administration and business, and so on. Many of the analysis packages promote a better understanding of molding process and the interrelationships among correlated parameters. This contributes to a better ability to control previously mysterious phenomena (such as warpage). Instead of the past costly trial-and-error manufacture process, prediction and optimization of the product quality at the lowest cost has now become possible [30].

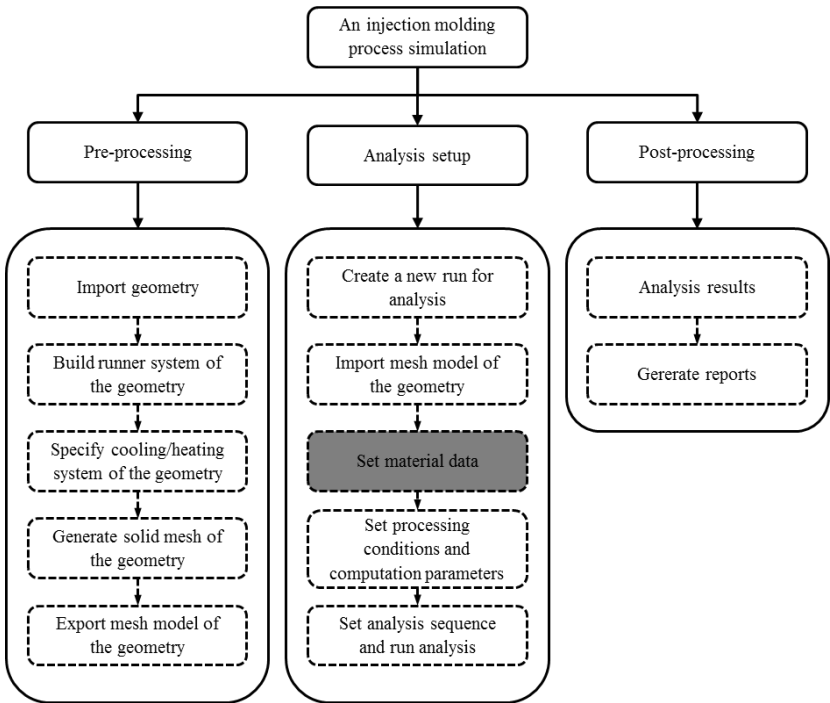


Figure 2.6 Schematic of an injection molding simulation process (both thermoplastics and thermosets)

Table 2.1 Required material properties for filling, packing and cooling/curing simulation process

Title	Input
Viscosity	A viscosity model and its coefficients
Heat capacity	The value of heat capacity
Thermal conductivity	The value of thermal conductivity
Density	The value of density
Curing data	A curing model and its coefficients
PVT	PVT model and its coefficients

In the field of injection molding simulation process, good simulation result relies on many crucial factors, as shown in Figure 2.6. There are three main steps for an injection molding process simulation (both thermoplastics and thermosets), including pre-proceeding, analysis setup and post-processing. A simulation software usually offers comprehensive options to help users complete each step during simulation process. However, the content should be mentioned here is set material data. For simulation, it is necessary to know some properties of the material. Material properties required to simulation injection molding depend on the simulation to be undertaken. For flow analysis (filling, packing, and cooling/curing) the input material properties are required, as shown in Table 2.1. If users of simulation software want to simulate shrinkage and warpage, additional properties are required, such as elastic modulus, shear modulus and coefficient of thermal expansion. With thermoplastics injection molding simulation, polymer injection molding simulation packages always provide accurate and comprehensive material data sheet of most thermoplastics' injection molding compounds. Users could easily choose thermoplastics material data sheet already embedded in the material data bank of simulation tools to simulate the entire phases of thermoplastics injection molding process. There have been some significant achievements in application of simulation packages to simulate the entire phases of thermoplastics injection molding process. The computations are found in good agreement with experiments [31, 32, 33, 34]. Nevertheless, thermosets material data sheet is found in limited sources and is seldom available from databank of simulation tools because of complication not only in material properties measurement but also in modelling rheological and thermal mathematical equations. Therefore, before setting material data, it is necessary to create its own material data sheet.

To create thermoset material data sheet for filling, packing and curing simulation process, as shown in Table 2.1, firstly, it is necessary to measure critical material properties including density, heat capacity, thermal conductivity, reactive viscosity and degree of cure. After that, based on the experimental data, optimization algorithm must be written to get all fitted coefficients in rheological and thermal mathematical models used to describe properties of material and being embedded in simulation tools. Rheological mathematical models are reactive viscosity models and thermal mathematical models are cure kinetics models.

2.2.1 Material properties

2.2.1.1 Rheological property

The rheological behavior of plastic melt is termed viscoelastic [35, 36]. This means that molten plastics behave viscously like a liquid, but also elastically like an elastic solid [37]. In most cases the viscous properties dominate in the molten state. The viscous properties can be characterized by the viscosity, which is a measure of the melt's inner resistance to flow processes. All flow processes in the plasticizing or in the mold are strongly influenced by the rheological behavior.

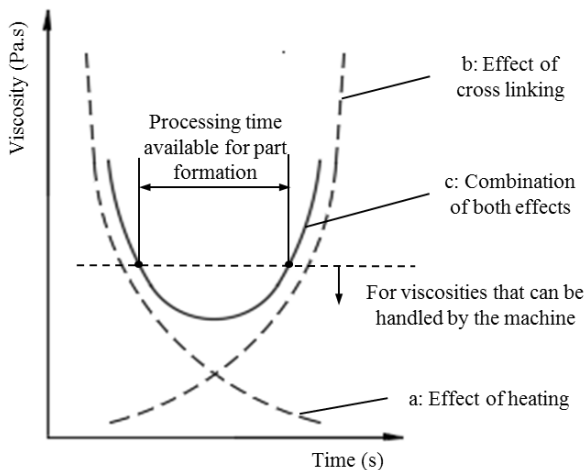


Figure 2.7 Flow/curing behavior of thermosets [38, 39, 40]

In thermoplastics processing the results of viscosity measurements show that the viscosity depends mainly on temperature and shear rate. In the range of high shear rates viscosity declines noticeably and viscosity decreases as temperature

rises. However, viscosity of thermoset compounds is more complicated because it not only depends on temperature and shear rate but also on degree of cure. Therefore, during the processing of thermoset compounds, the viscosity curve results in two opposing effects. At low degree of cure, the viscosity of thermoset resins will decrease due to the elevated temperature (Figure 2.7 graph a), which is the same for thermoplastic resins. As the temperature reaches a certain level, the rapid increase in the degree of cure and the cross-linking will cause a significant increase in viscosity (Figure 2.7 graph b). Consequently, the viscosity curve of thermoset materials is characterized by a parabolic-curve (Figure 2.7 graph c). Depending on the degree of condensation and reactivity, parabolic shape can form deep or shallow and narrow or broad [41, 42].

To simulate the flow behavior of polymer during the injection molding process, it is necessary to model the viscosity functions. A complete function for characterizing viscosity of a reacting polymer must contain the effects of shear rate ($\dot{\gamma}$), temperature (T) and degree of cure (α) [43], as shown in Eq. (2.1).

$$\eta = \eta(T, \dot{\gamma}, \alpha) \quad (2.1)$$

Temperature influences viscosity in two opposing ways. Raising the temperature will cause viscosity to drop but will increase the reaction rate, causing an increase in conversion and viscosity. In order to separate these effects, the kinetics must be measured independently. The variation of viscosity and extent of reaction must be monitored at the same heating rate. Castro and Macosko [44, 45] have followed such an approach to obtain the following empirical relation.

$$\eta(T, \dot{\gamma}, \alpha) = \eta_0(T) \left(\frac{\alpha_g}{\alpha_g - \alpha} \right)^{(c_1 + c_2 \alpha)} \quad (2.2)$$

With $\eta_0(T) = B \exp(T_b/T)$

It could be seen from Cross-Macosko Model, as shown in Eq. (2.2) that the viscosity depends on temperature and degree-of-cure only and does not depend on shear rate. Therefore, a complete reactive model was developed and embedded in some simulation packages such as Moldex3D and Moldflow simulation tool [46], as shown in Eq. (2.3).

$$\eta(T, \dot{\gamma}, \alpha) = \frac{\eta_0(T)}{1 + \left(\frac{\eta_0(T) \cdot \dot{\gamma}}{\tau^*} \right)^{1-n}} \left(\frac{\alpha_g}{\alpha_g - \alpha} \right)^{(c_1 + c_2 \alpha)} \quad (2.3)$$

With $\eta_0(T) = B \exp(T_b/T)$

The complete reactive viscosity model, as shown in Eq. (2.3) is an extension to Castro Macosko model, with power-law type shear rate dependence. The reactive viscosity model is a linear combination of two following terms. The first term is a Cross-WLF model [47] which shows the influence of temperature and shear rate on viscosity. The second term is related to gel model that shows the curing dependence of viscosity. Therefore, the name of Eq. (2.3) is Cross-Castro-Macosko Model which can easily be found in some commercial injection molding software [46]. In Castro-Macosko and Cross-Castro-Macosko Model, η , T , $\dot{\gamma}$ are viscosity, temperature and shear rate sensitivity, respectively. η_0 is the viscosity as shear rate gradually approaches zero. B is the pre-exponential and T_b represents the η_0 temperature sensitivity. τ^* is shear stress at transition from Newtonian to non-Newtonian flow. n is power-law index with value between 0 and 1. α_g is cross-linking density (gel point) at which flow is no longer possible. c_1 , c_2 are constants that fit experimental data. α is degree of cure and the value of α is between 0 and 1.

2.2.1.2 Cure kinetics property

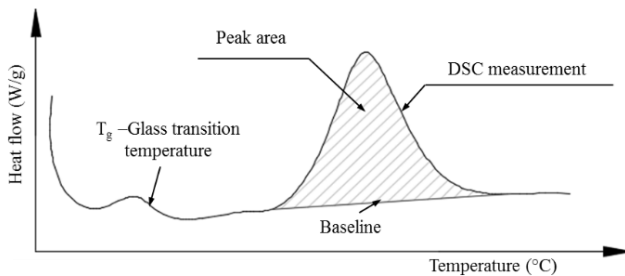


Figure 2.8 Schematic DSC heat flow results of an uncured thermoset resin [48]

Degree of cure (α) in shown in Equations (2.2) and (2.3) is not be directly measured during doing rheological test. It is independently measured by using differential scanning calorimetry (DSC) [49, 50, 51, 52, 53, 54, 55]. For example, Figure 2.8 shows the heat rate released during non-isothermal cure of a thermoset injection molding compound. The plot shows the heat flow as a function of the sample temperature. The glass transition temperature (T_g) represents the region in which the resin transforms from a hard, glassy solid to a viscous liquid. With a further increase in the temperature of sample, the resin eventually undergoes a curing process that is observed as a large exothermic peak area. The onset of cure is the temperature at which the heat flow deviates from a linear response and the exothermic peak temperature reflects the maximum rate of curing of the resin. At the completion of curing or conversion, the DSC heat flow returns to a

quasilinear response. The value of the peak area can be integrated to give the heat of cure ΔH (J/kg). As a thermoset cures or crosslinks, two main things happen [56], which are increase in T_g and decrease in exothermal heat of cure. The changes in T_g and the heat of cure can be used to characterize and quantify the degree of cure of the resin systems. As the resin system approaches complete cure, the T_g will achieve a maximum value, T_{gmax} . The increase in the T_g observed as a function of curing represents the increase in the molecular weight of the resin system. The actual value of T_{gmax} is dependent upon the chemical make-up of the particular resin system. As the resin becomes more cross-linked, the heat of curing becomes increasingly smaller and as the material becomes completely cured, the heat of cure becomes undetectable.

In order to study the influence of degree of cure (α) on viscosity and simulate the curing process of thermoset injection molding compounds it is necessary to define the curing model and fitted coefficients. Several curing functions are available for reactive injection molding simulation. Some of the most popular are Kamal model, modified Kamal model and Deng-Isayev-Law Model. The model that best represents the curing kinetics of thermoset resins and is embedded in some current injection molding software to describe the degree of cure of thermoset resins over temperature or time is Kamal model [57, 58, 59, 60, 61]. To model autocatalytic cure kinetics, the model can be applied as

$$\frac{d\alpha}{dt} = (k_1 + k_2 \alpha^m)(1-\alpha)^n \quad (2.4)$$

Where m and n are the reaction orders and k_1 , k_2 are the Arrhenius overall constants defined by:

$$k_i = a_i \exp\left(\frac{-E_i}{RT}\right) \quad (2.5)$$

For $i = 1, 2$ and a_i is the fitted rate coefficient, E_i is the activation energy, R is the universal gas law constant, and T is the cure temperature.

2.2.1.3 Specific heat capacity

Specific heat capacity of a material is measure of how much energy is required to raise the temperature of the material, and conversely, how much energy is contained in a material at a given temperature. For convection into the mold, the key property governing the heat into the mold is the specific heat capacity. To define this, suppose we have some mass of material to which we add some heat, Q , to bring about an increase in the temperature of ΔT . The mean heat

capacity denoted, \bar{C} , of the body is defined to be the ratio of the change in heat to the change in temperature:

$$\bar{C} = \frac{Q}{\Delta T} \quad (2.6)$$

The heat capacity of the body, C , at a particular temperature, is then defined as the limit approached by \bar{C} as temperature difference tends to zero:

$$C = \lim_{\Delta T \rightarrow 0} \frac{Q}{\Delta T} \quad (2.7)$$

The specific heat capacity is defined to be the heat capacity per unit mass of material. The unit of specific heat is Joule per kilogram degree Kelvin (J/kg.K). Specific heat capacity may be measured under conditions of constant volume or pressure, and is denoted c_v or c_p , respectively. Due to the large stresses exerted on the containing vessel when heating a sample for constant volume measurements, the use of c_p is more common.

Table 2.2 Specific heat of some Polymers and Metals [62, 63]

Material	Specific heat (J/kg.K)
ABS	1300
PA66	1700
Polyethylene	2300
Polypropylene	1900
Polystyrene	1300
Steel (AISI 1020)	460
Steel (AISI P20)	460

In reactive injection molding simulation, specific heat is used to calculate the heat gain from the heating system to the melt during the filling, packing and curing. It is also used to calculate the heat generated by viscous dissipation as the melt flows through the runner system and cavity. Table 2.2 shows some values for common polymers and steels used for injection molding.

2.2.1.4 Thermal conductivity

Thermal conductivity is a measure of how conductive to heat a material is. Materials with a high thermal conductivity are used to draw heat away from heat source. Materials with low thermal conductivity are insulators. In simulation of molding, the thermal conductivities of the mold and polymer are required.

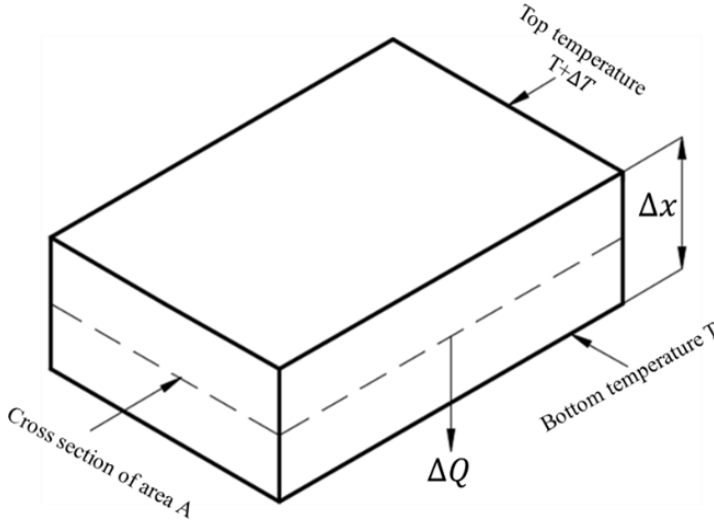


Figure 2.9 Definition of thermal conductivity [64]

More formally, imagine a slab of material with thickness Δx , for which one side is at a temperature, T , and the other at a higher temperature, $T + \Delta T$, as illustrated in Figure 2.9. Let ΔQ be the heat flow across the cross section of area A , in time Δt . The average heat flow across the cross section is then $\Delta Q / \Delta t$. Experimentally, it has been determined that the average rate of heat flow is proportional to the area and the temperature difference, and inversely proportional to thickness of the slab:

$$\frac{\Delta Q}{\Delta t} \propto A \frac{\Delta T}{\Delta x} \quad (2.8)$$

Introducing the positive constant of proportionality k , we have

$$\frac{\Delta Q}{\Delta t} = -kA \frac{\Delta T}{\Delta x} \quad (2.9)$$

And in the limit, as $\Delta x \rightarrow 0$ and $\Delta t \rightarrow 0$, we obtain:

$$\frac{\Delta Q}{\Delta t} = -kA \frac{dT}{dx} \quad (2.10)$$

Eq.(2.10) defines the thermal conductivity, denoted k , of the material. The units of thermal conductivity are Joules per meter second Kelvin (J/m.s.K) or Watts per meter Kelvin (W/m.K).

Table 2.3 Thermal conductivity of Polymers and Metals [65]

Material	Conductivity (W.mK)
ABS	0.25
PA66	0.3
Polypropylene	0.60
Polystyrene	0.14
Aluminum	250
Steel (AISI 1020)	51.9
Steel (AISI P20)	51.9

Being complex materials, the thermal conductivity of polymers varies with temperature. Polymers generally have low thermal conductivities whereas metals are much more conductive and have high thermal conductivities. Some examples are given in Table 2.3. Due to their low values, thermal conductivity is a difficult property to measure for polymers. The most important aspect of thermal conduction, as it relates to simulation, is Fourier's law, which can be deduced from Eq.(2.10) by dividing by A and generalizing the derivative to get:

$$\mathbf{q} = -k\nabla T \quad (2.11)$$

Where \mathbf{q} is the local heat flux vector. Most simulation software will assume k is a scalar.

2.2.1.5 Pressure-Volume-Temperature (PVT) data

Expansively and compressibility

Several thermodynamic properties are required for molding simulation. These are obtained from the equation of state of the material. This is often referred to as the *PVT* data. An equation of state relates these three variables, pressure p , specific volume V , and temperature T [66]. For any material, we could write the equation of state in the form

$$f(p, V, T) = 0 \quad (2.12)$$

Given any two variables, the third may be obtained from the equation of state. In particular, we can write

$$V = g(p, T) \quad (2.13)$$

Where g is some function. Graphing the function g , we obtain *PVT* surface as in Figure 2.10. Imagine that the material at a temperature, T_a , undergoes a change in temperature while the pressure is held constant. What is the subsequent change in volume? This can be answered by Figure 2.10, where this is illustrated as a

change from point a to b . A change in temperature from T_a to $T_a + \Delta T$ causes a change in volume equal to $g(p_a, T_a + \Delta T) - g(p_a, T_a)$. The average change in the volume over temperature change is therefore

$$\begin{aligned} \frac{\Delta V}{\Delta T} &= \frac{g(p_a, T_a + \Delta T) - g(p_a, T_a)}{\Delta T} \\ &= \frac{V(p_a, T_a + \Delta T) - V(p_a, T_a)}{\Delta T} \end{aligned} \quad (2.14)$$

In the limit as $\Delta T \rightarrow 0$, we obtain the instantaneous change in volume for the material which we demote by

$$\left(\frac{\Delta V}{\Delta T} \right)_p \quad (2.15)$$

Where the subscript p indicates that the pressure is constant.

The coefficient of volume expansion, β , of the material, is defined as

$$\beta = \frac{1}{V} \left(\frac{\Delta V}{\Delta T} \right)_p \quad (2.16)$$

And has units of reciprocal Kelvin (K^{-1}). The coefficient of volume expansion is also called the expansivity of the material.

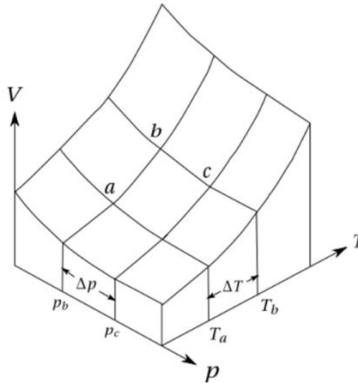


Figure 2.10 PVT surface [65]

Now consider the change in volume due to a change in pressure while keeping the temperature constant. This is illustrated by moving from point b to c in Figure 2.10. The average change in volume due to a change in pressure is given by

$$\begin{aligned}\frac{\Delta V}{\Delta T} &= \frac{g(p_a + \Delta p, T_b) - g(p_a, T_b)}{\Delta T} \\ &= \frac{V(p_a + \Delta p, T_b) - V(p_a, T_b)}{\Delta T}\end{aligned}\quad (2.17)$$

In the limit as $\Delta p \rightarrow 0$, we obtain the instantaneous change in volume for the material which we demote by

$$\left(\frac{\Delta V}{\Delta T}\right)_T \quad (2.18)$$

The isothermal compressibility coefficient k , is defined as

$$k = -\frac{1}{V} \left(\frac{\Delta V}{\Delta T}\right)_T \quad (2.19)$$

Where negative sign indicates that the volume decreases with increasing pressure. The isothermal compressibility coefficient has units of one square meter per Newton (m^2N^{-1}).

PVT model

For polymers, the equation of state is of the type $V = V(p, T)$ and is usually provided as a *PVT* diagram that gives the specific volume as a function of p and T . A commonly used equation is the Tail equation

$$V(p, T) = V_0(T) \left[1 - C \ln \left(1 + \frac{p}{B(T)} \right) \right] + V_t(p, T)$$

$$\text{With } V_0(T) = \begin{cases} b_{1,s} + b_{2,s}(T - b_5), & \text{if } T \leq T_{trans} \\ b_{1,m} + b_{2,m}(T - b_5), & \text{if } T > T_{trans} \end{cases}$$

$$B(T) = \begin{cases} b_{3,s} \exp[-b_{4,s}(T - b_5)], & \text{if } T \leq T_{trans} \\ b_{3,m} \exp[-b_{4,m}(T - b_5)], & \text{if } T > T_{trans} \end{cases} \quad (2.20)$$

$$\text{And } V_t(p, T) = \begin{cases} b_7 \exp[b_8(T - b_5) - b_9 p], & \text{if } T \leq T_{trans} \\ 0 & \text{if } T > T_{trans} \end{cases}$$

$$\text{with } T_{trans} = b_5 + b_6 p$$

Where $C = 0.0894$ is a constant, and considered to be universal. the superscripts l, s represents the solid and, melt state of the polymer, respectively. T_{trans} is the transition temperature. The $b_i (i = 1 \div 9)$ is fitted coefficients in the Tait equation.

2.2.2 Influence of material properties on simulation process

The polymer melt is assumed to be Generalized Newtonian Fluid (GNF) [65]. That is

$$\boldsymbol{\sigma} = -p\mathbf{I} + 2\eta\mathbf{D} \quad (2.21)$$

$$\nabla \cdot \boldsymbol{\sigma} = \nabla \cdot (-p\mathbf{I} + 2\eta\mathbf{D}) = -\nabla p + 2\nabla \cdot \eta\mathbf{D} \quad (2.22)$$

$$\begin{aligned} \boldsymbol{\sigma} : \nabla \mathbf{v} &= (-p\mathbf{I} + 2\eta\mathbf{D}) : \nabla \mathbf{v} \\ &= -p\mathbf{I} : \nabla \mathbf{v} + 2\eta\mathbf{D} : \nabla \mathbf{v} \\ &= -p\nabla \cdot \mathbf{v} + \eta[\nabla \mathbf{v} + (\nabla \mathbf{v})^T] : \nabla \mathbf{v} \\ &= -p\nabla \cdot \mathbf{v} + \frac{1}{2}\eta[\nabla \mathbf{v} + (\nabla \mathbf{v})^T] : [\nabla \mathbf{v} + (\nabla \mathbf{v})^T] \\ &= -p\nabla \cdot \mathbf{v} + 2\eta\mathbf{D} : \mathbf{D} \\ &= -p\nabla \cdot \mathbf{v} + \eta\dot{\gamma}^2 \end{aligned} \quad (2.23)$$

The field of polymer transport is the basis of polymer processing. In the filling process, both plastic melt and air are assumed weak compressible. Therefore, the non-isothermal 3D flow motion can be mathematically described by using the conservation principles of mass, momentum, and energy.

Conservation of mass:

$$\frac{\partial \rho}{\partial t} + \nabla \cdot \rho \mathbf{v} = 0 \quad (2.24)$$

Conservation of momentum:

$$\frac{\partial}{\partial t}(\rho \mathbf{v}) = \rho \mathbf{g} + \nabla \cdot \boldsymbol{\sigma} - \nabla \cdot (\rho \mathbf{v} \mathbf{v}) \quad (2.25)$$

Conservation of energy:

$$\begin{aligned} \rho c_p \left(\frac{\partial T}{\partial t} + \mathbf{v} \cdot \nabla T \right) &= \beta T \left(\frac{\partial p}{\partial t} + \mathbf{v} \cdot \nabla p \right) + \nabla p \cdot \mathbf{v} \\ &\quad + \boldsymbol{\sigma} : \Delta \mathbf{v} + \nabla \cdot (k \cdot \nabla T) + \dot{Q} \end{aligned} \quad (2.26)$$

We now consider implications and effects of material properties that was introduced in section 2.2.1 on these equations.

The conservation of mass equation remains unchanged and is the same as in Eq.(2.24). However, the material properties affect both the conservation of

momentum and energy equations. We deal with the conversation of momentum first. Substituting Eq.(2.22) into Eq.(2.25), we obtain

$$\frac{\partial}{\partial t}(\rho \mathbf{v}) = \rho \mathbf{g} - \nabla p + 2\nabla \cdot \eta \mathbf{D} - \nabla \cdot (\rho \mathbf{v} \mathbf{v}) \quad (2.27)$$

The left hand of Eq.(2.27) may be expanded to give:

$$\frac{\partial}{\partial t}(\rho \mathbf{v}) = \frac{\partial \rho}{\partial t} \mathbf{v} + \rho \frac{\partial \mathbf{v}}{\partial t} = -(\nabla \cdot \rho \mathbf{v}) \mathbf{v} + \rho \frac{\partial \mathbf{v}}{\partial t} \quad (2.28)$$

Where it must be used the conservation of mass equation, Eq. (2.24). The last term $\nabla \cdot (\rho \mathbf{v} \mathbf{v})$ of Eq.(2.27) may be expanded as follows:

$$\nabla \cdot (\rho \mathbf{v} \mathbf{v}) = \rho \mathbf{v} \cdot \nabla \mathbf{v} + (\nabla \cdot \rho \mathbf{v}) \mathbf{v} \quad (2.29)$$

Submitting Eq.(2.28) and (2.29) into Eq.(2.27), we obtain

$$-(\nabla \cdot \rho \mathbf{v}) \mathbf{v} + \rho = \rho \mathbf{g} - \nabla p + 2\nabla \cdot \eta \mathbf{D} - \rho \mathbf{v} \cdot \nabla \mathbf{v} - (\nabla \cdot \rho \mathbf{v}) \mathbf{v} \quad (2.30)$$

That is,

$$\rho \frac{\partial \mathbf{v}}{\partial t} = \rho \mathbf{g} - \nabla p + 2\nabla \cdot \eta \mathbf{D} - \rho \mathbf{v} \cdot \nabla \mathbf{v} \quad (2.31)$$

Now consider the energy equation, Eq.(2.26). Assuming constant thermal conductivity, and substituting Eq.(2.23) into Eq.(2.26), we get

$$\rho c_p \left(\frac{\partial T}{\partial t} + \mathbf{v} \cdot \nabla T \right) = \beta T \left(\frac{\partial p}{\partial t} + \mathbf{v} \cdot \nabla p \right) + \eta \dot{\gamma}^2 + k \nabla^2 T + \dot{Q} \quad (2.32)$$

In equations from (2.24) to (2.32) σ is stress tensor, p is pressure, ∇p is pressure gradient, $p\mathbf{I}$ is thermodynamic pressure, \mathbf{D} is deformation tensor, η is viscosity function, \mathbf{v} is velocity vector, ρ is density, \mathbf{g} is the total body force per unit mass. c_p is heat capacity, k is thermal conductivity, T is temperature, ∇T is temperature gradient, β is coefficient of volume expansion and \dot{Q} represents the heat source.

Most computation codes will be based upon the Equations (2.24), (2.31) and (2.32) for conservation of mass, momentum, and energy, respectively [65, 67]. All symbols of material properties such as viscosity (η), heat capacity (c_p), thermal conductivity (k), density (ρ) appear in the most important equations that is employed to write the codes for simulating the flow behavior of polymer

compounds. To improve the simulation results, there is a need to develop material modelling techniques that allow users to transform the measured data to data that is relevant in simulations. The challenge for code developers-commercial and academic, is to provide a more complete modelling of the injection molding process; particularly the modelling of material properties.

2.2.3 Modelling material properties

2.2.3.1 Optimization algorithm

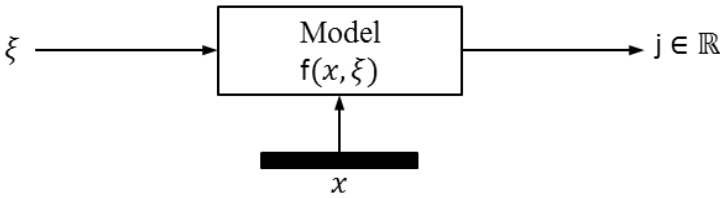


Figure 2.11 Schematic of a model with parameter $x \in \mathbb{R}^n$ which is to be adjusted so that the prediction j by the model agrees as well as possible with the available measurements.

Numerous problems in the engineering and economic sciences are of the following type. We have a functional model $f(\xi)$ which describes a relation $j = g(\xi)$ between the independent variables $\xi \in \mathbb{R}^r$ and dependent quantity $j \in \mathbb{R}$. This quantity contains parameters $x \in \mathbb{R}^n$ which are yet unknown, and we express this as follows:

$$j = f(x; \xi) \quad (2.33)$$

The problem is to choose the parameter $x \in \mathbb{R}^n$ in such a way that the model will fit available measurements $(j_i, \xi_i) \in \mathbb{R}^r \times \mathbb{R}, i = 1, \dots, m$, best possible. Finding the best parameter vector $x \in \mathbb{R}^n$ (in a sense to be made precise) is known as parameter identification, parameter estimation, model calibration, curve fitting, or data assimilation. In fact, the data pairs $(j_i, \xi_i) \in \mathbb{R}^r \times \mathbb{R}, i = 1, \dots, m$ are given, and they lead to the residuals

$$r_i(x) := f(x, \xi_i) - j_i, \quad i = 1, \dots, m \quad (2.34)$$

We are looking for a global (or at least a local) minimizer of the least-squares problem

$$\text{Minimize } \sum_{i=1}^m r_i(x)^2, x \in \mathbb{R}^n \quad (2.35)$$

To solve the optimization problem, as shown in Eq.(2.35), the optimization algorithm, namely, the least-squares estimation algorithm (LMA) developed by Levander- Marquardt [68]. In the field of mathematics and computing, the LMA was used to model mathematical models based on experimental data [69, 70, 71]. A good comparison between fitted curves and experimental curves was found, as shown in Figure 2.12.

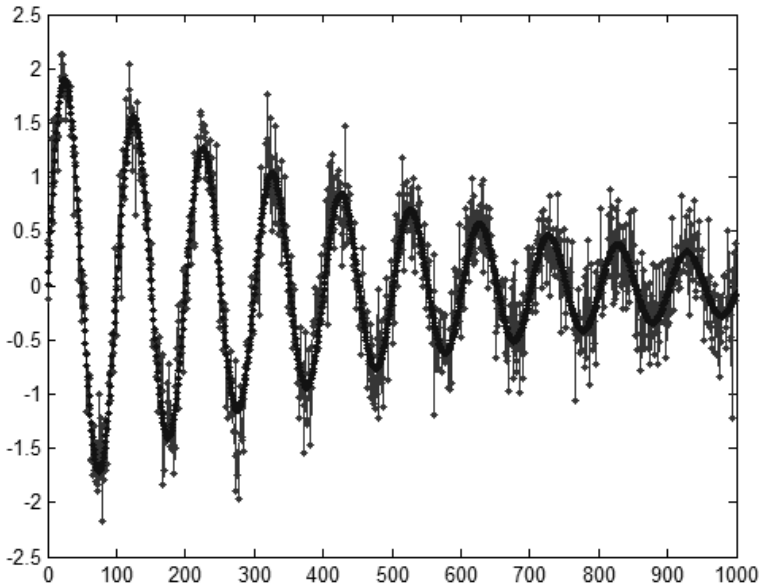


Figure 2.12 Fit a damped sine wave [72]

2.2.3.2 *Application of optimization algorithm in modelling material properties*

Up to know, modelling of cure kinetics and reactive viscosity for the thermoset injection molding process simulation has not been adequately described. In another way, how to obtain the value of variables that is called as fitted parameters in cure kinetics and reactive viscosity models from experimental data has been found in limited knowledge only.

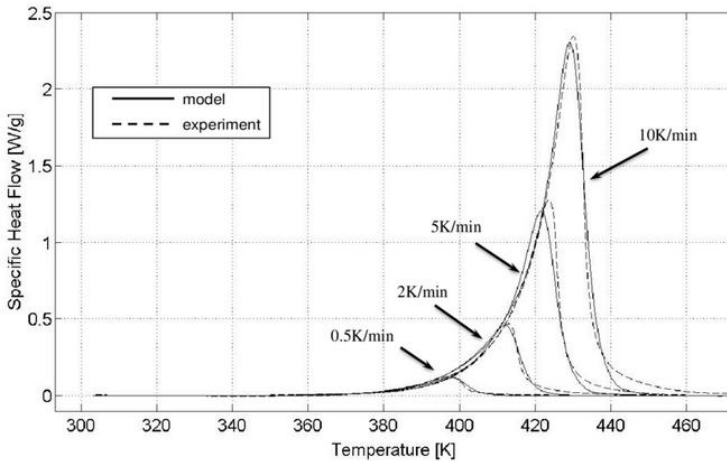


Figure 2.13 Dynamic validation of Kamal-Sourour model: Heat flow vs. temperature [73]

In the field of polymer processing, some studies have applied the LMA to write a fitting code to fit Kamal Model to the DSC scans data [74, 75, 76]. They reported that Kamal Model could describe the cure kinetics of thermoset injection molding compounds well, as shown in Figure 2.13. However, the fitted parameters were not used as fitted coefficients in Kamal model embedded in current reactive injection model of injection molding simulation packages to simulate flow behavior of thermoset polymer in a mold correctly. In additions, all these researches mentioned above have not yet shown the numerical method for predicting cure kinetics of thermoset resins for multiple heating rates different from the measured heating rates. In another way if DSC scans at only some heating rates such as 5 K/min and 20 K/min is conducted to measure the cure kinetics of thermoset resins, and then the challenge is how to predict the cure kinetics of thermoset resins at various heating rates that is different from 5 K/min and 20 K/min. Finally, the degree of cure (α) in all these studies was not used as a necessary input data for modelling a reactive viscosity model such as Cross Castro Macosko Model. It could be seen from Eq.(2.3) that there is appearance of the degree of cure (α) in Cross Castro Macosko model. Therefore, the input experimental data during modelling Cross Castro Macosko model includes not only viscosity over temperature and shear rate, but also the degree of cure (α). Nevertheless, the degree of cure (α) which happens during rheological tests is not be measured directly. It must be measured independently by cure kinetics measurement and could be calculated from a cure kinetics model such as Kamal

model. Due to these complexes, there was drawback in witting numerical method to model reactive viscosity for thermoset injection molding compounds. These problems are leading to the users 'dependency on the material data bank of simulation tools and restriction in application of computer simulation in thermoset injection molding simulation and comparison between experimental and simulation results.

2.2.4 Reactive injection molding simulation

Up to now, there is only few reports related to reactive injection molding simulation. Ramarino used Moldflow 6.2 CAE software to simulate the injection molding process for an engineering rubber component [77]. However, the rheological tests were performed on compounds without cross-linking agent, for mold flow simulation, only the parameters concerning the shear rate dependence of viscosity were determined from the experimental data. In addition, the filling results such as temperature distribution, viscosity variation, conversion of rubber component in a mold has not been shown. Kallien [78] used Sigma tool to optimize the injection molding of thermosets with 3D simulation. In his study, Cross-Castro-Macosko Model embedded in Sigma tool was used to characterize the viscosity distribution of thermoset polymer. The mold filling characterization of a thermoset compound predicted by simulation was compared to short-shot molded part generated by doing injection molding. Sensor nodes were installed during simulation process to observe the variation of pressure and pressure profile. Unfortunately, the material data sheet of thermoset material compound used to do injection molding and simulation was not illustrated. The distribution of viscosity over temperature or time, which was measured by rheological test and fitted to Cross-Castro-Macosko Model has not been shown. In addition, comparison of pressure profile generated by simulation and experiment was not done, which reflect partly the accuracy of viscosity measurement and modeling of reactive viscosity model based on experimental data. Recently, in 2017, Raschke [79] investigated flow behavior of phenolic injection molding compounds by doing injection molding experiment and simulation. In her thesis, phenolic 1110 of Hexion GmbH (PF1110) was used to do injection molding experimental. A series of incomplete molded parts was molded and compared with incomplete molded part generated from simulation. Nevertheless, due to material data sheet of PF1110 for injection molding process simulation has not been found in any simulation tool so simulation had to be done with material data sheet of CRAFTIN[®]HTI619. The information about data sheet of

CRASTIN®HTI619 has not been shown. Finally, because the mold filling behavior of thermoset molding compounds has not been adequately described. The existing question concerning whether there is slip or no slip on the interface between thermoset melt and cavity [28, 29] has not yet been found an exact answer. Therefore, all literatures about thermoset injection molding simulation mentioned above has been done without consideration of slip boundary condition. In another way, the influence of wall slip on the mold filling characterization of thermoset injection compounds in the simulation process was neglected.

3 Experiment

3.1 Selecting experimental material

Table 3.1 Technical data sheet of Vyncolit X655 [80]

Properties	Unit	Value	Method
Density	g/cm^3	2.08	ISO 1183
Molding shrinkage	%	0.15	ISO 2577
Post shrinkage	%	0.3	ISO 2577
Water absorption	%	0.06	ISO 62
Flexural modulus	GPa	25	ISO 178
Tensile strength	MPa	95	ISO 527-1

A commercial phenolic mold compound, namely, Vyncolit X655 of Sbhpp was adopted as the experimental polymer. Vyncolit X655 is a glass fiber and mineral filled phenolic molding compound with excellent dimensional stability and high electrical insulation properties. It consists of 20 percent of resin, hardener, all other ingredients to improve molding process and 80 percent of short glass fiber and mineral. Some important material properties are shown in Table 3.1.

3.2 Rheological measurement

3.2.1 Rheometer samples

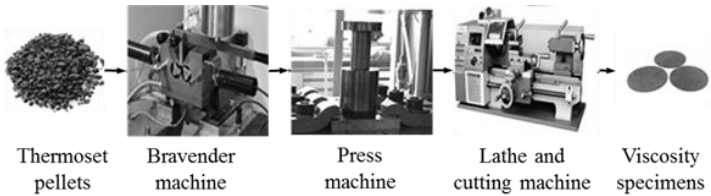


Figure 3.1 Sample preparation for measurement of viscosity of Vyncolit X655

Before doing rheology tests, rheometer samples must be prepared, as shown in Figure 3.1. Firstly, thermoset pellets were crushed into flour and lightly molten by using Brabender. In order to limit chemical reaction between components contained in thermoset resins occurs during crushing process, temperature of crushing machine used in this step was from 80°C to 90°C and the maximum torque of machine was 50 N.m. Secondly, the lightly molten polymer in the first step was put and pressed in a cylinder of the hydraulic press. The temperature and pressure of the hydraulic compression machine was 90°C and 20 MPa,

respectively. The pressing time was 4s. Finally, the cylinder samples generated by using the press was cut into test specimens of known dimensions (the diameter was 25 mm and the thickness was 1 mm) by using lathe and cutting machine. These test specimens were used as samples to measure viscosity distribution of thermoset resins over time or temperature.

3.2.2 Rotational rheometer tests

A plate-plate rheometer (AR 2000) was used to determine the flow curves of thermoset injection molding compounds under non-isothermal temperature and isothermal temperature. A specimen of known dimensions (the diameter is 25 mm and the thickness is 1 mm) was held between parallel plates so that the material acts as elastic and dissipative element in a mechanically driven oscillatory system. The drive motor provides the mechanical perturbation and the resulting torque transmitted through the test specimen was recorded by the torque sensor. With non-isothermal temperature (heating rate of 1 K/min, 2 K/min, 5 K/min), the system was used in oscillation mode with a frequency of 1 Hz and a deformation of 0.1 %. With isothermal conditions, the viscosity test was conducted under constant temperature of 100°C and 110°C, respectively, the system was used in oscillation mode with a variation in frequency from 0 Hz to 100 Hz and a deformation of 0.1 %.

3.3 Thermal properties measurement

3.3.1 Cure kinetics measurement

Differential scanning calorimeter equipment, namely DSC Q2000, manufactured by TA instruments was used to measure the reaction heat of samples under non-isothermal conditions. The mass of the samples was about 10 mg of powder. Open aluminum pans were used to contain materials. The samples were heated from -60°C to 350°C by using multiple scanning rates of 5 K/min, 10 K/min and 20 K/min.

3.3.2 Heat capacity measurement

Heat capacity of a full cured thermoset injection molding compound (Vyncolit X655) was measured via DSC Q2000. The range of temperature was from 110°C up to 200°C.

3.3.3 Thermal conductivity measurement

DTC 300 manufactured by TA instruments was used to measure thermal conductivity of full a cured thermoset injection molding compound (Vyncolit X655). The range of temperature was from 20°C up to 300°C.

3.4 Injection molding experiment

3.4.1 Developing technical method for investigating wall slip phenomenon

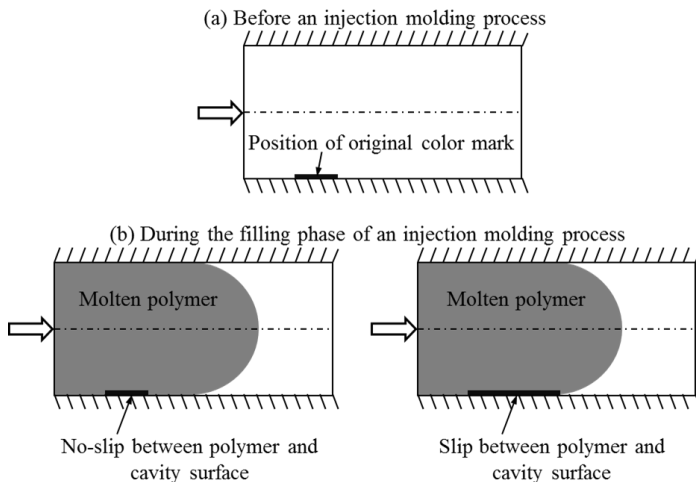


Figure 3.2 The spotwise painting of the mold wall surface method

The ‘no-slip’ is a fundamental assumption and generally-accepted boundary condition in rheology, tribology and fluid mechanics with strong experimental support. The violations of this condition, however, are widely recognized in many situations, especially in the flow of non-Newtonian fluids. Wall slip could lead to large errors and flow instabilities, such as shark skin formation and spurt flow, and hence complicates the analysis of fluid systems and introduces serious practical difficulties. In this content, a new method, namely, the spotwise painting of the mold wall surface method was developed and applied to investigate slip on the interface between polymer and wall surface during filling phase. The principle of the spotwise painting of the mold wall surface method is described in Figure 3.2. Before doing a new shot of injection molding, white color will be employed to paint manually a rectangular mark on the cavity surface of a mold (Figure 3.2 (a)). After being ejected from the mold, via analysis the position of white color appeared on the surface of molded parts, for the existing question whether “there is slip or no-slip on the interface between polymer and cavity surface during the filling” will be found an exact answer. If the position of white color on the surface of molded parts is the same as the original white color mark, that means there is no-slip on the interface between polymer and cavity surface during the filling phase. However, if slip occurs during filling the

cavity, there will be frictional force on the interface between polymer and cavity surface. As a result, there will be movement of white color on the surface of molded parts, as shown in Figure 3.2 (b).

3.4.2 Study cavities

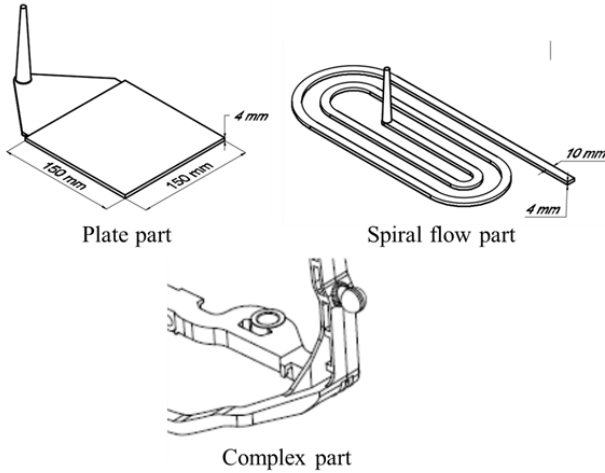


Figure 3.3 The studying objects

The study objects for injection molding experiments were 3 different parts. The first object was a plate with a dimension of 150 mm x 150 mm x 4 mm (Figure 3.3) with the film gate with a height of 2.5 mm, which was used to study slip phenomenon of thermoset polymer in the presence of a wall surface. A spiral part was the second studying object with flow length of 1385 mm and wall thickness is 4 mm. The purpose of using the spiral flow part is to investigate the maximum of flow length and degree of cure of thermoset injection molding compounds during the injection molding process. Finally, a complex part from industry was employed to study the formation of weld lines.

3.4.3 Experimental procedure

Table 3.2 Design of experiment for plate part

Parameters	Value	Unit
Cylinder temperature	100-80-60	°C
Mold temperature	160; 175; 190	°C
Injection speed	16; 32; 48	cm ³ /s
Surface roughness (R_a)	0.0846	μm

The injection molding experiments was performed with plate part, spiral part and complex part respectively. With the injection molding process of plate part, Hydraulic Krauss Maffei injection molding machine KM150-460B with three-zone plasticizing cylinder, a screw diameter of 45 mm and the maximum pressure is 180 MPa, was employed. A simple standard two plate mold was used. Processing conditions for thermoset phenolic resin injection molding of molded parts consist of a variation of mold temperature and injection speed, as shown in Table 3.2. Firstly, the mold temperature was constantly kept at 170°C for the different injection rates of 16 cm³/s, 32 cm³/s and 48 cm³/s. After that the injection speed was constantly kept at 32 cm³/s and the mold temperature was 160°C, 170°C, and 190°C, respectively.

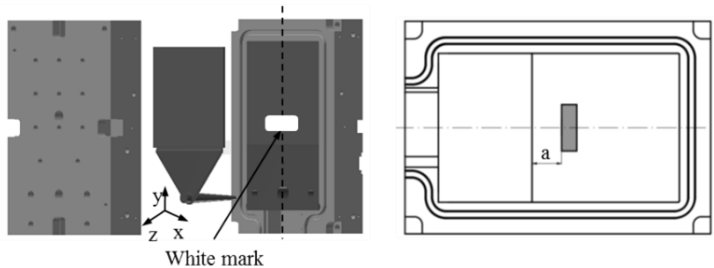


Figure 3.4 Schematic location of white marks on the mold wall surface

In order to study mold filling characteristics of phenolic injection molding compounds, with each processing parameter, a series of the incomplete molded parts were molded by setting different metering strokes in the controls of injection molding machine. Before doing a new shot of injection molding, the white marks were manually painted on the surfaces of the mold. Figure 3.4 shows schematically the position of the white mark, which was painted on the wall surfaces of the mold. The white mark was painted on the surface of the mold by which the behavior of the phenolic melts dyed white on the interface between the phenolic melt and the mold wall surface was observed. In these experiments, distance (a-mm) between the location of the white mark and the boundary line between the cavity and the film gate was 0 mm and 20 mm, respectively. The white mark was applied in different shapes.

Table 3.3 Design of experiment for spiral part

Parameters	Value	Unit
Cylinder temperature	100-80-60	°C
Mold temperature	175	°C
Injection speed profile	32-16-8	cm ³ /s

For the spiral flow injection molding, Hydraulic Krauss Maffei injection molding machine KM160-750CX with three-zone plasticizing cylinder, a screw diameter of 35 mm and the maximum pressure is 230 MPa, was used. Processing conditions for doing the spiral injection molding is summarized in Table 3.3.

Table 3.4 Design of experiment for complex part

Parameters	Value	Unit
Cylinder temperature	105-80-60	°C
Mold temperature	175	°C
Injection speed profile	13-09-07 20-18-14 40-36-28	cm ³ /s

To understand the formation of weld lines of thermoset injection molding compounds, the commercial part from industry was selected to do experiments. With the complex part injection molding experiment, injection molding machine KM125-520C, with three-zone plasticizing cylinder, a screw diameter of 45 mm and the maximum pressure is 180 MPa, was used. The injection molding process was conducted with constant temperature and different injection speed profile, as summarized in Table 3.4.

3.5 Summary of chapter

This chapter illustrates technical methods to measure rheological and thermal properties of thermoset injection molding compounds. Furthermore, a rather simple but effective and useful method, namely, the spotwise painting of the mold wall surface was developed to investigate slip between plastics melt and wall surface during the filling phase of injection molding process. The geometry of studying objects and processing conditions was designed and summarized.

4 Experimental results

4.1 Material properties

4.1.1 Viscosity

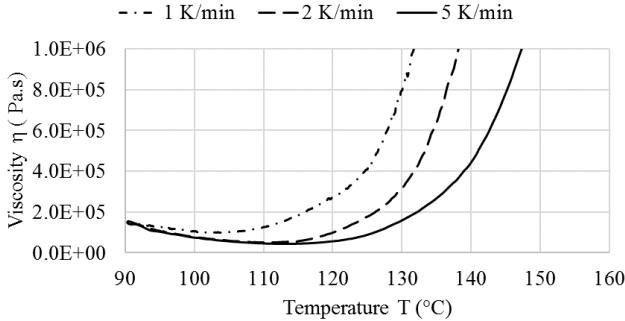


Figure 4.1 Influence of temperature on viscosity

The influence of temperature on viscosity is shown in Figure 4.1. In general, at the beginning viscosity decreases, followed by a significant increase. However, the temperature at which viscosity increases is different among heat rates. Specifically, with heating rate of 1 K/min, at 105°C viscosity increase while its numbers are 110°C and 115°C with heating rates of 2 K/min and 5 K/min, respectively. The main factor leading to these differences is influence of degree of cure on viscosity. At lower heating rate, there is more time for curing reaction. As a result, the point of temperature at which curing process starts is earlier than higher heating rates.

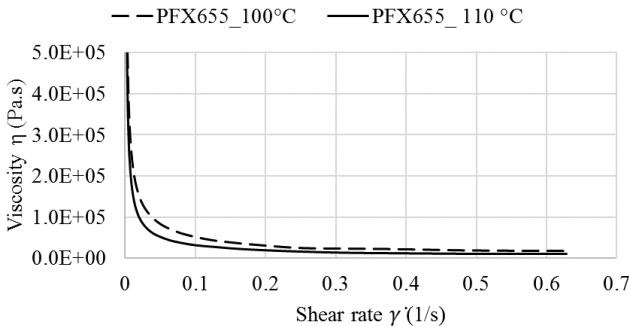


Figure 4.2 Influence of shear rate on viscosity

Viscosity in Figure 4.1 was measured by using the oscillation mode with a frequency of 1 Hz and a deformation of 0.1 %, which means the dependence of

viscosity on shear rate is not shown. In order to show the shear rate dependence of viscosity. A plate-plate rheometer, namely, AR 2000, by TA instruments was also used to determine the flow curves of Vyncolit X655 at constant temperatures of 100°C and 110°C, respectively. The system was used in oscillation mode with a variation in frequency from 0 Hz to 100 Hz and a deformation of 0.1 %. The influence of shear rate on viscosity is illustrated in Figure 4.2. Viscosity decreases significantly as shear rate increases.

4.1.2 Cure kinetics

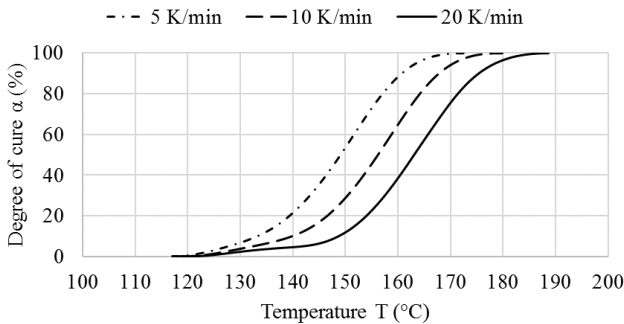


Figure 4.3 Degree of cure of Vyncolit X655 over temperature

Figure 4.3 shows the degree of cure of Vyncolit X655. The temperature at which curing process begins depends on heating rates. In particular, the lower the heating rate the earlier the curing process is. The reaction rate ($d\alpha/dt$) values as function of time (t) described in Figure 4.4, is easily calculated from plots of α over t . These data will be used to obtain the fitted coefficients of Kamal model to characterize the cure kinetics of the material, which will be shown in the next chapter.

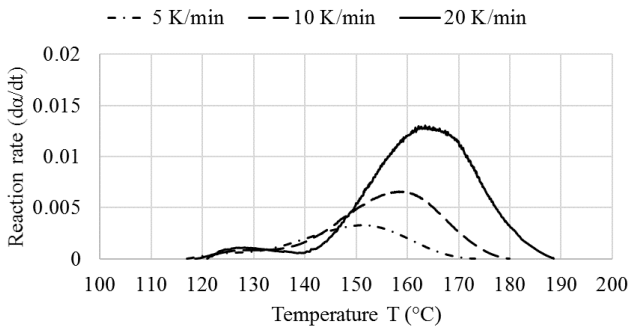


Figure 4.4 Reaction rate of Vyncolit X655 over temperature

4.1.3 Heat capacity

Heat capacity of full cured thermoset injection molding compound was measured via DSC Q2000. Heat capacity data is summarized in Table 4.1.

Table 4.1 Heat capacity data

Temperature (°C)	110	120	130	140	150	160	170	180	190	200
Heat capacity data C_p (J/kg.K)	894	926	946	974	1010	1042	1072	1087	1093	1099

4.1.4 Thermal conductivity

Thermal conductivity data of full cures Vycolite X655 was measured and is given in Table 4.2.

Table 4.2 Thermal conductivity data

Temperature (°C)	Thermal conductivity k (W/m.K)
60	0.86

4.2 Injection molding results

4.2.1 Slip phenomenon in the presence of a wall surface

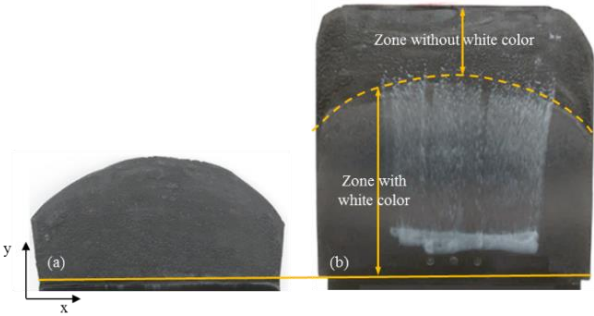


Figure 4.5 Distance $a \approx 20$ mm. Slip of the white stripes on the surface of the incomplete molded parts

The surface of incomplete molded parts and the distribution of the phenolic polymer dyed white on the interface between the phenolic melt and the wall

surface in the x-y plane are shown in Figure 4.5. The original position of the white mark in this case is 20 mm from the boundary line between the film gate and the cavity. It can be seen from Figure 4.5 (a) that at the beginning of injection molding, there is no white stripe on the surface of the incomplete molded part, which means the phenolic melt had no contact with the wall surface at the beginning of flow. As the cavity volume is filled with more amount of the phenolic polymer as shown in Figure 4.5 (b), the white stripes appear clearly on the surface of the molded parts and there is a slip of the white stripes in the flow direction. The length of the phenolic polymer region dyed white does not reach the melt front that means near to the melt front, the polymer without the white stripes is found, which seems that this polymer region originated from the initial polymer portion which flew into the cavity before reaching the original white mark.

The visual analysis of slip of the phenolic resin during injection molding process with another position of the white mark is shown in Figure 4.6. In this case, the white mark was painted at the boundary line between the film gate and the cavity ($a = 0$ mm). Therefore, the phenolic polymer must contact and flow through before reaching the cavity. It could be seen from Figure 4.6 that there are long stripes from the original white mark to the melt front. These white stripes demonstrate that the slip of the phenolic polymer begins immediately as the phenolic melt contacts the white mark and extends to the melt front. The white stripes appear clearly at the melt front of all incomplete molded parts, which means that the polymer region originated from the initial polymer portion which touched the white mark will reach the melt front. More specially, the white stripes still appear on areas where the polymer portion has an interrupted contact with the wall surface.

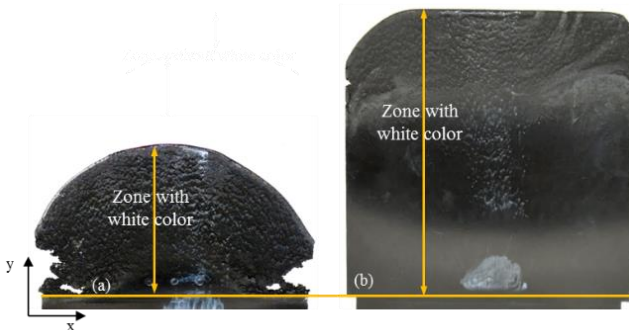


Figure 4.6 Slip of the white stripes on the surface of the incomplete molded parts

The spotwise painting of the mold wall surface was employed for all processing conditions, which have been investigated, it was found that there is a strong slip on the interface between the phenolic polymer and the mold wall surface, as shown in Figure 4.7.

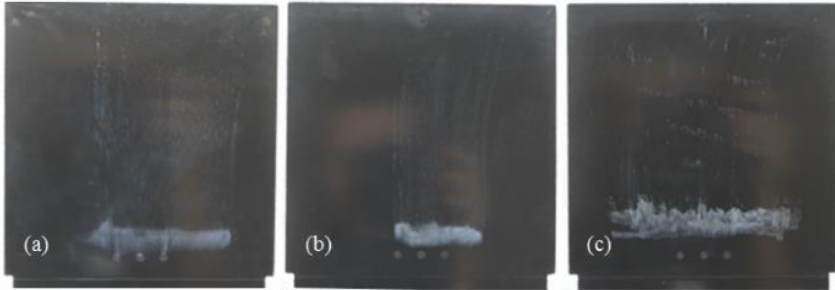


Figure 4.7 Slip of the white stripes on the cavity surface along the section x-y with constant mold temperature at 170°C and different injection rates (a) 16 cm³/s, (b) 32 cm³/s, (c) 48 cm³/s

With the spiral part and commercial complex part, the experimental results show also that there is strong slip between the phenolic melt and wall surface for all processing conditions, as shown in Figure 4.8 and Figure 4.9.

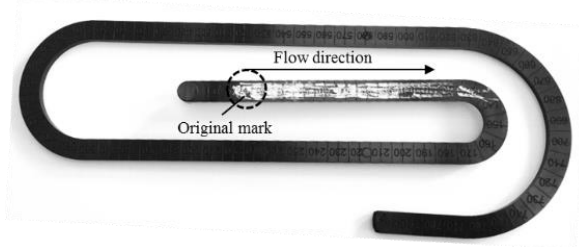


Figure 4.8 The movement of white stripe on the surface of spiral flow part

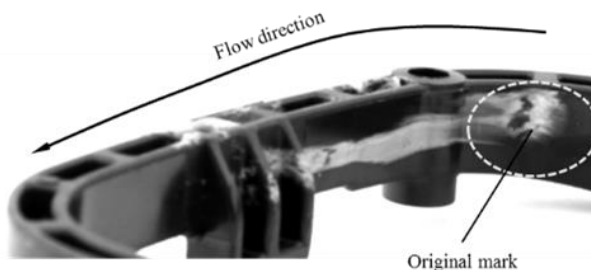


Figure 4.9 The movement of white stripe on the surface of complex part

4.2.2 Difference in the mold filling behavior between thermosetting and thermoplastic materials

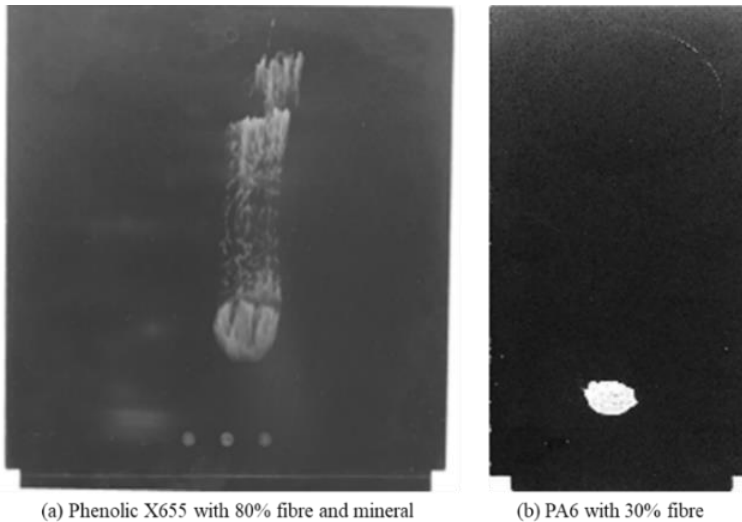


Figure 4.10 Difference in the flow behavior between thermosets and thermoplastics

The method of painting the wall surfaces of a mold was applied to thermoplastic injection molding to compare the movement of the phenolic melt and of a (wall sticking) thermoplastics melt on the cavity surface. Figure 4.10 shows a complete difference in the distribution of the white stripes on the surface of the molded parts made of thermoset phenolic resin and thermoplastic PA6 resin, respectively. For these thermoset phenolic injection molding, there is a strong slip between the phenolic melt and wall surface, which is not found for the injection molding of the PA6 with 30 percent of glass fiber. The factors which could lead to these differences are not only the influence of resin, high mold temperature but also the amount of fiber and filler. These opposite results help us to conclude that it is impossible to apply the thermoplastics injection molding concepts and rheological theory, simulation packages, respectively for thermosets. In addition, these differences will be leading to new thinking about influence of slip on calculation, analysis and simulation of fiber orientation during the filling process of the glass fiber reinforced thermoset resins injection molding compounds.

4.2.3 Mechanism of slip phenomenon between thermoset polymer and cavity surface

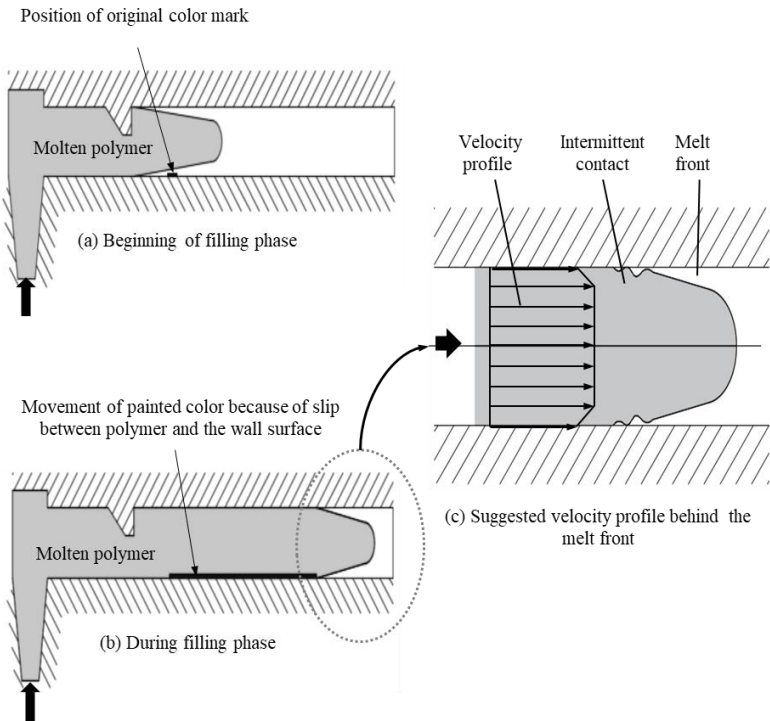


Figure 4.11 Mechanism of slip on the interface between phenolic resins and the wall surface in a rectangular cavity (a, b) and suggested velocity profile behind the melt front flow (c)

To summarize, mechanism of slip phenomenon of the phenolic melt is shown in Figure 4.11 (a) and (b). At the beginning of the filling phase the phenolic melt does not have contact to the wall surface so that there is no slip between the phenolic melt and the wall surface. The color stripes do not appear on the surface of incomplete molded parts in this case. As the cavity is filled with more polymer, there is contact between the phenolic melt and the wall surface. The wall slip starts immediately, leading to the movement of the color stripes on the surface of molded parts. As a result, velocity of the phenolic melt near to wall surface must be different from 0 and the mold filling behavior of these phenolic injection molding compound is plug-shear-flow, as shown in Figure 4.11 (c).

4.2.4 Wall contact of thermoset melts

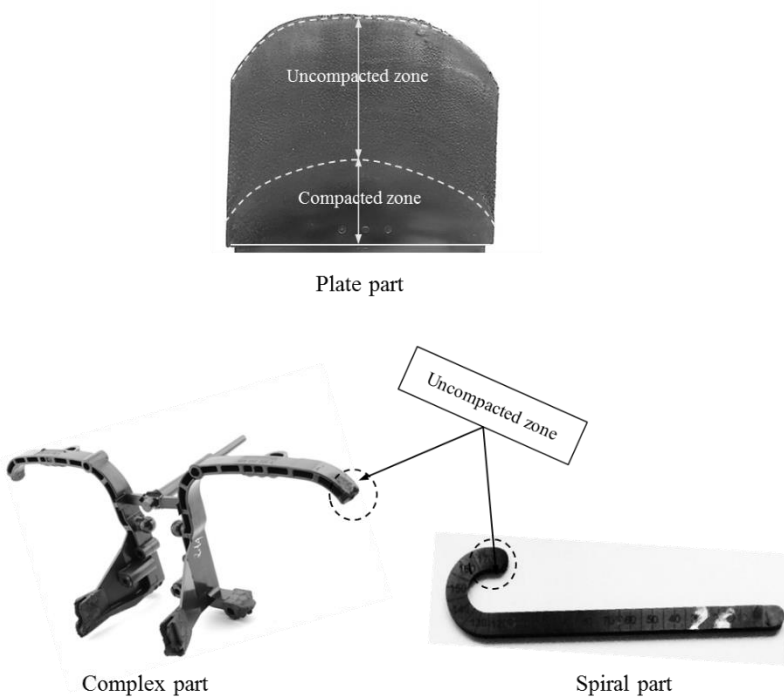


Figure 4.12 Uncompacted zone of injection-molded parts

It could be seen from Figure 4.12 that a series of the incomplete molded parts were molded by setting different metering strokes in the controls of injection molding machine. During the filling cavity, there are two different zones, including compacted zone and uncompacted zone. In compacted zone, the polymer has contact with the cavity surface while uncompacted zone the polymer has interrupted contact with the cavity surface. The length of uncompacted zone depends strongly on rheology of molded parts. It was clearly found on the surface of plate part. However, with spiral flow and complex part, the length of the thermoset polymer region that has interrupted contact with the cavity surface is very short.

4.2.5 Weld line formation of thermoset polymer

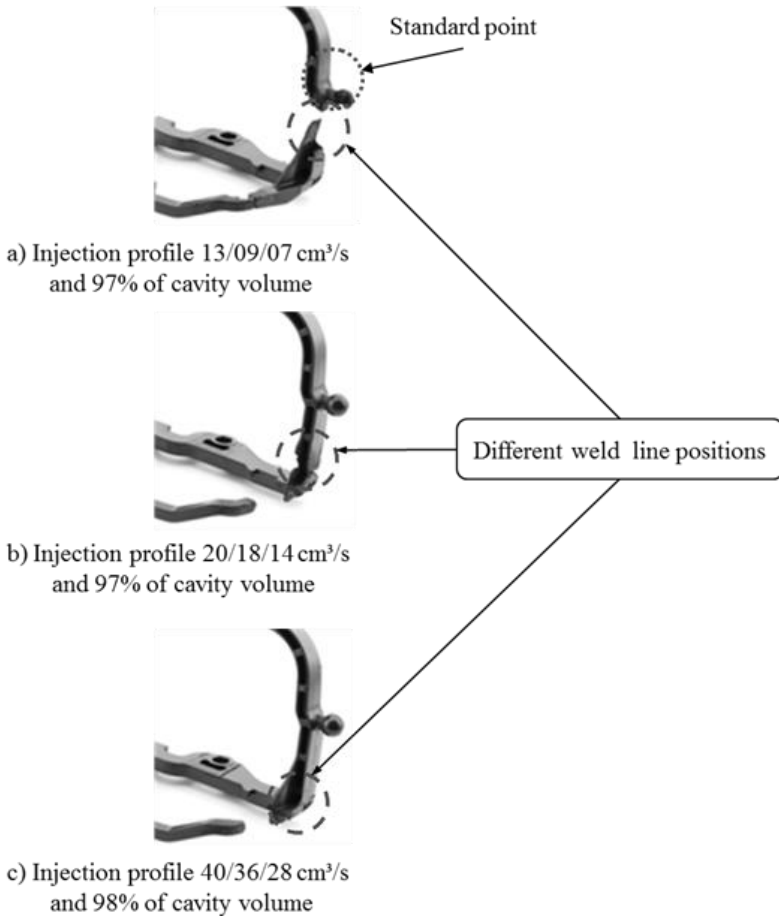


Figure 4.13 The weld line positions of different incomplete molded commercial parts

In polymer processing there are many primary situations where a polymer melt stream is separated and then reunited. The recombined areas are called weld-lines and they often show a weakness in mechanical properties as well as a distribution of the surface appearance of the molded or extruded part. With incomplete molded commercial injection parts, as shown in Figure 4.13, the positions of weld-line are different. It depends strongly on the injection speed profile. With

lowest injection speed profile, the position of weld line is near to the standard point. However, its position is far from the standard point with highest injection speed profile.

4.2.6 Degree of cure

Phenolic resins can be either resoles or novolacs type. Resoles are polymerized under alkaline environment and excess of formaldehyde. Furthermore, each phenol ring consists of one methyl group that gives the resoles their self-curing character. Under an acid environment and an excess of phenol, novolacs are polymerized, that are not self-curing. To start the curing reaction, a curing agent is

needed. Therefore, mostly hexamethylenetetramine is used [81, 82, 83] Hexamethylenetetramine hydrolyses at circa 120°C to form dimethylamine which finally acts as a hardener. Phenolic injection molding compounds are mainly novolac-based. The curing process runs in two steps. At first, when the temperature is more than 120°C, novolac reacts with dimethylamine under creation of methylene amine bridges. At temperatures above 170°C, the nitrogen-containing methylene amine bridges are transformed into methylene bridges. Both reaction steps lead to an elimination of ammonia (condensation product) [84, 85]. The curing of novolac can be monitored with differential scanning calorimetry (DSC) analysis. Both reaction steps show an exothermal character [86, 87, 88, 89, 90]. To calculate the real degree of cure of molded part during curing phase of injection molding process, it is also necessary to determine the residual reactivity of the injection- molded samples using the DSC. After being injected from the mold, samples of 10 mg were taken out from injected molded

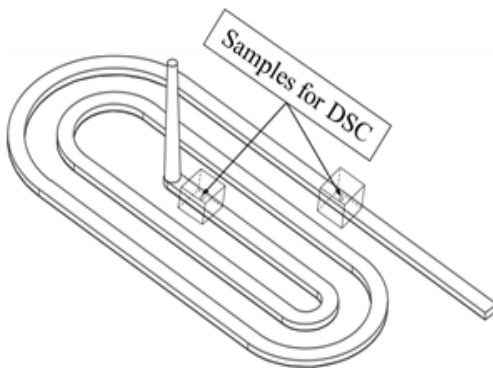


Figure 4.14 Positions of DSC specimens for measuring post degree of cure of molded part

part, as shown in Figure 4.14. These samples were used to measure the post degree of cure of molded part as shown in Figure 4.15.

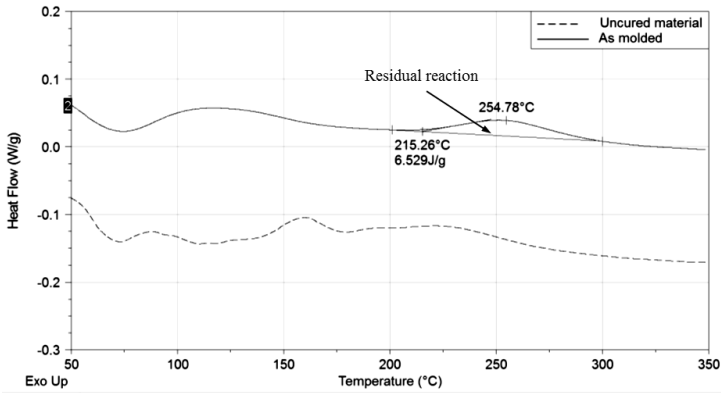


Figure 4.15 Vyncolit X655. DSC graph of uncured materials and injection-molded part. The real degree of cure of thermoset polymer during the filling and curing phase of injection molding process, as shown in Figure 4.16 could be calculated by applying following equation

$$\alpha_{real} = \frac{\Delta H_1 - \Delta H_2}{\Delta H_1} \cdot 100 \quad (4.1)$$

Where ΔH_1 is the heat of cure of uncured samples and ΔH_2 is the heat of cure of cured samples.

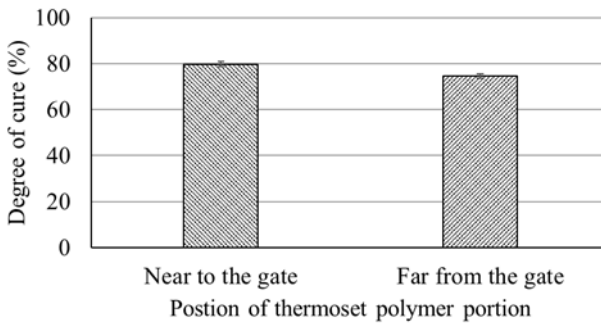


Figure 4.16 Degree of cure of Vyncolit X655 in the filling and curing phase

Generally, it could be seen from Figure 4.16 that the degree of cure of the molten polymer at the end of curing phase is around 80 %. It depends on location of polymer specimens for DSC scan. The polymer specimens near to the gate has a higher degree of cure in comparison with the polymer specimens far from the gate. The main reason leading to this phenomenon is the difference in the distribution of mold temperature. At different points on the surface of cavity the temperature is not equal. In addition, after being injected from the cavity, the surface temperature of the injection-molded part is more or less the same as the mold temperature and not equal to the environment. Therefore, it takes time for cooling the injection- molded part. During the cooling time chemical reaction inside the injection-molded part still occurs, which influences the accuracy of calculation the amount of the degree of cure of the injection-molded part during the curing phase of the injection molding process. The real value of the degree of cure of phenolic injection molding resin compounds in the curing phase should be lower than its value that is shown in Figure 4.16.

4.3 Summary of chapter

In this chapter, the thermal properties and viscosity of phenolic injection molding compounds were successfully measured and analyzed.

In the filling phase of thermoset injection molding process, for all processing conditions, which have been done, it was found that there is a strong slip on the interface between the phenolic polymer compound and the mold wall surface. The slip it believed to begin immediately when the phenolic melt contacts the wall surface.

Difference found between the slip phenomenon of thermosets and thermoplastics polymer on the cavity surface in the process of filling a mold help us to confirm that it is impossible to apply thermoplastics injection molding concepts such as fountain flow for explaining the mold filling behavior of thermoset injection molding compounds.

The mold filling study of different molded parts from simple to complex parts such as flow length, the calculated degree of cure has been done, which will be used in comparison with simulation results.

5 Creating thermoset material data for simulation process

In this content, based on experimental data including viscosity and curing data, numerical method was written to get all fitted parameters in cure kinetics and reactive viscosity model. These fitted parameters were employed to create material data sheet of thermoset injection molding compound. In addition, a numerical algorithm was developed and applied to predict mater curves of degree of cure and viscosity over temperature at multiple heating rates.

5.1 Modelling cure kinetics

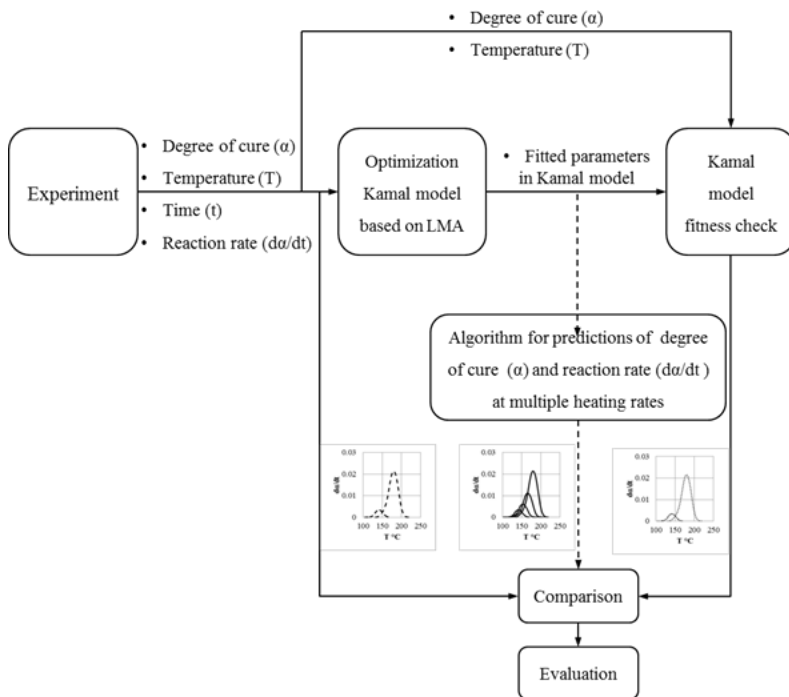


Figure 5.1 Schematic of fitting cure kinetics model based on experimental data and predictions of cure kinetics behavior at various heating rates

A process of creating cure data sheet of a thermoset resin based on experimental data illustrated in Figure 5.1. Experimental data and the LMA will be employed in writing a curing kinetics code to get fitted parameters in a cure kinetics model, namely, Kamal Model. After that a comparison of the experimental data and the fitted data will be conducted to evaluate the precision of numerical method. The fitting technique was tested in fitting the Kamal model based on DSC data of

Vyncolit X655 shown Figure 4.4. The fitted of Kamal model for all used heating rates are summarized in Table 5.1. A comparison between the experimental curves shown in dot lines and fitted curves illustrated in solid lines is found in good agreement, as shown in Figure 5.2.

Table 5.1 Fitted parameters in Kamal model

Phenolic material	Fitted parameters in Kamal model					
	m	n	$a_1(1/s)$	$a_2(1/s)$	$E_1(K)$	$E_2(K)$
Vyncolit X655	0.892	0.988	6.86e+08	5.06e+08	9.29 e+04	8.518e+04

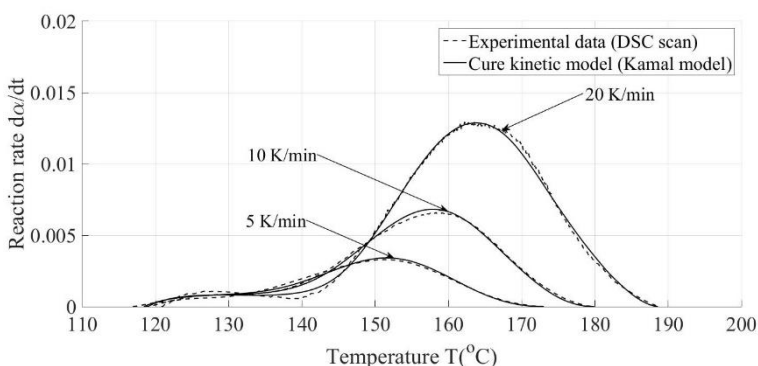


Figure 5.2 Vyncolit X655. Solid lines represent the fitted Kamal model and the dot lines represent the experimental data (DSC scans)

After having fitted parameters in the Kamal model, the reaction rate of Vyncolit X655 at heating rates of 5, 10 and 20 K/min was generated and shown in Figure 5.2. However, the master curves of reaction rate ($\frac{d\alpha}{dt}$) and degree of cure (α) at multiple heating rates has not yet been shown. By following the below mathematical analysis, a prediction code of the resin's behavior at multiple heating rates were written. Given a postulated function (functionally known as regression function) associated with certain parameters (considered unknowns) and a set of numerical experimental data, the primary purpose of the LMA is to find the parameter vector that best adapts the function to the obtained data. This is done by minimizing the sum of the squares of the differences between the function's outputs and that of the experiment. The set-up of the experiment involves data that are used as the input for the regression function; these are termed independent variables, while the output is functionally referred to as dependent variable. In our work, the LMA is employed to estimate the

parameters of the Kamal reaction model for a thermoset resin. If $\frac{d\alpha}{dt}$ is taken to be its output, then α and T are the input and thus the independent variables. However, since α and T in reality are closely correlated and the Kamal reaction model is a differential equation, there are implicit constraints that LMA may not be able to consider and might fail to fulfil. In particular, the fact that the definite integral of $\frac{d\alpha}{dt}$ wrt. t from $0 \rightarrow \infty$ must equal 1 is not guaranteed with the current implementation of the LMA. Moreover, while the function in the Kamal model is a 2-D function (since it has two independent variables, namely α and T), it is clear that the relation between α and T follows some S-shaped curve, as shown in Figure 4.3. Therefore, if the data were collected from an experiment with only one single heating rate, then the optimization would be rather locally done; in other words, the region for optimization would be quite limited, which negatively affects the accuracy of the outcomes. For these reasons, the experiment should be repeated at multiple heating rates to ensure a relatively significant region for optimization (in our experiment, three heating rates were tested). Doing so, on the other hand, could also lessen the degree of incorrectness due to the lack of consideration for the implicit constraints of the differential equation, as the surface generated by plotting $\frac{d\alpha}{dt}$ wrt. α and T is better curved to asymptotically conform to the dynamic behavior of the resin's rheological process.

Essentially, despite the fact that α and T are closely correlated, for simplicity they are regarded as independent variables for the fitness check of the LMA. To evaluate the performance of our work, first we tend to be oblivious of the relation between α and T , then take more meticulous care to analyze the predictions of the resin's behavior at other heating rates using the accumulation function, which numerically approximates the integration of $\frac{d\alpha}{dt}$ in a discretized way. The *raison d'être* of the first evaluation step is to observe the LMA's fitness for the parameter estimation given α and T as the independent input, while that of the second step is also to predict the behavior of both $\frac{d\alpha}{dt}$ and α wrt. T at different heating rates. The primary difference between these two steps is that step one assumes the existing samples of α associated with T acquired from the experiment, while step two finds them. It is natural that the oblivious method (i.e., step one) cannot make predictions because no experimental data is given at other heating rates. Finally, a comparison of the experimental data and predictions will be conducted to evaluate the precision of numerical method.

To the best of our knowledge, no closed-form solution has been found to compute the integral of $\frac{d\alpha}{dt}$ (from here on will be replaced by the symbol c for brevity), as

far as the Kamal reaction model is concerned. Therefore, the role of the accumulation function is to numerically calculate the integral of c wrt. T . Given the heating rate q , an array of temperature $T = [T_0, \dots, T_n]$, and the estimated parameter vector β of the Kamal equation (obtained from the LMA), the accumulation function is implemented to predict reaction rate and degree of cure of Vyncolit X655 over temperature at multiple heating rates. The result of predicted master curves is shown in Figure 5.3 and Figure 5.4. Reaction rate and degree of cure at multiple heating rates from 1 K/min to 40 K/min was successfully predicted and found in good agreement with experimental data.

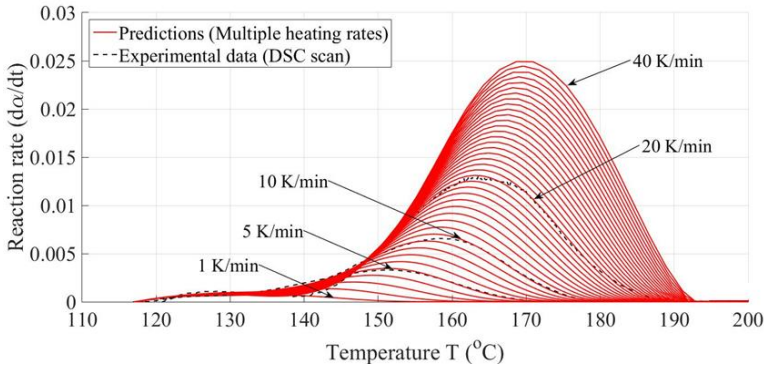


Figure 5.3 Vyncolit X655. Predicted reaction rate at multiple heating rates. The red solid lines represent predicted curves and the dot lines represent the experimental data (DSC scans)

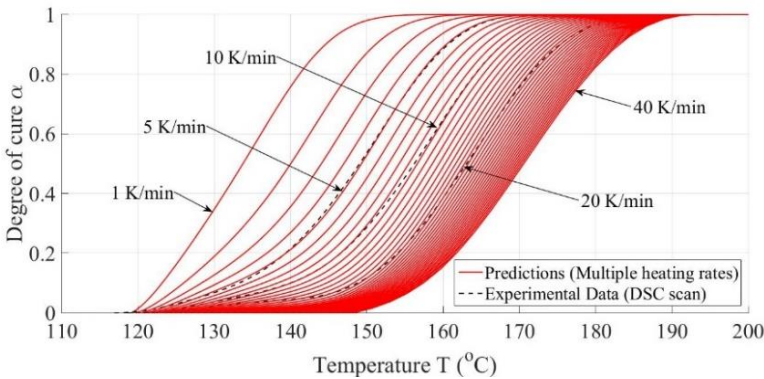


Figure 5.4 Vyncolit X655. Predicted degree of cure at multiple heating rates. The red solid lines represent predicted curves and the dot lines represent the experimental data (DSC scans)

This numerical method was applied to fit and predict the reaction rate and the degree of cure of some phenolic injection molding compounds including phenolic 6510 (GB 35, GF 20), phenolic 6680 (GB 35, GF 30), phenolic 1110 (GB35, GF 45) and another thermoset material (Epoxy EME-G760W of Sumitomo Bakelite Co., Ltd). The computations were found in good agreement with experimental results, as shown in Figure 5.5, Figure 5.6 and Figure 5.7, indicating that the written numerical algorithm for predictions master curves of degree of cure and reaction rate of thermoset injection molding compounds is useful.

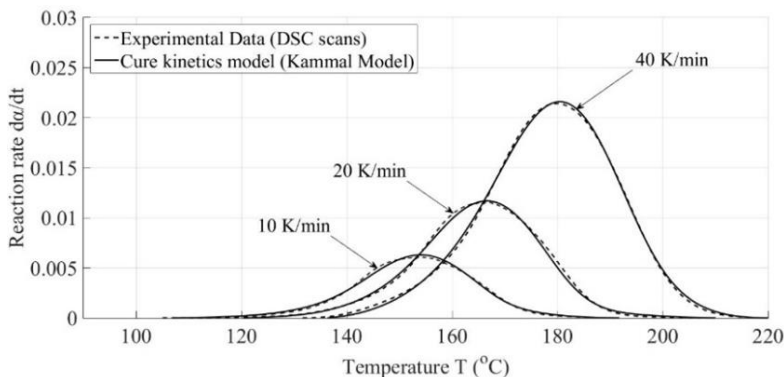


Figure 5.5 Epoxy EME-G760W. Solid lines represent the fitted Kamal model and the dot lines represent the experimental data (DSC scans)

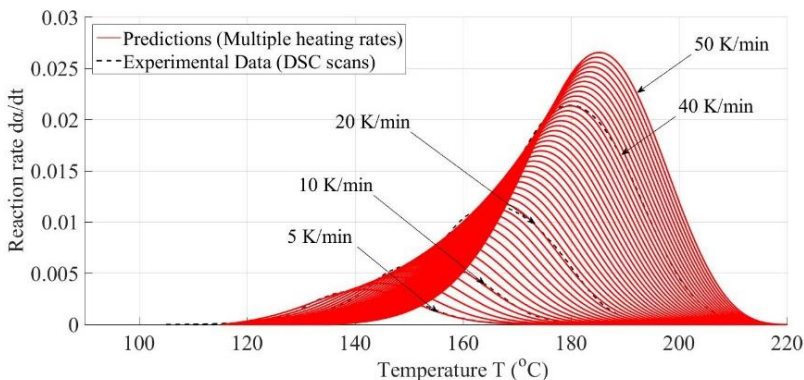


Figure 5.6 Epoxy EME-G760W. Predicted reaction rate at multiple heating rates. The red solid lines represent predicted curves and the dot lines represent the experimental data (DSC scans)

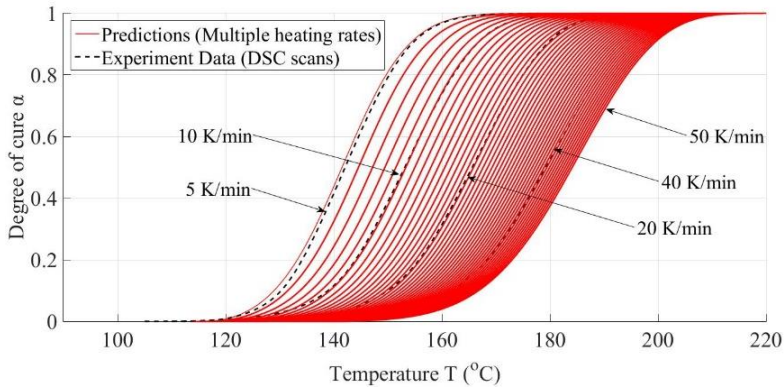


Figure 5.7 Epoxy EME-G760W. Predicted degree of cure at multiple heating rates. The red solid lines represent predicted curves and the dot lines represent the experimental data (DSC scans)

5.2 Modelling reactive viscosity

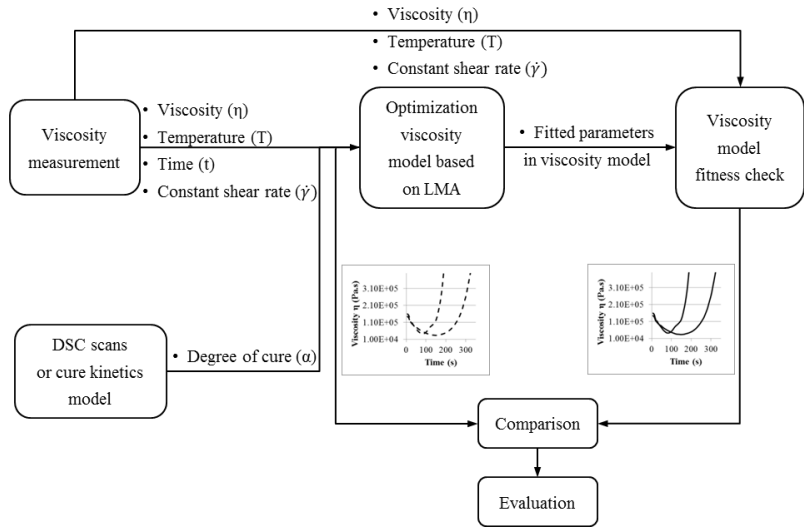


Figure 5.8 Schematic for fitting the reactive viscosity model based on experimental data

A process of fitting the reactive viscosity model based on experimental data is clearly shown in Figure 5.8. The fitted parameters in a reactive viscosity model (Cross-Castro-Macosko model) can as well be obtained based on the

experimental data using the LMA. After that, a comparison between the diagram of viscosity curve over time or temperature plotted from experimental data and the diagram of viscosity cure over temperature or time generated by the Cross-Castro-Macosko's model will be conducted to evaluate the precision of the fitting technique.

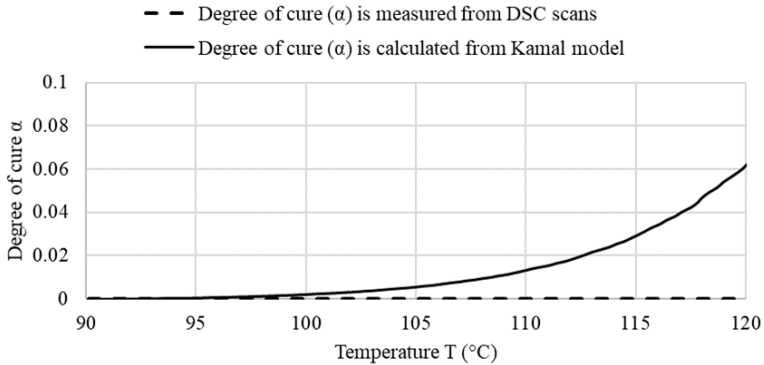


Figure 5.9 Vyncolit X655. A comparison between degree of cure measured by DSC scans and degree of cure calculated from Kamal model

The input experimental data used to fit a reactive viscosity model includes viscosity data over time, viscosity data over temperature, constant shear rate and the degree of cure (α). However, the degree of cure (α) is not measured during rheological measurements. Therefore, it is either measured by cure kinetics measurements or calculated from a cure kinetic model. In the case, the degree of cure (α) is measured by cure kinetic measurements, as shown in Figure 4.3, the curing process starts as temperature is more than 120°C. It means before reaching 120°C, the value of degree of cure (α) is 0. Therefore, the influence of degree of cure (α) at low range temperature (from 90°C to 120°C) on viscosity will not be considered during fitting a reactive viscosity model. Figure 5.9 displays a difference in the value of cure degree (α), which was measured by DSC scans and calculated from Kamal model. The value of cure degree (α) calculated from Kamal model is different from 0 after 90°C, which is not found in the plot of cure degree (α) measured by DSC scans. To solve this problem, the degree of cure calculated from Kamal model was used in fitting reactive viscosity model. A comparison of fitted curves and experimental cures was found in good agreement and shown in Figure 5.10. The fitted parameters of Cross-Castro-Macosko Model is summarized in Table 5.2.

Table 5.2 Fitted parameters of the Cross-Castro- Macosko-Model

Phenolic material	Fitted parameters of Cross-Castro- Macosko-Model						
	α_g	c_1	c_2	B (Pa. sec)	T_b (K)	n	τ^* (Pa)
Vyncolit X655	0.7	6.22	-5.05	1.7e+05	1.49e+04	0.432	2.8e-09

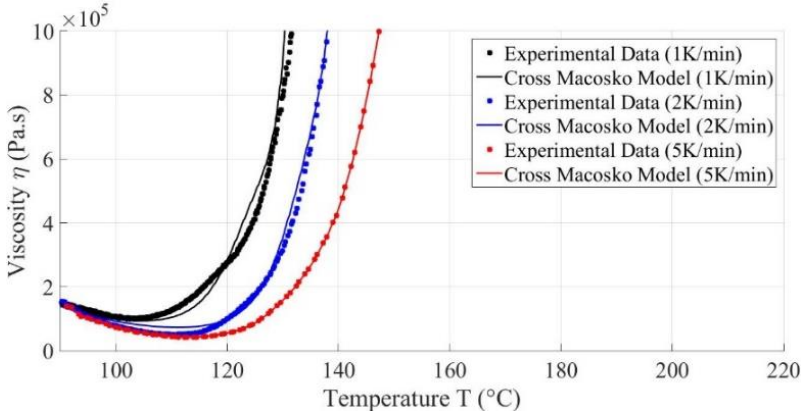


Figure 5.10 Vyncolit X655. Fitting reactive viscosity model based on experimental data

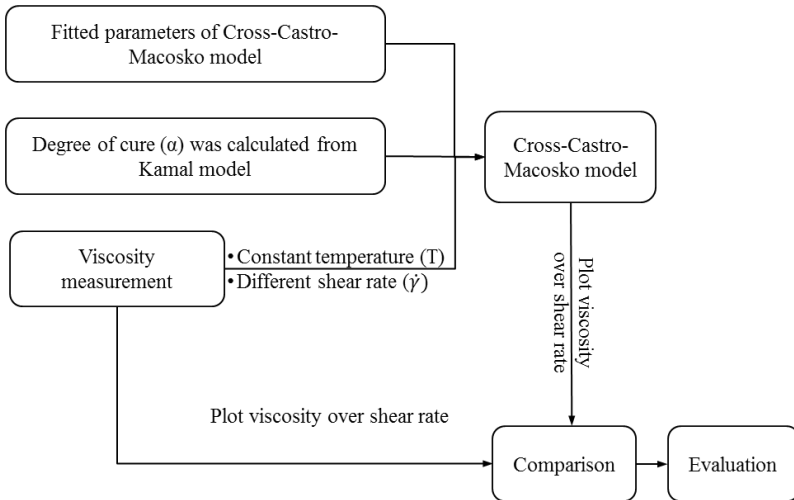


Figure 5.11 Schematic for fitting viscosity of thermoset materials over shear rate

During fitting process, as shown in Figure 5.8 the shear rate was kept constant. Therefore, the viscosity depends on only two factors, including temperature and degree of cure. The shear rate dependence of viscosity has not yet been considered. To be sure that fitted parameters in the reactive viscosity model (Cross-Castro-Macosko model) generated by numerical method shown in Figure 5.8 are fit to different shear rates. The all fitted parameters of Cross-Castro-Macosko model obtained in Figure 5.8 along with degree of cure calculated from Kamal model, experimental viscosity data shown in Figure 4.2 will be substituted into Cross-Castro-Macosko model to calculate viscosity distribution over shear rate, as shown in Figure 5.11. Finally, the comparison between viscosity over shear rate generated by Cross-Castro-Macosko model and measured by rheological tests will be conducted, as shown in Figure 5.12.

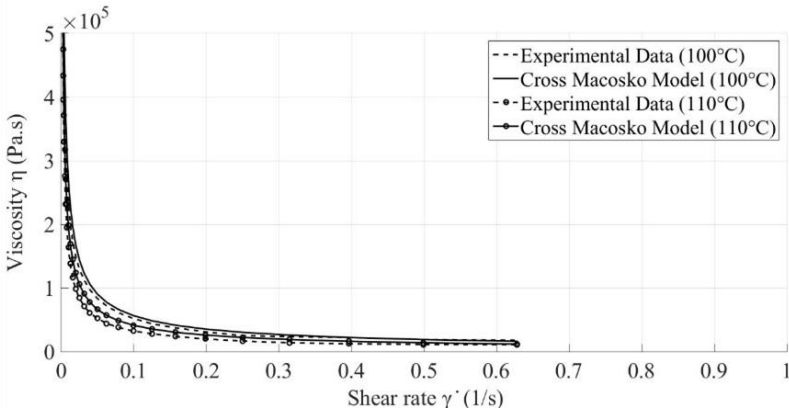


Figure 5.12 Fitted viscosity curves over shear rate

It could be seen from Figure 5.12 that the computation is found in remarkable agreement with the experimental results, indicating the accuracy of numerical method for finding fitted parameters of Cross-Castro-Macosko model summarized in Table 5.2. These fitted parameters are not only true in case of constant shear rate but also accurate in condition of various shear rates.

5.3 Prediction of viscosity

There are three main factors that influences on viscosity of thermoset injection molding compounds. Therefore Cross-Castro-Macosko model, as shown in Eq. (2.3) could be written in the following way:

$$\eta_{real}(T, \dot{\gamma}, \alpha) = \eta(T, \dot{\gamma}) \cdot A(\alpha) \quad (5.1)$$

With

$$\eta(T, \dot{\gamma}) = \frac{\eta_0(T)}{1 + \left(\frac{\eta_0(T) \cdot \dot{\gamma}}{\tau^*} \right)^{1-n}} \quad (5.2)$$

$$A(\alpha) = \left(\frac{\alpha_g}{\alpha_g - \alpha} \right)^{(c_1 + c_2 \alpha)} \quad (5.3)$$

And degree of cure (α) in Eq.(5.3) is calculated from a cure kinetics model such as Kamal model, as shown in Eq.(2.4) $\frac{d\alpha}{dt} = (k_1 + k_2 \alpha^m)(1 - \alpha)^n$.

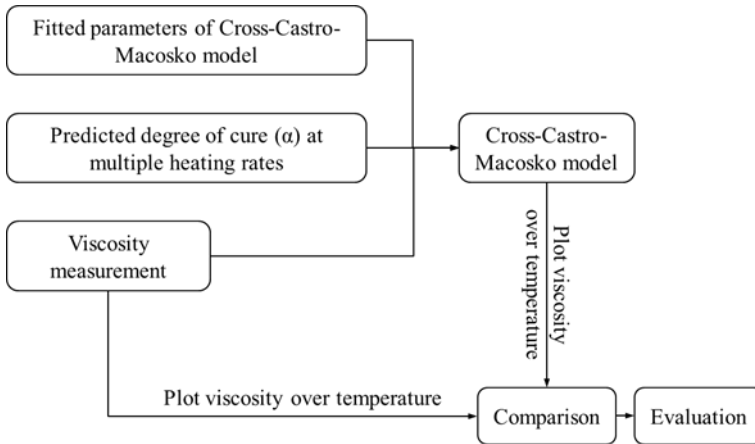


Figure 5.13 Schematic for predictions of viscosity of thermoset materials over temperature at multiple heating rates

By using the numerical method written and introduced in section 5.2, the viscosity curves of Vyncolit X655 at heating rates of 1, 2 and 5 K/min generated from Cross-Castro-Macosko Model was shown in Figure 5.10 . However, the master curves of viscosity over temperature at multiple heating rates has not yet been predicted. Therefore, a numerical algorithm for prediction of thermoset resin's viscosity behavior over temperature at multiple heating rates will be developed. The idea for writing prediction code in this case is to write a new numerical method that shows a link between two models. The first model is Cross-Castro-Macosko Model summarized in Eq. (5.1) and the second model is Kamal model, as shown in Eq. (2.4). A schematic of writing a code to predict

viscosity of thermoset materials over temperature at various heating rates is shown in Figure 5.13. Firstly, the fitted parameters in Cross-Castro-Macosko Model found in section 5.2 and the predicted degree of cure over temperature at multiple heating rates, as shown in section 5.1 are substituted into the reactive viscosity model (Cross-Castro-Macosko Model) as shown in Eq. (5.1). As a result, viscosity over temperature at specific heating rate is predicted. After that the comparison between viscosity over temperature generated by reactive viscosity model and measured by rheological tests is conducted to evaluate the accuracy of prediction of viscosity over temperature.

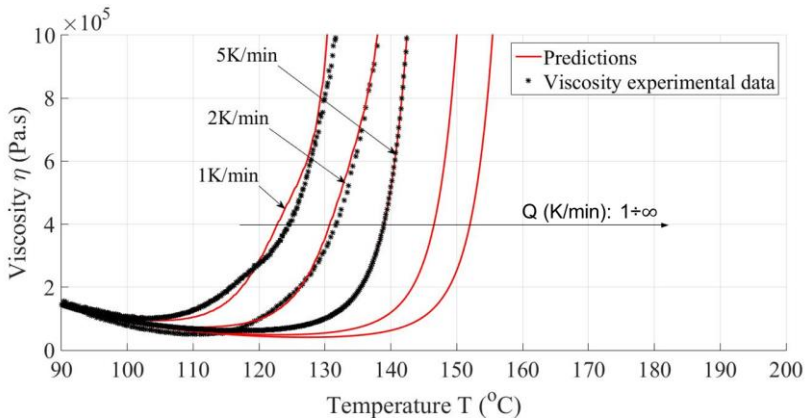


Figure 5.14 Vyncolit X655. Predicted master curves of viscosity at multiple heating rates

This numerical technique was applied in prediction of viscosity over temperature of Vyncolit X655 at multiple heating rates, as shown from Figure 5.14. Rheological tests were conducted under heating rates of 1, 2 and 5 K/min only while master curves of viscosity at any heating rate was predicted. A good agreement in comparison between predicted curves of viscosity and experimental curves is found, indicating that written prediction code is reasonable.

To evaluate the accuracy of the developed numerical method, the written code for prediction of master curves of viscosity was applied to predict the viscosity of some phenolic injection molding compounds including phenolic 6510 (GB 35, GF 20), phenolic 6680 (GB 35, GF 30), phenolic 1110 (GB35, GF 45). A good prediction result is shown in Figure 5.15.

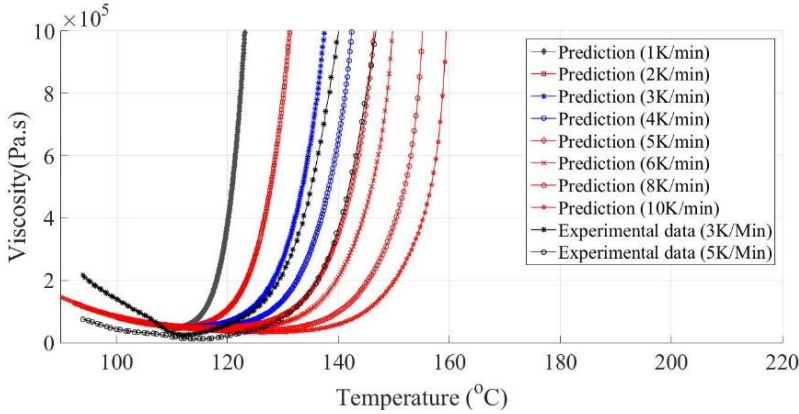


Figure 5.15 Phenolic 6510. Predicted master curves of viscosity at multiple heating rates.

5.4 Summary of chapter

A numerical method was written and applied to create material data sheet of thermoset injection molding compounds. The generated material data sheet of Vyncolit X655, which includes thermal conductivity data, heat capacity data, a cure kinetics model and its fitted parameters, a reactive viscosity model and its parameters will be directly imported into a simulation tool to simulate the filling and curing phase of thermoset injection molding.

Furthermore, in this chapter, the algorithm was developed to predict successfully master curves of cure kinetics and viscosity of thermoset resins at multiple heating rates. A remarkable agreement was found in comparison between predicted master curves and experimental curves.

6 Simulation model

The filling and curing process of Vyncolit X655 injection molding compound was simulated by using Moldex3D R15 simulation tool from CoreTech.

6.1 Characteristics of Moldex3D simulation tool

6.1.1 Meshing and numerical methods

The evolution of mesh techniques, as shown in Figure 6.1, started from the lay-flat method in the 1970s. Then, the 2.5D, called midplane, and shell methods were developed in the 1980s, followed by the quasi-3D and dual domain models in the 1990s, until the true 3D mesh models arrived in the 2000s. Because of the enormous growth of computational performance of computers, the number of mesh grids that can be processed has increased significantly. In theory, the 3D approach produces more accurate results.

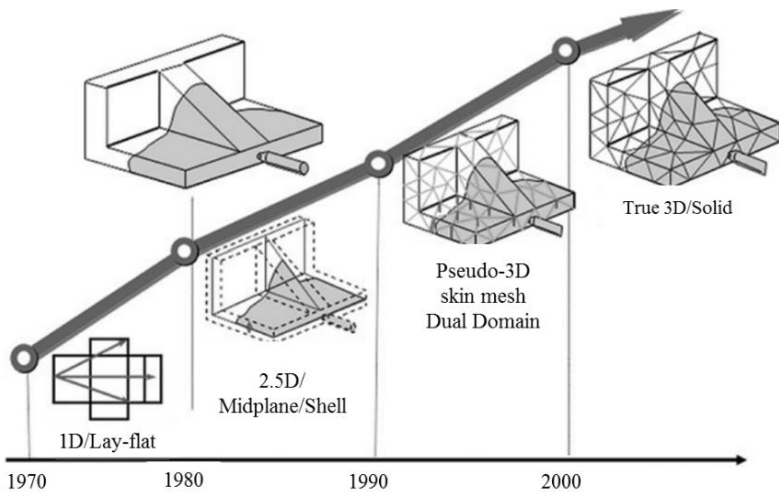


Figure 6.1 Brief history of mesh models for simulation [67]

After the layflat method, Cornell developed the 2.5D thin-shell mesh technique in the Cornell Injection Molding Program (CIMP), as shown in Figure 6.2. The basic assumption is to simplify a 3D model into 2.5D one and to take the geometric middle plane as the calculation elements. The theoretical basis of this 2.5D mid-plane method comes from the Hele-Shaw equation [91] (or generalized

Hele-Shaw). The theory utilizes the feature that the cavity of the injection mold is thinner in the direction of thickness and ignores the pressure gradient in the direction of thickness, that is, a simplified 2D pressure Poisson equation is used for the conservation of mass and momentum. For the conservation of energy, although the thermal convection in the direction of thickness and the thermal conduction in the flow plane are neglected, the 3D changes of the temperature in the system still have to be considered. As a result, the entire system is simplified into a problem of 2D pressure field coupled with a 3D temperature field, and thus it is called “2.5D.”

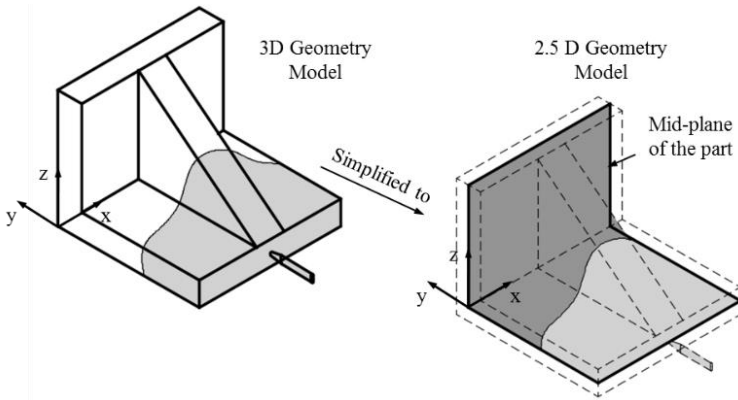


Figure 6.2 2.5D/midplane and shell [64]

The numerical methods appropriate for solving a 2.5D problem are FEM, which is used to solve the pressure equations, and FDM, which is used to deal with the temperature field in the direction of thickness. However, in certain flow areas as shown in Figure 6.3(a), in certain flow areas such as the injection flow area at the melt front, T-shaped areas like ribs, or where there is a sudden change in thickness, the assumption that ignores the pressure in the direction of thickness in Hele-Shaw equation becomes false and would generate errors to a certain degree. These errors can be very influential to predictions of fiber-reinforced plastics, because movements of these fibers, such as twists and turns in the 3D space, have to be considered. As shown in Figure 6.3(b), the 2.5D model cannot predict the out-of-plane direction of fiber orientation precisely in the zones with thickness change. In addition, the thermal convection in the direction of thickness and the thermal conduction in the flow plane are ignored due to the assumption of a Hele-Shaw flow. The 2.5D model does not provide a complete picture for

parts with inserts or pores where side-wall heat conduction can be significant. Another problem of the 2.5D approach is the creation of the midplane model from the 3D part, which is usually very time consuming.

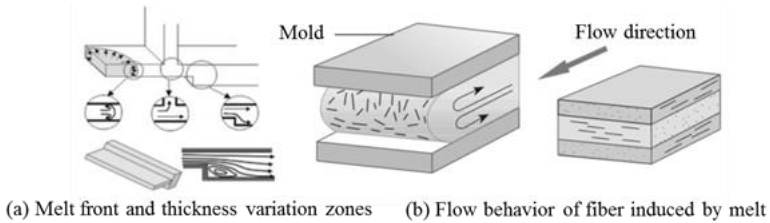


Figure 6.3 Limitations of 2.5D approach [92]

Simple as it may be, the dual domain method still has a risk when it comes to parts that are difficult to define the thickness. Errors such as discontinuity of melt may also occur with the dual domain method due to the connector approach. In comparison, only the true 3D mesh can produce correct simulation results.

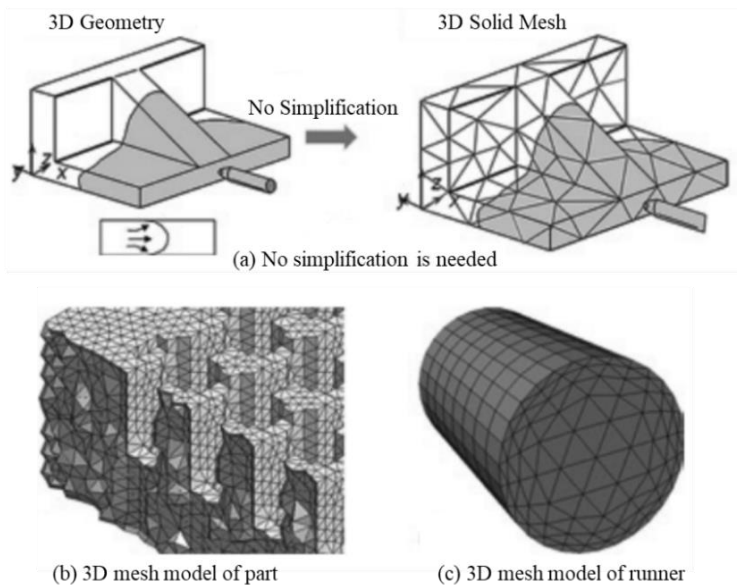


Figure 6.4 True 3D/solid model [92]

Of the evolved mesh techniques up to now, the 3D mesh model is still the most accurate method because it requires no geometrical simplification, as shown in

Figure 6.4 , and the governing equations (see section 2.2.2) describe exactly the 3D space of the system. By building products and runners using the 3D mesh model as shown in Figure 6.4 (b)-(c) the simulation results can be closer to the real situation. The key to the use of this meshing method is the solver's stability and performance.

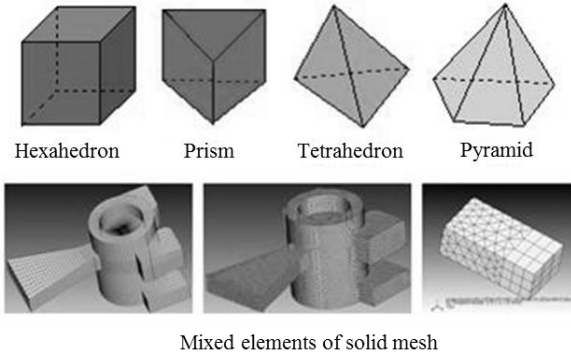


Figure 6.5 Geometry of solid model (3D elements)

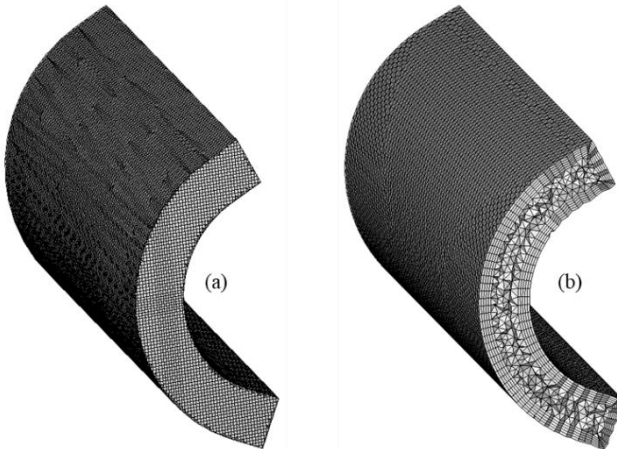


Figure 6.6 Meshing technology; (a) Traditional meshing method and (b) BLM method with generated multiple layers (5 layers) inward from the surface mesh [92]

In Moldex3D the following three-dimensional types of mesh are basically used: hexahedron, prism, pyramid, and tetrahedron, as shown in Figure 6.5. With increased demands for superior product quality and faster time-to-market, Moldex3D rolled out the new pre-processing module-Designer BLM (Boundary

Layer Mesh), which can help advanced users to generate multiple layers of prismatic meshes inward from the surface mesh and then filling up the remaining space with tetrahedral mesh, as shown in Figure 6.6 (b). BLM can precisely capture the drastic changes of temperature and velocity near these cavity wall during the filling process and could help users can accurately detect viscous heating and warpage problems in advance. Up to now, the supported mesh types in BLM are including tetra and 1÷5 layers BLM. As result, the solid mesh has minimum 2 layers across the thickness direction and can be increased up to 10 layers for higher accuracy requirements.

With Moldex3D simulation tool, the numerical method for solid/eDesign model is a High Performance Finite Volume Method (HPFVM) proposed by Chang any Yang [93] instead of FEM. The Finite Volume Method (FVM) due to its robustness and efficiency is used in this study to solve the transient flow field in three dimensions [92].

6.1.2 Slip boundary condition

Boundary conditions are quite specific to injection molding, which should be applied to conversions equations. Boundary conditions include the surface through which melt enters the cavity, the edge of the mold, the top surface of the mold, the bottom surface of the mold and the wall slip condition.

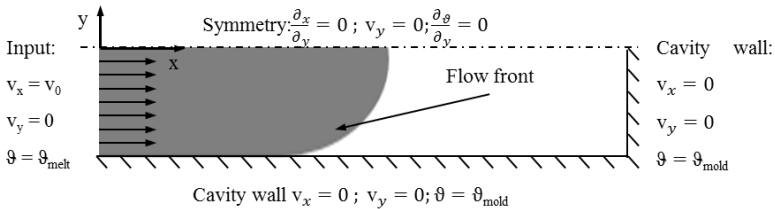


Figure 6.7 No-Slip boundary conditions for a filling simulation of a rectangular cavity

In general, the effect of wall slip on the cavity surface is ignorable during injection molding simulation process. At the inlet constant velocity and temperature of the melt are given; no slip condition and a constant mold temperature are imposed on the wall; the flow front is fraction free, at the symmetry line symmetry conditions are applied (Figure 6.7). However, with thermoset phenolic injection molding, there is a strong slip between the thermoset phenolic melt on the cavity surface. As a result, velocity of the phenolic melt near to wall surface must be different from 0 and the mold filling

behavior of these phenolic injection molding compound is plug-shear-flow instead of fountain flow like thermoplastics. Assumptions of neglecting the influence of wall slip on the mold filling characterization of the thermoset phenolic injection molding compounds during simulation process is not ignorable. Currently, with simulation tool Moldex3D users could take the influence of wall slip boundary condition (wall slip BC) on the flow behavior into account by two ways. Firstly, users might specify the wall shear stress threshold and the friction coefficient while setting the wall slip boundary condition. Friction coefficient is a dimensionless parameter. The friction coefficient indicates the relations between flow field, frictional drag, and wall shear stress threshold. The value of frictional coefficient can be set from 0 to 1. The wall shear stress threshold with unit of MPa means the critical shear stress at the moment when the flow behavior switches from non-slip to slip and the value of wall shear stress threshold is various from 0 to 1 MPa. The influence of the frictional coefficients and wall shear stress threshold on the onset of slip is shown in Figure 6.8.

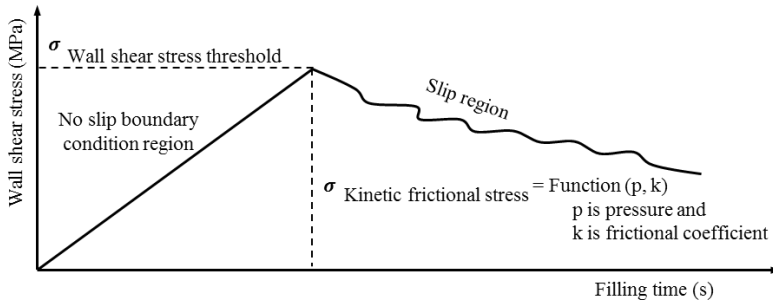


Figure 6.8 Wall slip boundary condition [92]

$$\begin{aligned}
 u_s &= 0 \text{ if } \sigma < \sigma_c \\
 u_s &= a \cdot \sigma^m \text{ if } \sigma > \sigma_c
 \end{aligned}
 \tag{6.1}$$

Secondly, another way to take the influence of slip boundary condition on flow behavior of polymer in the cavity during injection molding simulation is to implement directly the commonly mathematical slip model developed by Mooney [94, 95, 96] into the numerical model. The slip model in Eq.(6.1) shows the dependence of the slip velocity on shear stress.

6.2 Filling and curing phase simulation

6.2.1 Importing generated material properties

Material data sheet of thermoset injection molding compound, Vyncolit X655, is not found in material data bank of simulation tool Moldex3D. To simulate flow behavior during filling cavity and curing process, the first necessary step is to import material data sheet of Vyncolit X655 that was created in Chapter 5 into material data bank of Moldex3D. After importing in material data bank of Moldex3D, the influence of temperature viscosity of Vyncolit X655 and on degree of cure (conversion) is shown in Figure 6.10 and Figure 6.9, respectively.

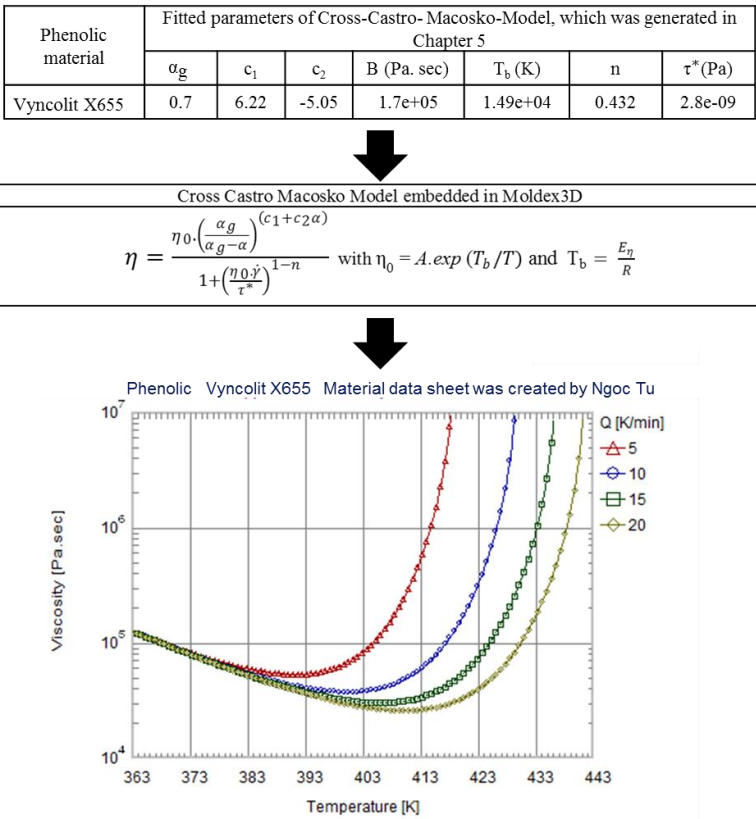


Figure 6.9 Importing generated reactive viscosity data sheet of Vyncolit X655 that was summarized in Table 5.2 into Cross-Castro Macosko Model embedded in Moldex3D

Phenolic material	Fitted parameters in Kamal model, which was generated in Chapter 5					
	m	n	a ₁ (1/s)	a ₂ (1/s)	E ₁ (K)	E ₂ (K)
Vyncolit X655	0.892	0.988	6.86e+08	5.06e+08	9.29 e+04	8.518e+04



Kamal model embedded in Moldex3D
$\frac{d\alpha}{dt} = (K_a + K_b \cdot \alpha^m) \cdot (1 - \alpha)^n$ <i>with</i> $K_a = A \cdot \exp\left(\frac{-T_a}{T}\right)$; $K_b = B \cdot \exp\left(\frac{-T_b}{T}\right)$; $T_a = \frac{E_a}{R}$; $T_b = \frac{E_b}{R}$

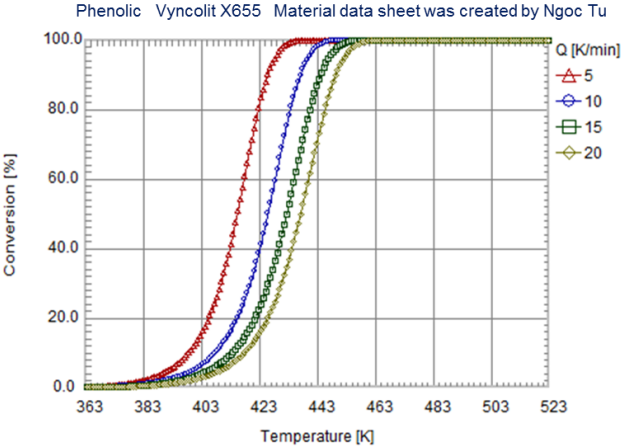


Figure 6.10 Importing generated cure kinetics data sheet of Vyncolit X655 that was summarized in Table 5.1 into Kamal Model embedded in Moldex3D

It can be seen that with only one value of fitted parameters in Cross Castro Macosko model and Kamal model, viscosity over temperature and degree of cure (conversion) at multiples heating rates was predicted by Moldex3D. These predicted curves are found similar to master curves of the viscosity and degree of cure over temperature at multiple heating rates that were generated and shown in Figure 5.14 and Figure 5.4 of Chapter 5. This similarity indicates that the numerical method for creating thermoset material data which was developed and described in Chapter 5 is a relevant scientific method.

6.2.2 Study cavities and sensor nodes

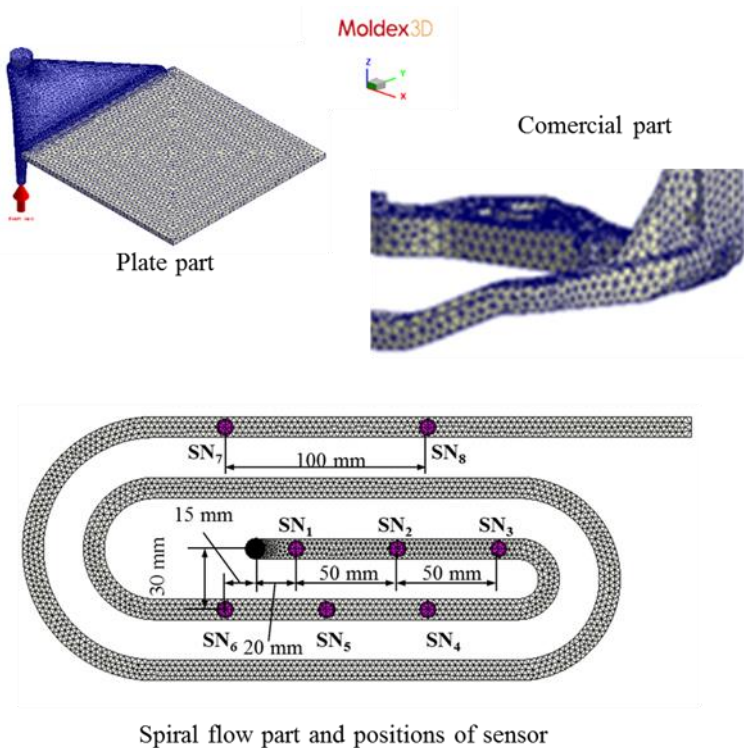


Figure 6.11 Mesh model of the components with runner system and sensor nodes

Study objects for simulation process were plate part, spiral flow part and commercial part that were used to do injection molding experiments in chapter 3. The mesh model of the components with runner system built in Moldex3D is shown in Figure 6.11. With the plate part, the volume of sprue and cavity is 150 cm^3 , the flow length is 150 mm and the number of elements is 403456. With the spiral part, sensor nodes were set in the meshing step. The total number of elements is 434613. The volume of sprue is 57 cm^3 and the cavity is 3.5 cm^3 . The flow length is 1385 mm. With the commercial part, the number of elements is 2676885, the volumes of sprue and the cavity are 109 cm^3 and 6 cm^3 , respectively.

6.2.3 Simulation procedure

The filling and curing phase of plate part, spiral flow part and commercial part were simulated respectively. The simulation processing conditions for each part is the same process conditions summarized in Table 3.2, Table 3.3 and Table 3.4 of Chapter 3. During simulation process, slip and no slip boundary condition is considered. Unfortunately, the value of frictional coefficient and shear stress threshold has not been yet measured, although there is a strong slip between the phenolic melt and wall surface. Therefore, reverse engineering method was employed, which means the injection molding experimental results, including flow length of incomplete molded part, positions of weld line, the melt pressure during filling the cavity simulation was used in comparison with the corresponding filling patterns and the melt pressure results predicted by simulation. In this case, simulation was done with slip boundary condition by choosing different values of frictional coefficient and shear stress threshold. These comparisons will be shown in the next chapter, which shows that with frictional coefficient of 0.5 and wall shear stress threshold of 0.09 MPa, the agreement appears remarkable. From this point to forward the frictional coefficient of 0.5 and wall shear stress threshold of 0.09 MPa will be used to discuss the filling and curing results.

6.3 Simulation results

6.3.1 Predicted melt front and position of weld line

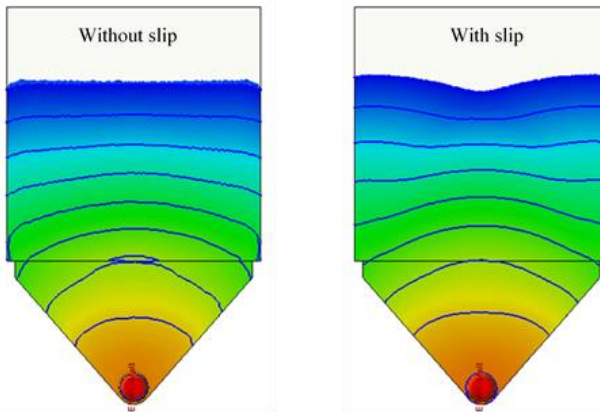


Figure 6.12 The profiles of melt front at current time in filling phase without and with considering wall slip impact

A fill analysis calculates the flow front that grows through the part incrementally from the injection location and continues until the velocity/pressure switch-over point has been reached. It could be seen from Figure 6.12 that with the same volume that was injected into the cavity, there is slight difference in the profile of melt front of plate molded part. However, with complex part, the influence of slip boundary condition on the profile of melt front and weld line position is more significant, as shown in Figure 6.13.

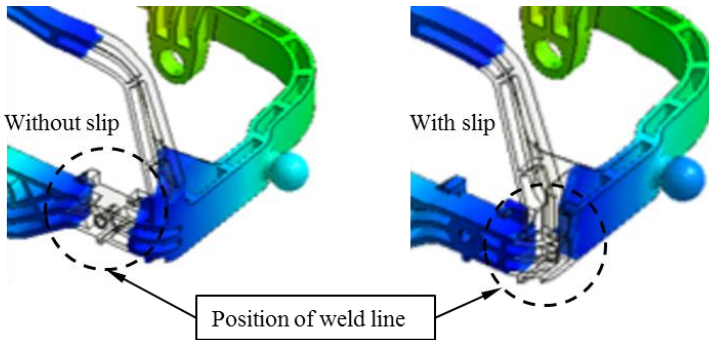


Figure 6.13 Predicted weld line position without and with considering wall slip impact

The difference in positions of weld line is because of changing frictional coefficient between polymer and cavity surface. Normally, with fountain flow term (without slip condition) and in the flow direction, when the polymer has a contact with the wall surface, it will stick on the cavity surface. Therefore, the velocity of polymer at the cavity surface is 0. Nevertheless, with plug flow (with slip condition) the velocity of polymer at the cavity surface is not 0. Due to the difference in velocity at the layer that has contact with the cavity surface and the geometry of cavity, the flow profile of the complex molded part is various, leading to disagreement in the positions of weld line. To prove this statement, simulation of the complex molded part was done with the same slip boundary condition but difference in injection speed. The predicted weld line position appears differently. It depends strongly on the injection speed. With lower injection speed, the weld line position is found far from to the corner A while it is near to the corner A with higher injection speed, as shown in Figure 6.14.

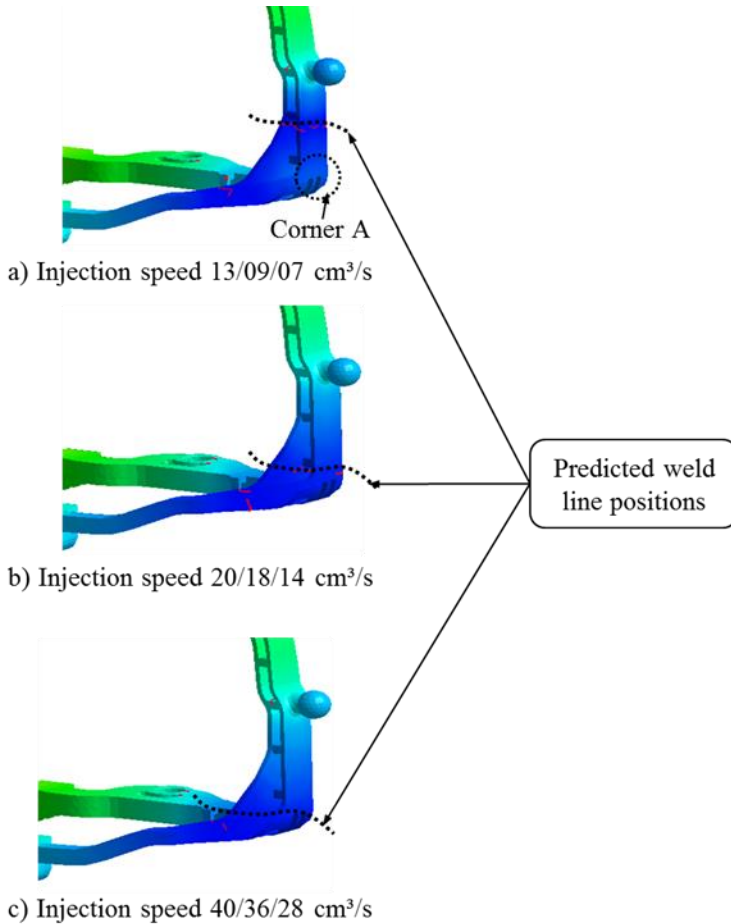


Figure 6.14 The dependence of weld line positions on injection speed

6.3.2 Predicted filling results

By simulation tools, users can set sensors on the interface between polymer and wall surface, as and even inside the injection molded part to observe the filling results, shown in Figure 6.11. Viscosity is one of the most important properties in fluids which can be considered as the resistance of flow. In general, viscosity of Vyncolit X655 thermoset melt decreases during filling the cavity. At the specific current filling time, for instance, at 2.5 s (VP-Switch point) in the filling

phase, viscosity of polymer portion that is near to the gate is higher than the polymer position far from the gate, as shown in Figure 6.15. This phenomenon is because of dependence of viscosity on shear rate, degree of cure and temperature. During the filling phase, the filling time is too short so that the degree of cure is very small as shown in Figure 6.16. Therefore, the viscosity degree of cure dependence could be ignorable, which means that mainly the influence of temperature and shear rate on viscosity should be considered.

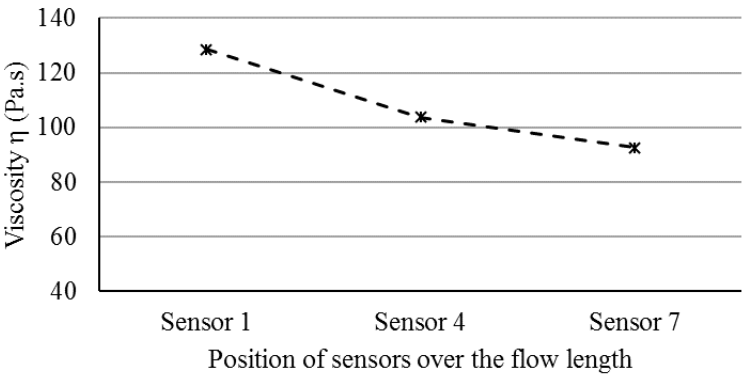


Figure 6.15 Viscosity of the molten Vyncolit X655 at the current filling time of 2.5 s

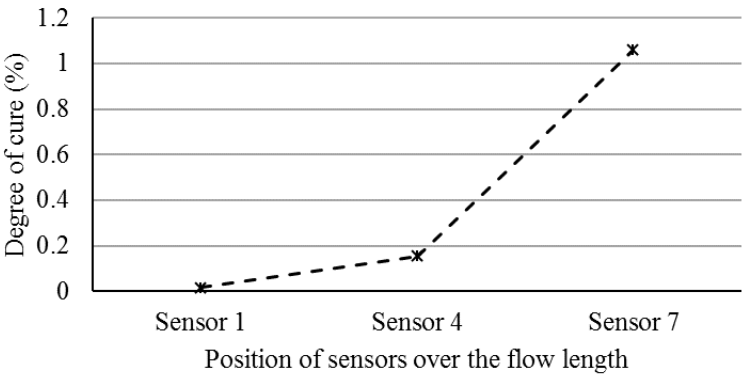


Figure 6.16 Degree of cure of the molten Vyncolit X655 at current filling time of 2.5 s

The temperature of the thermoset melt inside the cavity varies because of three reasons. Firstly, the shear heating or frictional heating, which is caused by

friction between adjacent laminas moving at different speeds. Secondly, the heat transfers from the cavity wall to the polymer. Finally, the heat generated by chemical reaction between substances inside thermoset injection molding compounds.

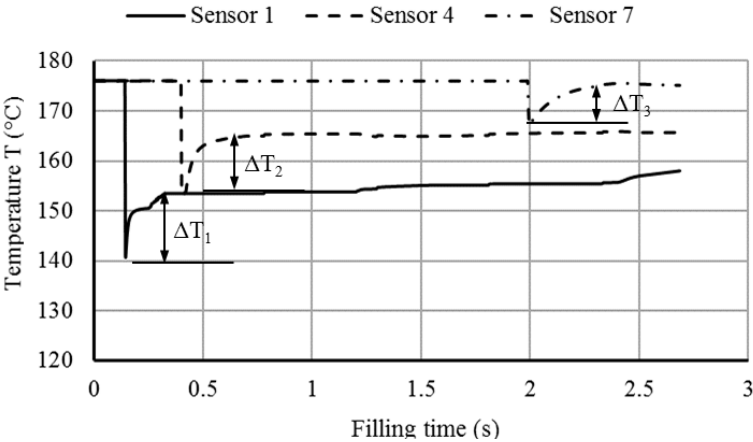


Figure 6.17 Temperature profile of the molten Vyncolit X655 during the filling phase

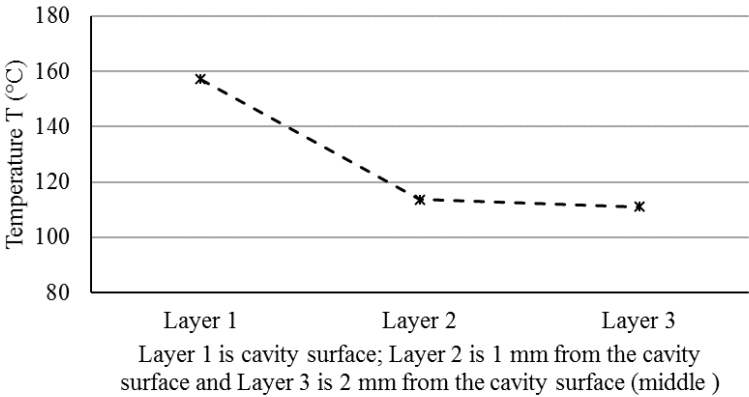


Figure 6.18 Temperature of the molten Vyncolit X655 at the same position (sensor 1) but in different layers via the thickness section and at the current filling time of 2.5 s

Temperature variation of the thermoset phenolic melt in the filling phase that was observed by using temperature sensors, as shown in Figure 6.17. After leaving screw, nozzle and runner, the polymer flows into the cavity and reaches the location of sensor 1. It could be seen from the temperature curve of sensor 1 that before a significant decrease in the temperature profile from the mold temperature of 175°C to 140°C because at the beginning of contact the temperature of polymer is lower than the temperature of cavity surface, there is a quick increase in the temperature of polymer melt due to heat transfer from the hot cavity to the polymer, followed by a slightly grow up until at the end of filling. The similar way in the temperature distribution of thermoset polymer is found in the temperature curves generated by sensor 4 and sensor 7, respectively. However, the temperature gradient of sensor 4 ($\Delta T_2 = 11^\circ\text{C}$) is lower than the temperature gradient of sensor 1 ($\Delta T_1 = 13^\circ\text{C}$) and higher than the temperature gradient of sensor 7 ($\Delta T_3 = 7^\circ\text{C}$). This is because of difference in residence time of the thermoset melt inside the cavity. The higher residence time of the thermoset melt inside the cavity, the higher heat transfer from the hot cavity to the polymer is the occurring, leading to the higher temperature of the polymer. At VP-Switch point the temperature of polymer portion that was calculated via sensor 1, sensor 4 and sensor 7 is 157°C, 166°C and 175°C, respectively. In addition, the temperature distribution of polymer at different layers via the thickness section was calculated, as shown in Figure 6.18. The highest temperature is found as expected in the cavity surface (layer 1), follow by layer 2 and layer 3.

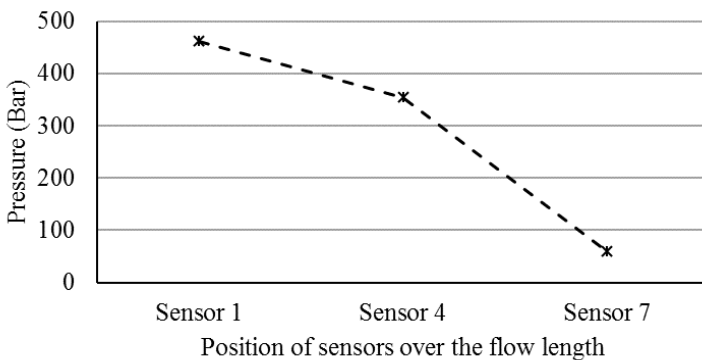


Figure 6.19 Pressure of the molten Vyncolit X655 at the current filling time of 2.5 s

During simulation process, the variation of polymer temperature leads to the difference in viscosity of polymer melt. As a result, the necessary pressure that is required to inject the polymer into the cavity will be affected. The pressure variation of molten polymer in the filling phase is shown in Figure 6.19. At the beginning of filling, the pressure is zero, or 1 atm in the absolute pressure scale, throughout the mold. The pressure at a specific location starts to increase only after the melt front reaches that location. The pressure continues to increase as the melt front moves past, due to the increasing flow length between this specific location and the melt front. The pressure difference from one location to another is the force that pushes the polymer melt to flow during filling. The pressure gradient is the pressure difference divided by the distance between two locations. Polymer always moves in the direction of the negative pressure gradient, from higher pressure to lower pressure, therefore, the maximum pressure occurs at the locations of polymer injection and the minimum pressure occurs at the melt front during the filling stage. The magnitude of the pressure or pressure gradient depends on the resistance of the polymer in the mold. This is because the polymer with high viscosity requires more pressure to fill the cavity.

6.3.3 Predicted curing results

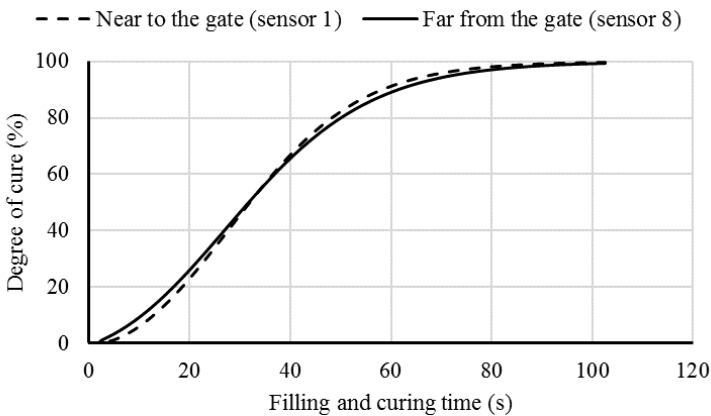


Figure 6.20 Degree of cure of molten Vyncolit X655 in the filling and curing phase

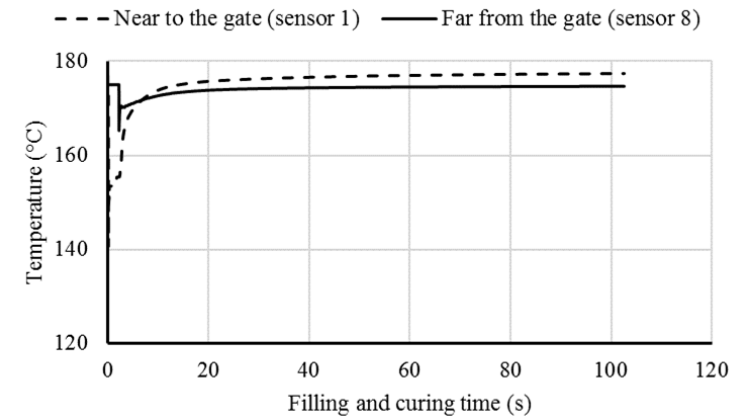


Figure 6.21 Temperature distribution of molten Vyncolit X655 in the filling and curing phase

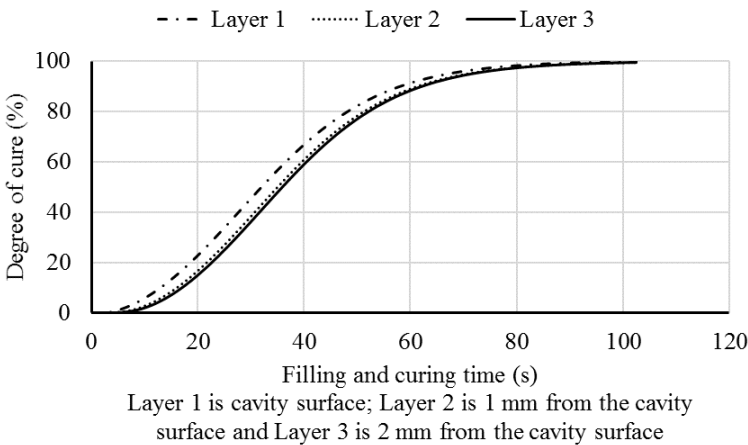


Figure 6.22 Degree of cure of molten Vyncolit X655 at the same position (sensor 1) but in different layers via thickness section

The degree of cure of molten polymer during the filling and curing phase of spiral injection molding process was predicted by using sensor nodes, as shown in Figure 6.20. With the injection speed of 32/16/8 cm³/s and the mold temperature of 175°C, the degree of cure of the molten polymer reaches 80% after 50 s. At the beginning of curing process, the degree of cure of polymer portion near to

the gate is little lower than the molten polymer far from the gate. However, from 35s to at the end of curing phase, an opposite phenomenon in the degree curve of polymer near to the gate and far from the gate is found. The cause leading to this variation is difference in the molten temperature distribution in the curing phase (Figure 6.21). Depending on curing time, the positions of hot channel and the heat from the mold to the molten polymer, the molten polymer temperature in the cavity at different positions is different. Even at the same position, but in different layers the degree of cure is also different, as shown in Figure 6.22.

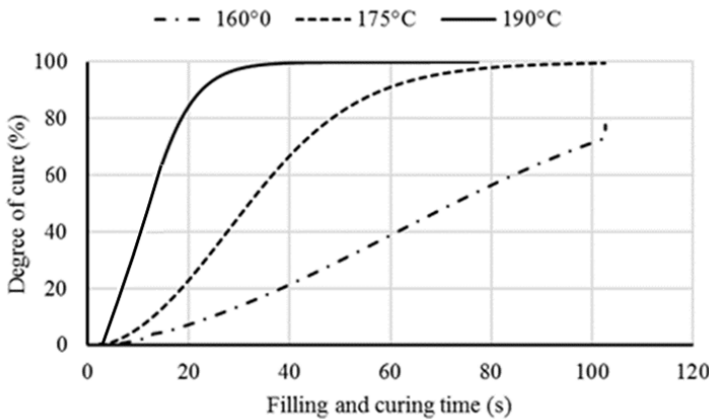


Figure 6.23 Influence of different mold temperatures on the degree of cure of molten Vyncolit X655 in the curing phase

The degree of cure predicted by simulation with other processing conditions was done and it was also found that there is a slightly higher in the degree of cure of the polymer near to the gate in comparison with the degree of cure of the polymer far from the gate. In addition, the influence of change in mold temperature on predicted degree of cure of the molten polymer during the curing process is illustrated in Figure 6.23. With the same injection speed, as shown in Figure 6.23, the mold temperature is 160°C, 175°C and 190°C, it requires at least 100 s, 50 s and 20 s, respectively, for the curing process to reach approximately 80 % conversion.

6.3.4 Influence of initial conversion on simulation results

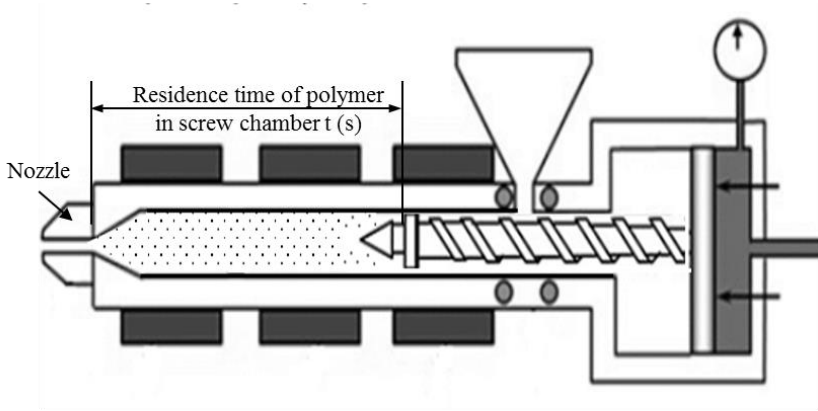


Figure 6.24 Screw chamber and nozzle of an injection molding machine

Initial conversion, which refers to the percentage of the material which starts reacting before being injected into the cavity. With thermoset injection molding process, before being injected into the cavity, the thermoset injection molding compounds are plasticized in screw, pushed in screw chamber and flows through a nozzle. The residence time of polymer in the screw chamber and the constriction at the nozzle increase the risk of premature curing [97, 98, 99, 100]. Particularly, the cure reaction is instigated immediately when the material enters the screw chamber and flows through the nozzle, as shown in Figure 6.24. Consequently, there is entanglement of the thermoset melt in the nozzle, which significantly increases viscosity and the flow resistance of thermoset melt during filling the cavity.

With Moldex3D simulation tool, users could take the influence of the initial conversion on the mold filling characterizations of thermoset injection molding compounds by setting the value of initial conversion during analysis setup. Figure 6.25 shows the influence of initial conversion on the predicted filling results. With only slight change in initial conversion (0.5 %), the degree of cure of polymer in the filling phase increases, leading to higher viscosity and a significant increase in injection pressure.

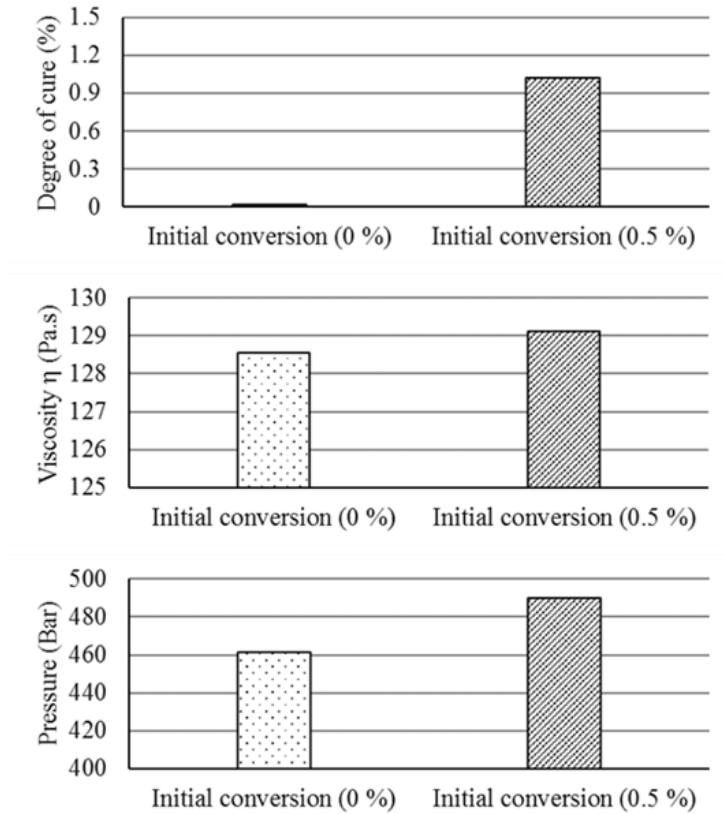


Figure 6.25 Influence of initial conversion on simulation results

6.4 Summary of chapter

In this chapter, the data sheet of the Vyncolit X655 generated in Chapter 5 was employed to import into Moldex3D simulation to investigate its application in simulate the filling phase and curing phase of the injection molding process with and without considering slip boundary condition.

The predicted filling and curing results, including viscosity, temperature, pressure and degree of cure was analyzed and will be used in comparison with the corresponding results that was generated in Chapter 4. Results of comparison will be shown in the next chapter.

7 Validation simulation results with experimental results

7.1 Filling results

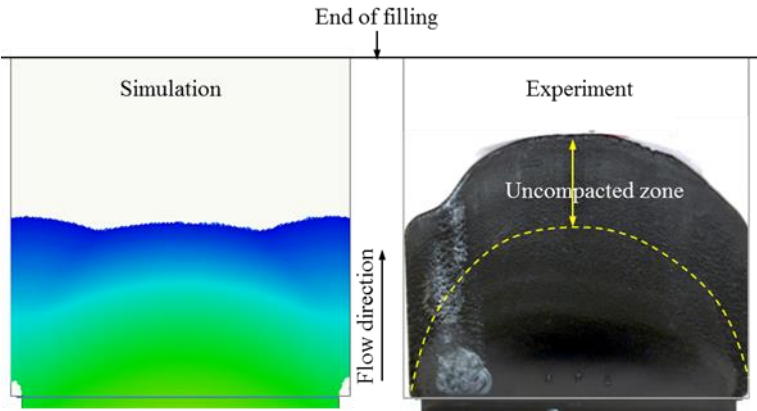


Figure 7.1 Plate part. Comparison between the pictures of the incomplete injection-molded parts and the corresponding filling patterns predicted by Moldex3D. Cavity volume is 60 %

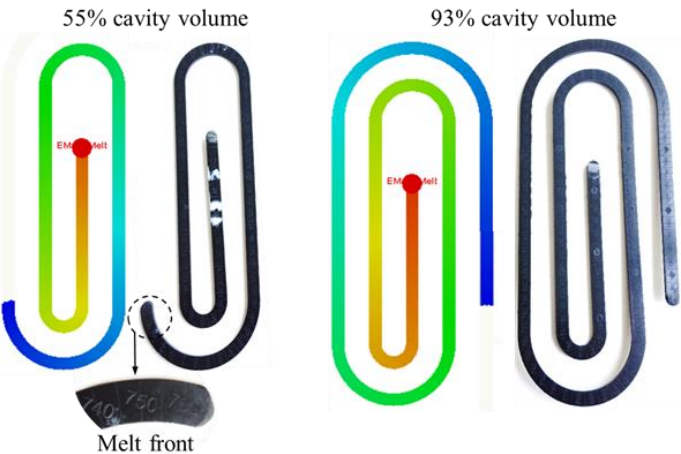


Figure 7.2 Spiral flow. Comparison between the pictures of the incomplete injection-molded parts and the corresponding filling patterns predicted by Moldex3D

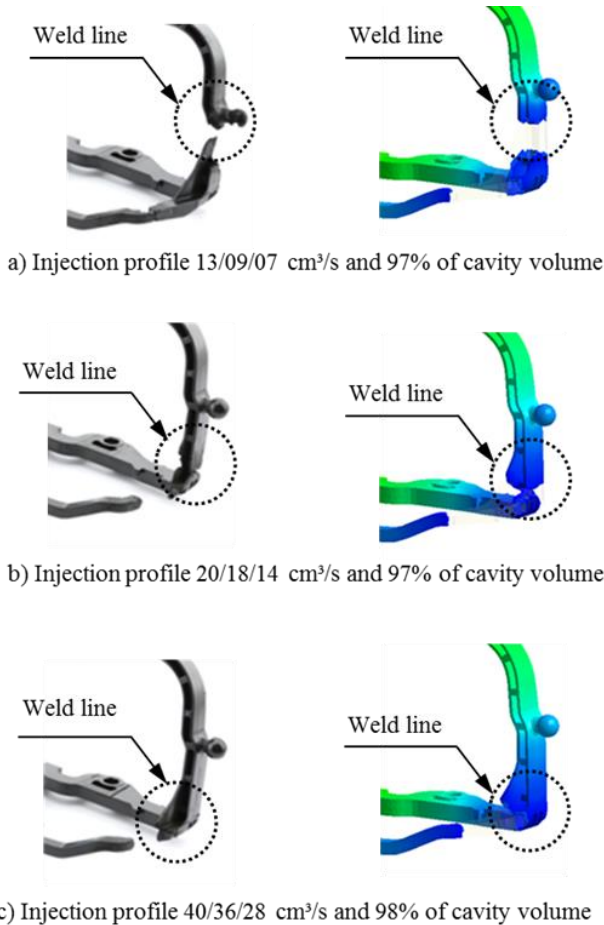


Figure 7.3 Complex part. Comparison between the positions of weld line pictures of the incomplete injection-molded parts (left) and the corresponding weld line positions (right) predicted by simulation

The experiment results of Vyncolit X655 generated by doing injection molding was employed to compare with the simulation results shown in chapter 6. It could be seen from Figure 7.1 that with frictional coefficient is 0.5 and wall shear stress threshold is 0.09 MPa, there is difference in the melt front and flow length of incomplete injection molded part and the corresponding filling patterns predicted by Moldex3D. Simulation has not yet been simulated exactly the uncompacted zone that has an interrupted contact with the cavity surface. Therefore, with the

same volume (60%) injected into the cavity the flow length of incomplete molded part predicted by simulation is shorter than the flow length of incomplete molded part generated by injection molding experiment. However, difference in the uncompacted zone and the flow length between simulation and experimental results depends on the geometry of cavity. For instance, with spiral flow part, the width and the thickness of part is only 10 mm and 4 mm, respectively, the uncompacted zone seems to be disappeared and the melt front and flow length generated by simulation and experiment is found in good agreement, as shown in Figure 7.2. In addition, a comparison between the positions of weld line of incomplete injection-molded complex parts and the corresponding weld line positions predicted by Moldex3D is conducted and also found in remarkable agreement, as shown in Figure 7.3. The experimental results show that the positions of weld line depend strongly on the injection speed profile, which is also found in simulation results. The agreement appears remarkable, indicating that the numerical methods for creating thermoset material data sheet that were written and shown in chapter 5 plays an important role for well-found prediction. And frictional coefficient of 0.5 and wall shear stress threshold of 0.09 MPa could be used to predict the flow length of injection molded part during filling the cavity.

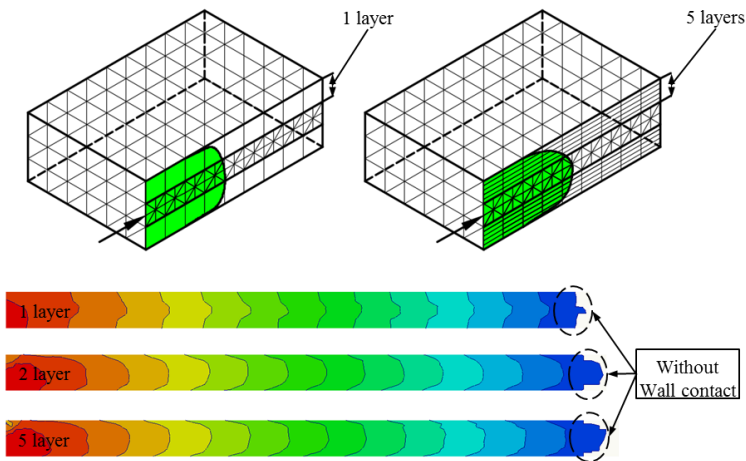


Figure 7.4 Influence of different skin layers on the uncompacted zone during filling the mold

Recently, Moldex3D rolled out the new pre-processing Module-Designer BLM (Boundary Layer Mesh), which can help advanced users to generate multiple layers of prismatic meshes inward from the surface mesh and then filling up the remaining space with tetrahedral mesh. Because of this development, Moldex3D

has been partly solved in simulation of the uncompacted zone of thermoset injection molding compounds during filling the rectangular cavity. It could be seen from Figure 7.4 that the higher the number of skin layers, the higher ability to simulate and capture the drastic changes of polymer near the cavity wall during the filling process such as temperature, velocity and the uncompacted zone. However, with simulation tools, users only change the value of friction coefficient and wall shear stress threshold to investigate the influence of slip boundary condition on the mold filling behavior of thermoset injection molding compounds. These adjustments may lead to unstable flow calculation and abnormal result and therefore the user must take serious consideration when adjusting these parameters. Therefore, to solve exhaustively this difference, a separate numerical fluid equation should be written with considering plug flow phenomenon into account instead of changing only the value of frictional coefficient and shear stress threshold in computation program.

7.2 Curing results

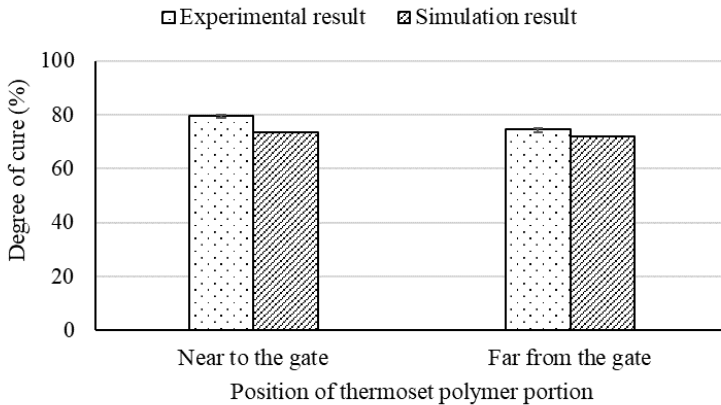


Figure 7.5 Comparison between the degree of cure of injection- spiral molded part and the degree of cure of molten polymer predicted by simulation (Filling and curing time is 43 s)

To investigate the accuracy of curing kinetics data that was generated in section 5.1 of chapter 5 and used in the simulation process of chapter 6, a comparison between the degree of cure of injection- spiral molded part and the degree of cure of molten polymer predicted by simulation was conducted and shown in Figure 7.5. Near to the gate, with the same processing conditions and curing time (43 s), the degree of cure predicted by simulation tool is 74 % while its experimental value is 79 %, which means that the degree of cure predicted by

simulation is 6.3 % lower than the degree of cure of molten polymer generated from experimental process. By simulation, as shown in Figure 6.20, it is found that it takes only 5 s more to the molten polymers reach the degree of cure of 79 %. Factors which could lead to these slight differences are the post curing process of the substances inside the injection molded parts and initial conversion. Because the mold temperature is 175°C, the temperature of injection-molded part after being ejected from the mold could be near to 175°C. Therefore, it takes time for cooling the injection molded part from 175°C to the ambient temperature so that the curing process still occur during the cooling time, leading to a slight increase in the real amount the degree of cure of the polymer in the curing phase. In addition, in this case simulation was done with the value of initial conversion is 0 %. If this number increases only 1%, the difference in the degree of cure predicted by simulation tool and experiment will be more or less the same.

7.3 Results of different phenolic injection molding compounds

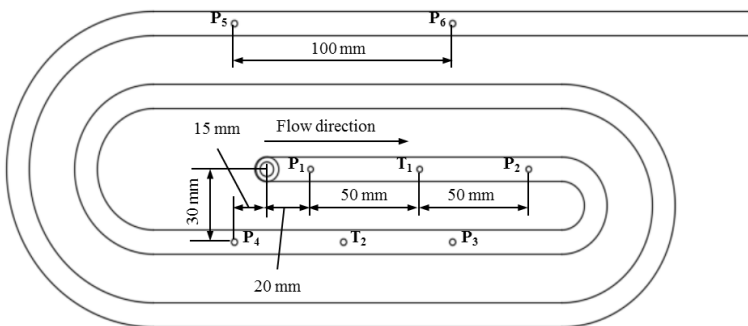


Figure 7.6 Positions of pressure sensors that was set during doing injection molding experiment of spiral flow

Filling and curing process of some phenolic injection molding compounds, namely, phenolic 6510 (GB 35, GF 20), phenolic 6680 (GB 35, GF 30), phenolic 1110 (GB35, GF 45) was simulated with frictional coefficient of 0.5 and wall shear stress threshold of 0.09 MPa. The subject study was also spiral flow part. Due to material data sheet of these phenolic injection molding compounds has not been found in any simulation tool now. Therefore, before conducting filling and curing simulation process, the numerical method that was developed and introduced in chapter 5 was employed to create their material data bank. Simulation results includes melt pressure and degree of cure was used to compare with experimental results that were available and kept in our laboratory [55]. During the injection molding process experiment, the pressure sensors was set

on the interface between polymer melt and cavity surface, as shown in Figure 7.6. The processing conditions consist of a variation of mold temperature and injection rate. Firstly, the mold temperature was constantly kept at 170°C for the different injection rates of 12 cm³/s, 24 cm³/s and 48 cm³/s. After that the injection rate was constantly kept at 24 cm³/s and the mold temperature was 155°C, 170°C, and 185°C, respectively. The curing time is 80 s, 40 s and 20 s as the mold temperatures is 155°C, 170°C, and 185°C, respectively.

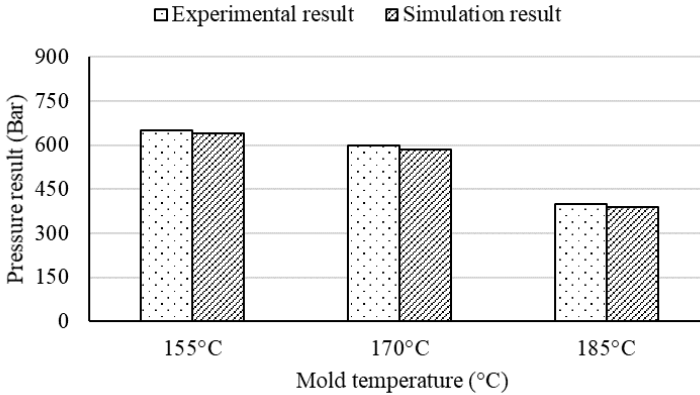


Figure 7.7 Comparison between the melt pressure measured by pressure sensor 1 and the melt pressure predicted by simulation. At the current filling time of 2 s

It could be seen from Figure 7.7 that the injection rate was constantly kept at 24 cm³/s and the mold temperature was 155°C, 170°C, and 185°C, respectively. Experimental results show that with higher temperature, the melt pressure decrease significantly. A decrease in the melt pressure is because in the filling phase, the filling time is too short so that the polymer viscosity depends strongly on temperature and shear rate, the influence of degree of cure on viscosity is small. Therefore, higher temperature leads to lower viscosity, which requires lower pressure to inject polymer into the cavity. This phenomenon is also found in simulation results. In general, there is good agreement in the melt pressure measurement between experiment and simulation, indicating that viscosity data sheet generated by applying the numerical method in chapter 5 is reasonable. To prove this statement, another comparison between the melt pressure measured by pressure sensor 1 and the melt pressure predicted by simulation was conducted and found in a remarkable agreement, as shown in Figure 7.8. In this case, the

mold temperature was constantly kept at 170°C for different injection speeds of 12 cm³/s, 24 cm³/s and 48 cm³/s.

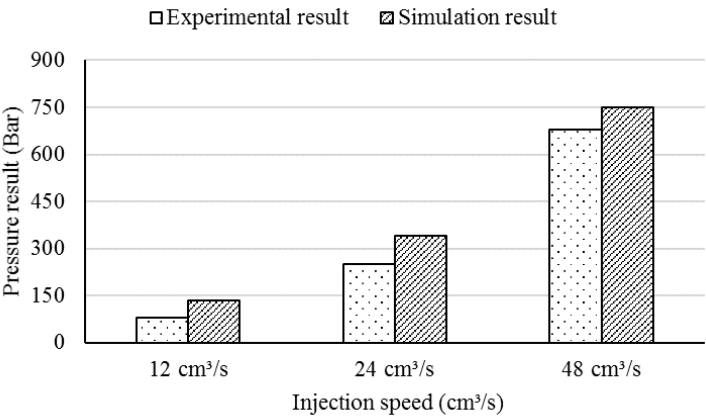


Figure 7.8 Phenolic 6510. Comparison between the melt pressure measured by sensor 1 and the melt pressure predicted by simulation. At the current filling time of 1 s

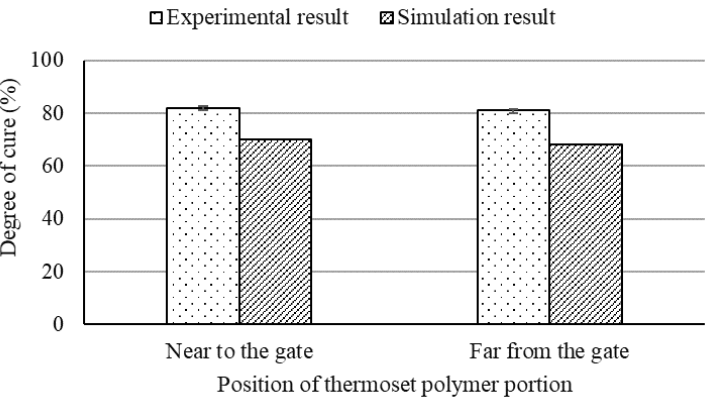


Figure 7.9 Phenolic 6510. Comparison between the real degree of cure of injection-spiral molded part and the degree of cure of molten polymer predicted by simulation

Finally, the real degree of cure of injection molded part was compared to the degree of cure predicted by simulation, as shown in Figure 7.9. There is only

slight difference in comparison, which demonstrates that the curing data sheet of Phenolic 6510 generated by applying the numerical method in chapter 5 makes sense.

7.4 Summary of chapter

In this chapter, simulation results were compared to the corresponding results generated from experiments. With frictional coefficient of 0.5 and shear stress threshold of 0.09 MPa, it was found that it depends on the geometry of cavity, the melt front and flow length of injection molded parts that predicted by simulation could be the same or slight difference from the experimental results. However, with the generated material data sheet, simulation results show that it is possible to full fill completely cavities, which was also found in experimental results. Filling results such as the distribution of melt pressure during filling the mold and curing results show a remarkable agreement with experimental results, concluding that the numerical method that was developed and written to create thermoset material data for reactive injection molding process, as shown in chapter 5 is reasonable.

8 Summary

8.1 Conclusions

This thesis focused on innovation of a new method to study the mold filling behavior of thermosets injection molding compounds and developing numerical method to create thermoset material data sheet for simulation of mold filling characterizations of thermoset injection molding compounds. The following works were accomplished

- a. A new method, namely, the spotwise painting of the mold wall surface was developed to investigate wall slip phenomenon on the interface between polymer and cavity surface during injection molding process.
- b. The flow behavior of the phenolic melt on the interface between the cavity and the mold wall under various processing conditions was investigated by using the spotwise painting of the mold wall surface.
- c. Developing and writing a new numerical method for not only creating thermoset material data sheet from rheological and thermal experimental data for reactive injection molding simulation process, but also for predicting the rheological and cure kinetics properties. It was applied to create material data sheet of some phenolic injections molding compounds, that has not been found any current simulation tools.
- d. The generated material data sheet of some thermoset phenolic injection molding compounds was directly imported into Moldex3D simulation tool to simulate the filling and curing process with and without considering slip boundary condition. The comparison between measured results and simulated results was performed.

Based on the accomplished works above, the research conclusions were shown follows

- a. Flow behavior of thermoset injection molding compounds during the filling process is plug-shear-flow instead of fountain flow as thermoplastics materials. Because of these differences will be leading to new thinking about influence of slip on calculation, analysis and simulation of fiber orientation during the filling process of the glass fiber reinforced thermoset resins injection molding compounds.

- b. A new material data sheet of all chosen phenolic injection molding compounds was successfully created and added to the data bank of simulation tools. In addition, master curves of viscosity over temperature and master curves of degree of cure over temperature at multiple heating rates was predicted and found in a good agreement with experimental results. The applicability of developed numerical method was not only published on the international polymer journals, but also recognized by a commercial simulation software company, namely Moldex3D from CoreTech, indicating that the developed numerical method of creating material data sheet for reactive injection molding simulation is reasonable and useful.
- e. With frictional coefficient of 0.5 and shear stress threshold of 0.09 MPa, it depends on geometry of cavity, the melt front and flow length of injection molded parts that predicted by simulation could be the same or different from the experimental results. The predicted melt pressure and degree of cure was found in a remarkable agreement with the corresponding results generated from injection molding experiments.

8.2 Future work

Although several works were accomplished, there are some relevant fields needed to be explored and studied.

- a. The spotwise painting of the mold wall surface should be applied for other phenolic injection molding compounds with different amount of fiber and filler to analysis the influence of amount of fiber and filler on the slip phenomenon. In addition, the influence of surface roughness on the slip phenomenon should be taken into account. During doing injection molding process, the mold wall surface should be painted with a scientific method instead of manual painting to observe more visually the influence of processing conditions on the dyed white color on the surface of injection-molded part.
- b. The developed and written numerical method should be used in modeling other reactive viscosity and cure kinetic models to evaluate which reactive viscosity and cure kinetic models fit the experimental data best.

- c. Studying the method to measure exactly the value of frictional coefficients, shear stress threshold, the relation between slip velocity and shear stress.
- d. Simulation will be done with the best reactive viscosity model, cure kinetic model and suitable frictional coefficient and shear stress threshold.
- e. PVT diagram of phenolic injection molding compounds should be measured to fit to the PVT mathematical model, which could be used to import into simulation tools to simulate the shrinkage and warpage of thermoset injection molding compounds.

9 References

- [1] Jeans. P.P, Henry. S, Jacques. V, Roberto. J.J.W, Thermosetting Polymers, New York: Marcel Dekker, 2002.
- [2] Biron. M, Thermosets and Composites: Technical Information for Plastics Users, Oxford: Elsevier Advanced Technology, 2004.
- [3] Yao. L, Heat transfer process between polymer and cavity wall during injection molding, Chemnitz: Technische Universität Chemnitz, 2015.
- [4] Malloy. R, Plastic part design for injection moulding: An introduction, Munich: Hanser, 2011.
- [5] Kazmer. D, Injection molding design engineering, Munich: Hanser, 2007.
- [6] Zheng. R, Tanner. R, Fan. X. J, Injection molding: Intergration of theory and modeling methods, Berlin: Springer, 2011.
- [7] Mennig. G, Klaus.S, Mold-Making Handbook, Munich: Carl Hanser, 2013.
- [8] Johannaber. F, Injection molding machines: A user's guide, Carl Hanser, 2016.
- [9] Coppetti. T, Krebs. R, "Vollhydraulische und Kniehebel-Schließsysteme," *Kunststoffe*, pp. 821-825, 1980.
- [10] Urbanek. O, Leonhartsberger. H, Steinbichler. G, "Hole Steifigkeit und viel Platz," *Kunststoffe*, vol. 81, pp. 1081-1084, 1991.
- [11] Coppetti. J, "Spritzgießen-Maschinentechnik, Antrieb, Steuerung," *Kunststoffe*, vol. 75, pp. 553-558, 1985.
- [12] N. N, "Einführung in das Spritzgießen von Duroplasten, Firmenschrift Arburg GmbH & Co KG," 2005.
- [13] N. N, "Verarbeitung von rieselfähigen duroplastischen Formmassen, Firmenschrift Raschig AG," 2006.
- [14] Weißler. E.P, Braun. U, "Duroplastische Formmassen, Expert-Verlag, Ehningen," 1989.
- [15] Pilato. L, Phenolic Resins: A Century of Progress, Berlin: Springer, 2010.
- [16] N. N, "1st Thermoset Exchange Days, Schulungsunterlagen Vyncolit," Gent, 2012.
- [17] Stang. C, Rezeptur- und Feuchteinflüsse auf die Standzeit von phenolharzgebundenen Trennschleifscheiben, Dissertation, Universität Erlangen Nürnberg, 2008.

- [18] Samou. M; Chung. B, Cohen. C, "Glass fiber - filled thermoplastics , II. Cavity filling and fiber orientation in injection molding," *Polymer engineering and science*, vol. 25, pp. 1008-1016, 1985.
- [19] Koponen. M, Enqvist. J, Nguyen-Chung. T, Mennig. G, "Advanced Injection Molding Mold and Molding Process for Improvement of Weld Line Strengths and Isotropy of Glass Fiber Filled Aromatic Polyester LCP," *Polymer engineering and science*, vol. 48, pp. 711-716, 2008.
- [20] Li. X.P, Zhao. G.Q, Yang. C, "Effect of mold temperature on motion behavior of short glass fibers in injection molding process," *The international journal of advanced manufacturing technology*, vol. 73, p. 639–645, 2014.
- [21] Kamal. M. R., "Thermoset characterization for moldability analysis," *Polymer engineering and science*, vol. 14, pp. 231-239, 1974.
- [22] Chang. D.E, *Rheology and processing of polymeric materials*, New York: Oxford University Press, 2007.
- [23] Kamal. M.R, Ryan. M.E, "The behavior of thermosetting compounds in injection molding cavities," *Polymer engineering and science*, vol. 20, pp. 859-867, 1980.
- [24] Thienel. P, Hoster. B, Schröder. T, Schröder. K, Kretzschnier. J, "Duroplast-spritzgießen mit Gasinnendruck," *Kunststoffe*, vol. 83, pp. 91-95, 1993.
- [25] Castro. J.M, Macosko. C. W, Tackett. L. P, Steinele. E.C, Critchfield. F.E, "Reaction injection molding: Filling of a rectangular mold," *Journal of elastomers and plastics*, vol. 12, pp. 3-17, 1980.
- [26] Ohta. T, "Visual analysis of cavity filling and packing process in injection moulding of thermoset phenolic resin by the gate-magnetization method," *Polymer Engineering and Science*, vol. 41, pp. 806-819, 2001.
- [27] Yokoi. H, Hayashi. T, Morikita. N, Todd. K, "Direct observation of jetting phenomena under a high injection pressure by using a prismatic-glass inserted mould," *SPE Technical Papers*, vol. 88, p. 329–333, 1988.
- [28] Englich. S, Scheffler. T, Gehde. M, "Specific mold filling characteristics of highly filled phenolic injection molding compounds," in *SPE-ANTEC 2013 Proceedings*, Cincinnati, 2013.
- [29] Englich. S, *Strukturbildung bei der Verarbeitung von glasfasergefüllten Phenolformaldehydharzformmassen*, Ph.D Thesis, Chemnitz: Technische Universität Chemnitz, 2015.
- [30] Huamin. Z, *Computer modeling for injection molding: Simulation, Optimization, and Control*, John Wiley & Sons, 2013.

- [31] Nguyen-Chung. T, Jüttner. G, Löser. C, Pham. T, Gehde. M, "Determination of the heat transfer coefficient from short-shots studies and precise simulation of microinjection molding," *Polymer science and engineering*, vol. 50, pp. 165-173, 2009.
- [32] Nguyen-Chung. T, Plichta. C, Mennig. G, "Flow disturbance in polymer melt behind an obstacle," *Rheologica Acta*, vol. 37, pp. 299-305, 1998.
- [33] Nguyen-Chung. T, "Flow analysis of the weld line formation during injection moulding of thermoplastics," *Rheologica Acta*, pp. 240-245, 2004.
- [34] Yao. L, Gehde. M, "Evaluation of heat transfer coefficient between polymer and cavity wall for improving cooling and crystallinity results in injection moulding simulation," *Applied Thermal Engineering*, vol. 80, pp. 238-246, 2015.
- [35] Manfred. P, *Praktische Rheologie der Kunststoffe und Elastomere*, VDI-Verlag, 1995.
- [36] Mezger. G.T, *The rheology book*, William Andrew Publishing, 2006, pp. 62-64.
- [37] Maxwell. B, "The application of melt elasticity measurements to polymer processing," *Polymer engineering and science*, vol. 26, pp. 1405-1409, 1986.
- [38] Becker. G.W, Braun. D, *Kunststoff Handbuch Band 10 - Duroplaste*, München: Carl Hanser, 1988.
- [39] Schönthaler. W, "Duroplaste Zukunft von Anfang an, Technische Vereinigung Würzburg," 1993.
- [40] Trenson. K, "The Basics of Thermoset Material Vyncolit 2nd Thermoset Exchange Days," Gents, 2014.
- [41] Bauer. W, *Technik der Preßmassenverarbeitung*, Carl Hanser: München, 1964.
- [42] Schönthaler. W, *Verarbeitung härtpbarer Kunststoffe*, Düsseldorf: VDI-Verlag, 1973.
- [43] Osswald. T.A, Menges. G, *Material science of polymer for engineers*, Munich: Carl Hanser, 2003.
- [44] Castro. J.M, Macosko. C.W, "Kinetics and rheology of typical polyurethane reaction injection molding systems," *Soc. Plast Eng. Tech. Papers*, vol. 26, pp. 434-438, 1980.

- [45] Castro J.M, Macosko.C.W, "Studies of mold filling and curing in the reaction injection molding process," *The American Institute of Chemical Engineers (AIChE) Journal*, pp. 250-260, 1982.
- [46] Tamil. J, Ore. S.H, Gan. K.Y, Bo. Y.Y, Ng. G, Wah. P.T, Suthiwongsunthorn. N, Chungpaiboonpatana. S, "Molding flow modeling and experimental study on void control for flip chip package panel molding with molded underfill technology,," *Journal of microelectronics and electronic packaging*, vol. 9, pp. 19-30, 2012.
- [47] Carreau, De Kee, Chhabra, *Rheology of Polymeric Systems: Principles and Applications*, Munich: Carl Hanser, 1997.
- [48] Ehrenstein. G.W, Riedel. G, Trawiel. P, *Thermal Analysis of Plastics-Theory and Praxis*, Munich: Carl Hanser, 2004.
- [49] Shiraz. S, Kamal .M.R, "Thermoset injection molding dynamics and the distribution of cure in thermoset molded parts," *Polymer engineering and science*, vol. 22, pp. 349-353, 1984.
- [50] Hülder. G, *Zur Aushärtung kalthärtender Reaktionsharzsysteme für tragende Anwendungen im Bauwesen*, Ph.D Thesis, Universität Erlangen Nürnberg, 2008.
- [51] Häßler. R, "Härtungsverhalten von Klebstoffen, Tagungsband Anwenderseminar TA Instruments," Würzburg, 2009.
- [52] Fuhrich. R, Gehde. M, John. J, "Werkstoffkennwertbestimmung von hochgefüllten reaktiven Substanzen, Tagungsband Anwenderseminar TA Instruments, Würzburg," 2010.
- [53] Schweiger. A, "Werkzeugkonzepte für Duroplaste, VDI Wissensforum Duroplast als High-Tech Werkstoff, Mannheim," 2011.
- [54] Knorr. L, "Grundlegende Materialcharakterisierung von duroplastischen Formmassen, FH Rosenheim, unveröffentlichte Masterarbeit," 2016.
- [55] Scheffler .T, *Werkstoffeinflüsse auf den Spritzgussprozess von hochgefüllten Phenol-Formaldehydharz-Formmassen*, Ph.D Thesis, Chemnitz: Technische Universität Chemnitz, 2018.
- [56] "<https://shop.perkinelmer.com>," [Online].
- [57] Kamal. M.R, Sourour. S, "Kinetics and thermal characterization of thermoset cure," *Polymer engineering and science*, vol. 13, pp. 59-64, 1973.
- [58] Kamal. M.R, Ryan. M.E, "Reactive polymer processing: Techniques and trends," *Advances in polymer technology*, vol. 4, pp. 323-348, 1984.

- [59] Arrillaga. A, Zaldua. A.M, Atxurra. R.M, Farid. A.S, "Techniques used for determining cure kinetics of rubber compounds," *European polymer journal*, vol. 43, pp. 4783-4799, 2007.
- [60] Arrillaga. A, Zaldua. A.M, Farid. A.S, "Evaluation of injection molding simulation tools to model the cure kinetics of rubbers," *Journal of applied polymer science*, vol. 123, pp. 1437-1454, 2012.
- [61] Garschke. C, Parlevliet. P.P, Weimer. C, Fox. B.L, "Cure kinetics and viscosity modelling of a high-performance epoxy resin film," *Polymer testing*, vol. 32, pp. 150-157, 2013.
- [62] Menges. G, Mohren. P, How to make injection molds, New York: Hanser, 2001.
- [63] Rodriguez. F, Principles of polymer system, Taylor and Francis, 2014.
- [64] Kennedy. P, Zheng. R, FLOW analysis of injection molds, Munich: Hanser, 2007.
- [65] Kennedy. P, Zheng. R, Flow analysis of injection molds, Munich: Carl Hanser, 2013.
- [66] Osswald. T, Hermendes-Ortiz. J.P, Polymer Processing :Modeling and simulation, Munich: Carl Hanser, 2006.
- [67] Wang. M.L, Chang. R.Y, Hsu. C.H, Molding simulation Theory and Practice, Munich: Carl Hanser, 2018.
- [68] Marquardt. D.W, "An algorithm for least squares estimation of nonlinear parameters," *J. Soc. Indust. Appl. Math*, vol. 11, pp. 431-441, 1963.
- [69] Madsen. K, Nielsen. N.B, and Tingleff, "Methods for nonlinear least squares problems," Technical Report, Informatics and Mathematical Modeling, Technical University of Denmark, 2004.
- [70] Lourakis. M.I.A, "A brief description of the Levenberg-Marquardt algorithm implemented by levmar," Institute of Computer Science, Foundation for Research and Technology - Hellas, 2005.
- [71] Transtrum. M.K, Machta. B.B, Sethna. J.P, "Why are nonlinear fits to data so challenging?," *Physical review letters*, vol. 104, pp. 060201-06204, 2010.
- [72] "<https://de.mathworks.com>," [Online].
- [73] Raffaele. D, Gilles. D, "Cure kinetics of a polysilazane system: Experimental characterization and numerical modelling," *European Polymer Journal*, vol. 76, pp. 40-52, 2016.

- [74] Arrillaga. A, Zaldua. A.M, Atxurra. R.M, Farid. A.S, "Techniques used for determining cure kinetics of rubber compounds," *European polymer journal*, vol. 43, p. 4783–4799, 2007.
- [75] Hernandez-Ortiz. J.P, Osswald. T.A, "A novel cure reaction model fitting technique based on DSC scans," *Journal of polymer engineering*, vol. 25, pp. 23 -37, 2005.
- [76] Lopez. L.M, Cosgrove. A.B, Hernandez-Ortiz. J.P, Osswald. T.A, "Modeling the Vulcanization Reaction of Silicone Rubber," *Polymer engineering and science*, pp. 675-683, 2007.
- [77] Ramorino. G, Girardi. M, Agnelli. S, Franceschini. A, Baldi. F, Viganò. F, Riccò. T, "Injection molding of engineering rubber components: A comparison between experimental results and numerical simulation," *International journal of material forming*, vol. 3, pp. 551-554, 2010.
- [78] Kallien. T, "Optimization of the injection molding process for thermoplastics with 3D simulation," Sigma Engineering GmbH, Aachen, 2011.
- [79] Raschke. K, Grundlagenuntersuchungen zur Prozess- und Struktursimulation von Phenolharzformmassen mit Kurz- und Langglasfaserverstärkung, Ph.D Thesis, Chemnitz: Technische Universität Chemnitz, 2017.
- [80] "Internet side <https://www.sbhpp.com>," [Online].
- [81] Holland. C, Stark. W, Hinrichsen. G, "Dielectric investigations on novolak phenol-formaldehyde resin," *Acta Polymerica*, vol. 46, pp. 64-67, 1995.
- [82] Carotenuto. G, Nicolais. L, "Kinetic study of phenolic resin cure by IR spectroscopy," *Journal of applied polymer science*, vol. 74, pp. 2703-2715, 1999.
- [83] Korosec. R.C, Meznar. L.Z, Bukovec. P, "High pressure DSC of phenol-formaldehyde molding compounds," *Journal of thermal analysis and calorimetry*, vol. 95, pp. 235-240, 2009.
- [84] Ehrenstein. G.W, Bittmann. E, Duroplaste - Aushärtung, Prüfung, Eigenschaften, Munich: Hanser, 1997.
- [85] Becker. G.W, Braun. D, Kunststoff Handbuch Band 10 - Duroplaste, München: Carl Hanser Verlag, 1988.
- [86] Wang. X.M, Riedl. B, "Differential scanning calorimetry of the effects of temperature and humidity on phenol-formaldehyde resin cure," *Polymer*, vol. 35, pp. 5685-5691, 1994.

-
- [87] Gill. P.S, Sauerbrunn. S.R, Reading. M, "Modulated differential scanning calorimetry," *Journal of thermal analysis and calorimetry*, vol. 40, pp. 931-939, 1993.
- [88] Benzler. B, "Anwendung der dynamischen Differenzkalorimetrie an duroplastischen Werkstoffen," *UserCom*, vol. 12, pp. 9-10, 2000.
- [89] Krüger. S, Stark. W, Goering. H, Michel. U, "Thermoanalyse der Phenolharzhärtung," *Materials Testing*, vol. 48, pp. 556-561, 2006.
- [90] Stark. W, "Investigation of curing behavior of melamine/phenolic (MP) thermosets," *Polymer testing*, vol. 29, pp. 723-728, 2010.
- [91] Fernandez. J, Kurowski. P, Petitjeans. P, Meiburg. E, "Density-driven unstable flows of miscible fluids in a Hele-Shaw cell," *Journal of Fluid Mechanics*, vol. 451, pp. 239-260, 2002.
- [92] "<http://support.moldex3d.com>," [Online].
- [93] Rong. Y.C, Wen. H.Y, "Numerical simulation of mold filling in injection molding using a three-dimensional finite volume approach," *International journal for numerical methods in fluids*, vol. 37, pp. 125-148, 2001.
- [94] Mooney. M, "Explicit formulae for slip and fluidity," *Journal of rheology*, vol. 2, pp. 210-222, 1931.
- [95] Hatzikiriakos. S.G, Dealy. J.M, "Wall slip of molten high density polyethylene," *Rheological Acta Journal*, vol. 35, pp. 497-253, 1991.
- [96] Hatzikiriakos. S.G, "Wall slip of molten polymers," *Progress in Polymer Science*, vol. 37, pp. 624-643, 2012.
- [97] Bronke. D, "Herstellung von duroplastischen Präzisionsteilen," *Plastverarbeiter*, vol. 36, pp. 24-25, 1985.
- [98] Schönthaler. W, Handbuch Duroplaste - Zukunft von Anfang an, Technische Vereinigung der Hersteller und Verarbeiter von Kunststoff-Formmassen, 1996.
- [99] Singh. R, Chen. F, Jones. F.R, "Injection molding of reinforced phenolic composites," *Polymer composites*, vol. 19, pp. 37-47, 1998.
- [100] Berthold. J, Verarbeitung von duroplastischen Formmassen im Spritzprägeverfahren, Ph.D Thesis, RWTH Aachen, 2000.

10 List of symbols and abbreviations

Symbols		
T_g	[°C]	Glass transition temperature
T	[°C]	Temperature
ΔH	[J/kg]	Heat of cure
Q	[J]	Heat amount
c	[J/(kg.K)]	Specific heat
ρ	[kg/m ³]	Density
k	[W/m.K]	Thermal conductivity
h	[W/m ² .K]	Heat transfer coefficient
η	[Pa/s]	Melt viscosity
η_0	[Pa/s]	Zero shear viscosity
$\dot{\gamma}$	[1/s]	Shear rate
τ	[Pa]	Shear stress
α		Degree of cure
$\frac{d\alpha}{dt}$		Reaction rate
α_g		Gelation point
n		Power law index

B, T_b, τ^*, c_1, c_2		Data fitted parameters for Cross Castro Macosko Model
k_1, k_2		Arrhenius overall constants
a_i		Data fitted parameters for Kamal model
E_i		Activation energy
R		Universal gas law constant
p	[Bar]	Pressure
t	[s]	Time
\mathbf{v}		Velocity vector
ΔT	[°C]	Temperature difference between two sensors
α_{real}		Real degree of cure of molded part
∇p		Pressure gradient
σ		Stress tensor
\mathbf{D}		Deformation tensor
\mathbf{g}		Total body force per unit mass
β		Coefficient of volume expansion
\dot{Q}		The heat source

Abbreviations

PF	Phenol-formaldehyde resins
EMC	Epoxy injection molding compound
DSC	Differential scanning calorimetry
TMA	Thermal dynamic analysis
DMA	Dynamic mechanical analysis
TTT	Time temperature transformation
CTE	Coefficient of thermal expansion
2D	2 dimensional
2.5D	2.5 dimensional
3D	3 dimensional
FEM	Finite element method
FVM	Finite volume method
LMA	Least-square estimation algorithm developed by Lavender-Marquart
BLM	Boundary layer mesh